



AKADEMIA GÓRNICZO - HUTNICZA
IM. STANISŁAWA STASZICA W KRAKOWIE

WYDZIAŁ FIZYKI I INFORMATYKI STOSOWANEJ

UNIVERSITEIT ANTWERPEN

FACULTEIT WETENSCHAPPEN DEPARTEMENT FYSICA

Ph.D Thesis

Design and computer simulations of nanodevices with applications to quantum computing

Author:

mgr inż. Paweł SZUMNIAK

Promotor:

Prof. dr hab. Stanisław BEDNAREK

Co-promotor:

Prof. dr. Bart PARTOENS

June 2013



This dissertation is dedicated to my wonderful wife Sylwia

Abstract

In this thesis we propose several nanodevices that exploit the self-focusing effect of a hole or an electron wave function as well as the spin-orbit interaction in order to realize various operations on an electron and hole spin confined in semiconductor gated nanodevices without application of a magnetic field. The proposed devices fulfill the criteria for the physical implementation of quantum computation and are promising candidates for basic building blocks of an all-electrically controlled spin based scalable semiconductor solid state quantum computer architecture. The thesis consists of six chapters: chapter (1) contains the introduction in which we give a short historic overview of the ideas which lay behind quantum computation, list most popular proposals for the physical implementation of quantum computers, describe the spin based proposals for the realization of quantum computers and finally give a short overview of the proposed devices. The summary of the articles which were published as a result of the research done within this PhD are included in chapter (2). The articles are attached in chapters (3)-(6). In chapter (3) nanodevices for single electron spin initialization and read out are proposed that exploit the Dresselhaus spin-orbit interaction. Chapter (4) contains the description of improved nanodevices of the previous chapter (3) which now are capable to realize high fidelity spin accumulation of single electrons and nondestructive single electron spin read out, both without application of a magnetic field, while this time the Rashba spin-orbit interaction is employed. In the next chapter (5) we propose a method for the coherent manipulation of single heavy-hole spin qubits, based on the hole motion-induced heavy-hole spin rotations in the presence of the Dresselhaus spin-orbit interaction and present a nanodevice which can act as a single quantum logic NOT gate. Nanodevices which can realize several all-electrically controlled single quantum logic gates (i.e. Pauli X, Y and Z) on heavy-hole spin qubits based on the method from chapter (5) are proposed in the last chapter (6). Furthermore, in chapter (6) “a combo” nanodevice which can realize an arbitrary sequence of single quantum logic gates on heavy-hole spin qubits is proposed as well as a fragment of a scalable quantum computer architecture containing four qubits. At the end the summary of the thesis is included.

Streszczenie

Niniejsza praca dotyczy projektowania i symulacji działania nanourządzeń wykonujących kwantowe operacje logiczne na spinie elektronu (dziury) uwięzionego w półprzewodnikowej nanostrukturze bez konieczności stosowania pola magnetycznego. Wykorzystany jest w nich efekt samoogniskowania funkcji falowej elektronu lub dziury oraz oddziaływanie spin-orbita. Zaproponowane nanourządzenia spełniają kryteria fizycznej implementacji komputerów kwantowych i są bardzo obiecującymi kandydatami na podstawowe elementy skalowalnej architektury komputera kwantowego opartej o nanostruktury półprzewodnikowe, ponieważ qubit spinowy jest kontrolowany wyłącznie za pomocą niewielkich napięć przykładanych do elektrod. Praca składa się z sześciu rozdziałów: w rozdziale (1) zawarty jest wstęp obejmujący krótki rys historyczny dotyczący idei obliczeń kwantowych, lista najpopularniejszych propozycji fizycznej realizacji komputerów kwantowych ze szczególnym uwzględnieniem rozwiązań wykorzystujących jako kubit spin elektronu uwięzionego w półprzewodnikowych nanostrukturach. Rozdział kończy się krótkim opisem zaproponowanych w pracy nowych nanourządzeń. Podsumowanie artykułów zawierających wyniki uzyskane podczas realizacji doktoratu zawarte są w rozdziale (2). Publikacje tworzące dysertację zamieszczone są w rozdziałach kolejno od (3) do (6). W rozdziale (3) dyskutowane są nanourządzenia służące do ustawiania oraz do odczytu spinu pojedynczego elektronu. Rozdział (4) zawiera propozycję i opis nanourządzeń zdolnych do ustawiania i nieniszczącego odczytu stanu spinowego elektronu bez konieczności stosowania pola magnetycznego. Są one w dużym stopniu ulepszone w stosunku do nanourządzeń zaproponowanych w rozdziale (3). W kolejnym rozdziale (5) przedstawiamy metodę wykonywania koherentnych operacji na kubicie realizowanym przez stan spinowy dziury ciężkiej. Tego typu rozwiązanie jest korzystne ponieważ spin dziury ciężkiej w porównaniu do spinu elektronu cechuje się znacznie dłuższym czasem koherencji. Proponujemy nanourządzenie wykonujące na spinie dziury kwantową operację logiczną NOT. W ostatnim rozdziale (6) przedstawiona jest propozycja nanourządzeń, które są w stanie wykonywać, różne kwantowe operacje logiczne (np. bramki Pauligo X, Y i Z) na pojedynczym dziurowym kubicie spinowym. W rozdziale (6) zaproponowane jest ponadto nanourządzenie "combo" zdolne do wykonywania dowolnej sekwencji jednokubitowych operacji logicznych oraz fragment skalowalnej architektury (zawierającej cztery kubity) składającej się z takich nanourządzeń. Na końcu pracy znajduje się podsumowanie.

Abstract

In deze thesis stellen we een aantal nanodevices voor die gebruik maken van het zelf-focusing effect van een holte of elektron en van de spin-baan interactie om verschillende logische operaties te implementeren op de spin van een elektron en holte in halfgeleider nanodevices met gates en zonder een uitwendig aangelegd magneetveld. De voorgestelde devices voldoen aan de criteria voor de fysische implementatie van kwantumcomputatie en zijn veelbelovende bouwstenen voor een volledig elektrostatich gecontroleerde spin gebaseerde schaalbare halfgeleider kwantumarchitectuur. De thesis omvat 6 hoofdstukken. Hoofdstuk (1) geeft een inleiding met een kort historisch overzicht met de ideeën achter kwantumcomputatie. Daarnaast bespreekt het de meest populaire voorstellen voor de fysische implementatie van een kwantumcomputer, de spin gebaseerde voorstellen in het bijzonder. Tot slot wordt een kort overzicht gegeven van de devices die voorgesteld worden in deze thesis. Een samenvatting van de artikels die gepubliceerd werden voortvloeiende uit het onderzoek dat verricht werd in dit doctoraat wordt gegeven in hoofdstuk 2. De artikels zijn toegevoegd als hoofdstukken (3) tot (6). In hoofdstuk (3) worden de nanodevices voor de initialisatie en uitlezing van een enkele elektron spin voorgesteld. Deze devices maken gebruik van de Dresselhaus spin-baan interactie. In hoofdstuk (4) komen verbeterde versies van deze nanodevices aan bod die het mogelijk maken om de spin van een elektron niet-destructief uit te lezen, en dit zonder gebruik te maken van een uitwendig aangelegd magneetveld. Hierbij wordt gebruik gemaakt van de Rashba spin-baan koppeling. In het volgende hoofdstuk (5) stellen we een methode voor voor de coherente manipulatie van een enkele heavy-hole qubit, gebaseerd op de beweging van de holte door geïnduceerde holte spin rotaties door de aanwezigheid van de Dresselhaus spin-baan interactie. Hier beschrijven we een nanodevice dat een kwantum logische NOT gate realiseert. Nanodevices voor verschillende volledig elektrostatich gecontroleerde kwantum logische operaties (i.e. Pauli X, Y en Z) op heavy-hole spin qubits, gebruik makende van de methode van hoofdstuk (5), worden voorgesteld in hoofdstuk (6). Bovendien wordt in hoofdstuk (6) ook een "combo" device voorgesteld dat in staat is om een willekeurige sequentie van kwantum logische operaties uit te voeren op een heavy-hole qubit, en een fragment van een schaalbare kwantumcomputerarchitectuur met vier qubits. Tot slot volgt een samenvatting.

Acknowledgement

This thesis would not have been possible without the involvement of my promoters prof. Stanisław Bednarek and prof. Bart Partoens to whom I wish to express my sincere gratitude. On this page I would like to thank them for giving me an unique opportunity to work on interesting research topics, for their motivation, invaluable support and guidance during my PhD studies. This thesis is a result of their consistent encouragement and the fruitful discussions I had with them. It was a great privilege for me to work with them.

I would like to thank all my colleagues from the Theory of Nanostructures and Nanodevices Group for fruitful and interesting and very often entertaining conversations. Especially, I thank my office roommates: Michał Nowak (actual) and Przemysław Gryniewicz (former), conference and lunch companions: Michał Zegrodnik, Paweł Wójcik, Jarosław Pawłowski and W. Pasek who have provided a cheerful atmosphere during the realization of my thesis. I have spent great time with you guys. I also thank all the professors and doctors from the NN group: prof. B. Szafran, prof. J. Adamowski, dr. T. Chwiej, and dr. B. Spisak who were always ready to help.

Also I would like to thank prof. F. Peeters for his hospitality during my one year stay at Antwerp University and all my colleagues from the Condensed Matter Theory group in Antwerp with whom I have the privilege to make interesting and inspiring conversations. The possibility to do research in your group was an unique, valuable and unforgettable experience.

I would also like to thank Foundation for Polish Science for financial within the “Krakow Interdisciplinary PhD Project in Nanoscience and Advanced Nanostructures” programmes co-financed by the EU European Regional Development Fund. and the coordinator prof. Bartłomiej Szafran for his exceptionally good management of the project. I thank the NCN Polish National Science Center who also supported some part of research done within the thesis with the Grant no. DEC-2011/03/N/ST3/02963 and PL-Grid Infrastructure.

Finally, special thanks to my wonderful wife Sylwia for her love, encouragement and patience, my parents Zbigniew and Barbara, for their support throughout my life and my newborn son Jan whose smile has motivated me to work during the very end of the preparation of this thesis.

There is one more person I would like to thank, ks. prof. Jan Żelazny, thank you for the many inspiring discussions we had.

Contents

About the thesis	2
1 Introduction, motivation and context of the thesis	3
2 Summary of the articles which forms this thesis and conclusions	10
2.1 Article A1, <i>Nanodevice for High Precision Readout of Electron Spin</i>	10
2.2 Article A2, <i>Spin accumulation and spin read out without magnetic field</i> . .	12
2.3 Article A3, <i>Spin-Orbit-Mediated Manipulation of Heavy-Hole Spin Qubits in Gated Semiconductor Nanodevices</i>	15
2.4 Article A4, <i>All-electrical control of quantum gates for single heavy-hole spin qubits</i>	16
3 Nanodevice for High Precision Readout of Electron Spin	18
4 Spin accumulation and spin read out without magnetic field	22
5 Spin-Orbit-Mediated Manipulation of Heavy-Hole Spin Qubits in Gated Semiconductor Nanodevices	28
6 All-electrical control of quantum gates for single heavy-hole spin qubits	34
Summary	47
Podsumowanie	49
Samenvatting	51
Bibliography	53

About the thesis

The present dissertation consists of monothematic articles in which we propose several nanodevices that exploit the soliton effect of a hole or an electron wave function as well as the spin-orbit interaction in order to realize all-electrically controlled operations on electron and a hole spin qubits confined in gated semiconductor nanostructures for quantum computing applications. The dissertation is composed of the following articles:

- A1 P. Szumniak, S. Bednarek, P. Grynkiewicz, B. Szafran *Nanodevice for High Precision Readout of Electron Spin*,
Acta Physica Polonica A 119, 651 (2011).
- A2 S. Bednarek, P. Szumniak, and B. Szafran *Spin accumulation and spin read out without magnetic field*,
Phys. Rev. B 82, 235319 (2010).
- A3 P. Szumniak, S. Bednarek, B. Partoens, and F. M. Peeters, *Spin-Orbit-Mediated Manipulation of Heavy-Hole Spin Qubits in Gated Semiconductor Nanodevices*,
Phys. Rev. Lett. 109, 107201 (2012).
- A4 P. Szumniak, S. Bednarek, J. Pawłowski, and B. Partoens, *All-electrical control of quantum gates for single heavy-hole spin qubits*,
Phys. Rev. B 87, 195307 (2013).

The series of papers which constitute the dissertation are preceded by an introduction and a summary of the articles (which can be treated as a guide to the articles) with a description of the novel contribution to the existing field of solid state spin based implementation of quantum computation. At the end of the thesis a summary is included.

1 Introduction, motivation and context of the thesis

In 1982, preceded by some ideas related to quantum information theory [1, 2], Richard Feynman published an original article [3] in which he suggested that the time dependent numerical simulation of a many body quantum system will be an extremely challenging task to realize using standard computers. Together with David Deutch and other researchers [3, 4, 5, 6] they proposed an alternative computer architecture - a quantum computer - which exploits the basic and counterintuitive laws of quantum mechanics (such as quantum superposition, unitary evolution and quantum entanglement) to simulate in a very efficient way quantum physical systems. Shortly after scientists discovered that such a computer can not only be used to model physical systems but also to solve other challenging computational tasks [7, 8, 9, 10, 11, 12, 13, 14]. The most profound example is the algorithm proposed by Peter Shor [9, 10] for factorization products of large prime numbers in a polynomial time while classical algorithms can solve such a problem only in an exponential time. The next important algorithm which illustrates the power of quantum computation is the Grover algorithm for searching an unsorted database [11, 12]. Scientists also realized that a physical system that will realize quantum computation is unavoidably exposed to interactions with the environment, which causes decoherence and leads to errors and the destruction of quantum information. Fortunately, Peter Shor and Andrew Steane developed methods to circumvent this problem, called quantum error correction codes [15, 16, 17, 18, 19] which allow to protect quantum information from errors of different sources (like decoherence or imperfections of the quantum gates). In the same time huge progress has been made in nanofabrication as well as in the ability to study experimentally the behavior of individual quantum objects. Furthermore, Alain Aspect in his famous experiment [20] confirmed the quantum mechanical non-local character of Nature. For all these reasons searching for physical implementations of quantum computation has attracted an enormous attention of theoreticians and experimentalists in recent years and convinced scientists that quantum computers may become reality one day. However its realization will require extreme efforts and groundbreaking ideas.

Many promising proposals for the physical realization of quantum computation have been put forward [21, 22]. The most important ones are based on semiconductor quantum dots [23, 24, 25, 26, 27], cold trapped ions [28], cavity quantum electrodynamics [29, 30, 31, 32], bulk nuclear magnetic resonance [33, 34], Josephson tunnel junctions

[35, 36, 37, 38, 39, 40], linear optics [41], molecular magnets [42, 43], spin clusters [44], single dopants in solids like donor atoms in silicon [45, 46] or nitrogen vacancy centers in diamond [47, 48, 49]. These proposals are suitable for the realization of the so called circuit model of quantum computation. There are also some other approaches like adiabatic quantum computation [50, 51, 53] or topological quantum computation [54, 55, 56, 57, 58]. The latter proposal is particularly interesting since it employs exotic quasiparticles called anyons [59, 60] (particles which obey neither fermion nor boson statistics), or Majorana bound states (particles or excitations which are in the same time its antiparticles) [61, 62] which both are due to their topological nature are much more immune to the decoherence than standard qubits from the circuit model.

From the other hand, searching for the best physical candidate for a quantum computer has stimulated enormous progress in nanofabrication and in experimental techniques which now enable measuring and controlling individual quantum objects in many different physical systems. Some of these achievements were awarded by the Nobel Prize in Physics in 2012 to the experimentalists Serge Haroche and David J. Wineland for their groundbreaking experiments on manipulating and measuring the quantum state of individual physical systems of trapped ions and photons [63, 64, 65, 66, 67, 68, 69, 70]. Furthermore, studying the behavior of individual quantum systems and especially decoherence processes, gives also a unique opportunity to investigate the fascinating physics connected with the transition from the quantum to the classical world [71, 72, 73].

Since, as suggested by Rolf Landauer, quantum computation should be realized by a “physical apparatus not Hamiltonians” [74] any physical implementation of a quantum computer architecture (within the so called circuit model) should fulfill the list of challenging and even conflicting criteria which has been put forward by David DiVincenzo [75, 23]:

- i The physical system which realizes the defined basic unit of quantum information - a qubit - is needed. Usually, a qubit is encoded in a two level quantum system. Furthermore, in order to realize practical computation, scalability is required. It means that one has to be able to extend a system to a larger number of qubits arranged in a so called quantum register in which each qubit can be adressed individually (the amount of information stored in the Hilbert space should be increased exponentially without exponential cost of resources [22]).
- ii Before performing computation one has to be able to initialize qubits in the quantum

register in a given state with high fidelity.

- iii The quantum information should be characterized by a long coherence time T_2 which is limited by the interaction with the environment. Since it is extremely difficult to isolate individual quantum systems from the surrounding environment this criterion seems to be the most challenging one. Thanks to the existence of quantum error correction codes the coherence time could be finite but has to be long enough [15, 16, 17, 18, 19], i.e. much longer than the gate operation time τ_{OP} .
- iv The key criterion is the ability to control and manipulate qubits in the quantum register in a selective and precise manner to realize quantum logic gates (unitary operations) without undesired disruption of the state of other qubits in the quantum register. The one and two qubit quantum gates form a universal set of quantum gates which can realize an arbitrary quantum algorithm [76, 77]. Furthermore, as mentioned in (i) the quantum gate operation time τ_{OP} in certain proposals has to be sufficiently fast.
- v When a certain quantum computation is done one has to be able to read the outcome, i.e. to make a precise measurement of the state of the qubits. It is essential that the measurement should be done on each qubit individually (selectively) without affecting the state of other qubits in the quantum register and preferably in a nondestructive manner (i.e. a projective type measurement).

There are also two additional criteria related to the quantum communication and transfer of quantum information:

- vi The ability to transform stationary qubits between “flying qubits” [24, 78].
- vii The possibility to transfer “flying qubits” between the desired locations.

Within this thesis we propose a set of nanodevices which are designed in such a way that they fulfill some of these demanding criteria. Our proposals belong to the spin based solid state semiconductor electrostatically defined quantum dot category [23]. First we describe the basic concepts of this original approach to quantum computation [23, 25, 26, 27] and next describe how our proposal can solve some issues related to selective single spin control. Daniel Loss and David DiVincenzo in their original work [23] proposed that a quantum bit can be encoded in the spin state of an electron (which is a natural two

level quantum system) confined in an array of electrostatically defined coupled semiconductor quantum dots with electrically tunable tunnel barriers. Such electrically gated semiconductor quantum dots seem to be a very promising candidate for the realization of a quantum computer architecture since it allows to control spin qubits with electric fields, generated by top local electrodes. Two qubit gates are realized by controlling interdot coupling (switching on and off exchange interaction) by a voltage applied to the top electrodes while single electron spin qubit rotations may be realized mainly by the application of oscillating electric fields like electron spin resonance (ESR) techniques, by dragging electron wave function in inhomogeneous g-factor layer of quantum dot host in presence of static magnetic field, by optical methods, or by using the electric dipole spin resonance (EDSR) method.

Motivated by the original work [23] recently a vast number of state of the art experiments has been realized in which individual electron spins are initialized, manipulated in coherent manner and read out with high fidelity [79, 80, 81, 82, 83, 84, 85, 86, 87, 88, 89, 90, 91, 92, 93, 94, 95]. Despite these remarkable experiments, realization of a practical scalable quantum dot architecture where more than a few qubits can be manipulated selectively haven't been realized so far ¹.

One of the main problems is the scalability requirement and the related difficulty in addressing individual spin qubits in a quantum register in a selective manner. The selective single electron spin control, preparation and read out seems to be more challenging than the realization of two qubit quantum gates which can be implemented by employing the electrically controllable exchange interaction in quantum dots [101] and thus realize a fully all-electrical manipulation scheme. The single spin control usually requires application of a magnetic field which causes the continuous precession of spins of all the confined qubits which prevents to address individual qubits without affecting the state of others in the quantum register. This was the motivation for a proposal in which qubits can be encoded in the singlet and triplet states of two electrons in a double quantum dot instead of using the spin up and down states of a single electron [101]. In such systems single qubit gates can be realized all-electrically but more resources are needed: two electrons instead of one for each qubit.

¹The proposals for other physical implementations suffer from the same limitation. The experiments are made only on a few qubits. As an example the physical implementation of Shor's algorithm has been realized, and number 15 [96, 97, 98, 99] has been factorized and recently 21 [100] which is very promising but still far from practical applications.

The first step towards the realization of selective single electron spin control was proposed in articles [102, 103, 104] where the combination of the spin-orbit interaction, the static magnetic field and the oscillating electric fields (generated by the top local electrodes) are employed in order to control the electron spin electrically - EDSR technique. Such a method was recently implemented experimentally in electrostatic quantum dots [89] and in gated nanowire quantum dots [90, 91].

Another difficulty in using electron spins confined in quantum dots as qubits is their relatively short coherence time. The main source of electron spin decoherence in semiconductor quantum dot systems at low temperatures is the hyperfine contact Fermi interaction with the nuclear spins of the host material [105, 106, 107, 108]. If no special effort is made the electron spin loses its coherence in nanosecond timescale. Several appealing proposals have been made in order to suppress this type of decoherence to extend the electron spin coherence time from nanoseconds to microseconds and even milliseconds [109, 110]. One promising method which we consider in this thesis is to encode the qubit in the spin state of the valence hole instead of the electron [111, 112, 113]. The valence hole Bloch functions are described by p-type orbitals which vanish at the nuclear site of the host atoms and thus the contact hyperfine interaction is strongly suppressed. Unfortunately the hole spin still experiences interactions with nuclear spins which have a dipolar character which is about ten times weaker than the contact one for the electrons [114, 115, 116, 117, 118, 119, 120]. Consequently, the hole spin qubit coherence time is prolonged compared to the electron spin coherence time.²

These new concept proposals of electron and hole spin qubit manipulation, initialization and measurement methods have to be developed preferably all-electrical, without the need of the application of a magnetic field in any stage of the quantum computation process. In this thesis we propose several semiconductor gated nanodevices which operate on a single electron or hole spin qubit without the application of a magnetic field (except one nanodevice) which should potentially help in the realization of a scalable many qubit quantum computer. Furthermore, the proposed devices are designed in order to fulfill the criteria for physical implementation of quantum computation. This research is somehow a continuation of the pioneering work done by my promotor on the application of the electron soliton effect [121, 122, 123, 124, 125] to realize all-electrically controlled quantum

²The dipolar hyperfine interaction between a hole spin state and a nuclear spins for a hole occupying only heavy-hole (HH) band(i.e. absence of the heavy-hole / light-hole (LH) mixing) is of the Ising type [114, 115]. In this situation the hole spin coherence time reaches its maximum.

gates on electron spin qubits [126, 127].

The proposed devices exploit the interplay between a peculiar electron (hole) soliton effect [121, 122, 123, 124] which is present in so called induced quantum dots and wires [125] together with the spin-orbit interaction (SOI) (Dresselhaus [128] (DSOI) or Bychov-Rashba [129, 130] (RSOI) type) in order to realize various operations on single electron and hole spin states including read out, initialization and manipulation without application of a magnetic field. Since proposed devices are controlled only by weak static electric fields applied to the top local electrodes, such methods are highly suitable for addressing qubits individually and thus are promising for the realization of a scalable quantum computing architecture. In particular we propose several semiconductor gated nanodevices which are able to:

- a initialize the electron spin qubit state in a given spin orientation (with [A1] or without application of a magnetic field [A2]),
- b perform a read out of an electron spin (destructive [A1] or nondestructive [A2] without application of a magnetic field [A2]),
- c realize motion induced rotations of HH pseudospin mediated by the DSOI, and the quantum NOT gate,
- d realize an arbitrary sequence of Pauli X, Y, Z and U_S quantum gates [A4] using analogous methods as presented in the proposal from [A3] and which can be arranged in a scalable architecture [A4].

In all the proposed nanodevices a single electron or hole wave packet is confined in a semiconductor quantum well which is sandwiched between two blocking barriers. On top of this heterostructure nanostructured metal electrodes are deposited. The charge density associated with the presence of an electron or hole in the quantum well layer induces a response potential of the electron gas in the metallic gates which in turn leads to the lateral confinement of the charged particle wave function - i.e. the so called self-focusing mechanism [122]. As a result an electron or a hole is self trapped under the metal in form of a stable Gaussian wave packet which has soliton like properties. By applying a small electric field to the top metal gates one can force such a soliton to move. Its trajectory is determined by the geometry of the metal electrodes under which it moves. During the motion the electron or hole soliton maintains its shape. Furthermore, when it collides with an object - a quantum potential barrier - it can reflect or pass through it with 100%

probability and the shape of the wave packet after collision is not affected. While the electron or hole soliton behaves in “an almost” classical way, it possesses a spin which behaves fully quantum mechanically in which quantum information can be encoded.

The proposed nanodevices take also advantage of the SOI. Depending on the used material the Dresselhaus or Bychov-Rashba type of the SOI is employed. The former arises from bulk inversion asymmetry (BIA) and is characteristic for semiconductor compounds with the zinc blende crystal structure. The latter has its origin in structural inversion asymmetry (SIA) and can be induced by an electric field applied in perpendicular direction to the two dimensional electron or hole gas (which causes asymmetry in the quantum well potential profile) or structurally by using semiconductor barrier layers in a heterostructure with different band gaps to obtain asymmetric quantum well potentials. The main effect of the SOI in semiconductor nanostructures is coupling between the spin and the motional degree of freedom of an electron or hole.

In our proposals we exploit this effect in order to realize all-electrically controlled spin filtering devices and hole spin manipulation without a magnetic field. Thus the SOI can be treated as a mediator of electron or hole spin control which is realized by the electric fields.

We make a numerical time dependent simulation of all proposed nanodevices within the self consistent Poisson-Schrödinger formalism and in case of valence holes we apply additionally the four band k·p heavy-hole / light-hole model. Thus the confining potential which is felt by the electron or hole is not modeled by the approximate analytic function but determined by the solution of Poisson equation. We work within the effective mass theory which is, despite its simplicity, suitable for modeling semiconductor nanostructures of quantum dots and wires which confines single charge carriers. We apply a Poisson-Schrödinger self-consistent approach which was previously used [131] in order to model an electrostatic quantum dot which was experimentally realized [132]. The very high quantitative agreement between the theoretical and experimental results provides evidence of its correctness. Thus the presented work may be treated as a link between theoretical proposals and experimental realizations and its main goal is to stimulate experimental progress.

2 Summary of the articles which forms this thesis and conclusions

2.1 Article A1, *Nanodevice for High Precision Readout of Electron Spin*

Many extensive efforts have been made in order to develop and realize methods for an electron spin set up and read out which are two very important ingredients for the physical implementation of spin based quantum computation [75]. Most of the spin initialization techniques proposed and implemented so far in quantum dot structures exploit the application of large external magnetic field, the energy relaxation effect in the two electron quantum dot, optical methods [133, 134, 135, 136, 137], the Pauli spin blockade effect in a double quantum dot [81, 138, 139] and in nanowire quantum dots [90], while electron spin read out (single-shot read-out of an individual electron spin) utilizes mainly the spin to charge conversion method [82, 83, 86].

Within the work [A1] we propose an alternative approach and design gated semiconductor nanodevices which could serve as a single electron spin filter to accumulate single electrons in a given spin orientation in different parts of the nanodevices thus realizing an electron spin qubit initialization. Furthermore, we propose a method for electron spin read out based also on the idea of the spin filter. In both proposed devices the electron is transported within the zinc-blende semiconductor ZnTe quantum well in the $x - z$ plane sandwiched between two barriers stacked along the y axis. The considered semiconductor heterostructure is covered by metal electrodes under which the electron wave function is self focused and forms a stable soliton like wave packet [122].

Since in the considered system the electron is confined in the zinc-blende semiconductor (thus lacking crystal inversion symmetry) in the ZnTe quantum well DSOI is intrinsically present [128]³.

While in Ref. [127] DSOI was utilized to realize single electron spin rotations induced by the electron motion in an analogous manner as in the spin field effect transistor [140, 141], in the current proposal the electron trajectory can depend on its spin orientation thanks to the presence of the DSOI and this fact can be employed further to realize

³We take into account only linear part of the DSOI because the quantum well height $h \approx 10$ nm is a few times smaller than the lateral diameter $d \approx 50$ nm of the induced quantum dot. The cubic Dresselhaus terms are much smaller than the linear ones to be specific they are $(\frac{h}{d})^2$ times smaller.

a spin filtering device. A similar effect of a spin dependent electron trajectory in spin-orbit coupled semiconductors was originally considered and observed within the Spin Hall Effect⁴ which was predicted by M.I. Dyakonov and V.I. Perel in 1971 [143, 144] and observed very recently [145, 146].

In the first step of the filtering process the electron travels initially in the “+z” direction along the path determined by the specially designed electrodes. Due to presence of the DSOI (within the considered system) only electrons with their spin oriented either up \uparrow or down \downarrow ⁵ can move straight while the electrons with other spin orientations ($\alpha \uparrow + \beta \downarrow$ where $\alpha \neq 0, \beta \neq 0$) turn either in the “+x” or “-x” direction and then are intercepted by the appropriate neighbor electrodes. Finally only spin up \uparrow or spin down \downarrow electrons can pass through this part of the nanodevice.

The main purpose of the second step of the filtering process is to spatially separate electrons with spin up orientation from those with spin down and consequently realize electron spin accumulation or read out. We present two nanodevice variants for achieving this goal. The first proposed approach is to place an diluted semimagnetic semiconductor $Zn_{1-x}Mn_xTe$ on the electron trajectory (i.e. an area in which part of the Zn ions are replaced by Mn ions). By applying an external magnetic field in the z direction one can polarize the Mn ions. The semimagnetic area becomes a barrier or a quantum well for an electron depending on its spin orientation. Consequently, a spin up electron can pass through the semimagnetic area (quantum well) while a spin down electron is reflected from it (barrier) analogous as in the proposal presented in Ref. [147]. In this variant, the presented nanodevice can be used to realize electron spin set up or read out. The main disadvantage of this nanodevice is the necessity to apply a magnetic field in order to polarize the Mn ions. Application of an external magnetic field can lead to the persistent precession of all electron spins qubits in the quantum register and thus limits the possibility to address individual electron spin qubits.

The second designed and simulated nanodevice is an alternative proposal which does not need the application of a magnetic field to separate spin down and spin up electrons. In order to distinguish between spin up and spin down electrons after passing the first filtering part of the nanodevice, the electron reflects from a potential barrier which is formed under a 45° cut corner edge of the electrode and starts to move in the “+x”

⁴This term was introduced in 1999 by J. E. Hirsch [142].

⁵The electron spin orientation is defined as an expectation value of the spin operators $\vec{s} = \langle \frac{\hbar}{2} \vec{\sigma} \rangle$ where the $\vec{\sigma}$ is the vector of the Pauli spin matrices. We use a convention where the spin up (down) orientation corresponds to the $s_z = \frac{\hbar}{2}$ ($s_z = -\frac{\hbar}{2}$).

direction. Then due to the presence of the DSOI, electrons with initial spin up (down) state are directed to the channel in the upper (lower) part of the nanodevice. Thus by measuring the presence of the electron either in the lower or upper channel (i.e. by utilizing a quantum point contact (QPC) [148]) one can identify what was the initial value of the electron spin. In this proposal, at the moment of the measurement, the electron spin is no longer in the same state as it was initially, because after reflection in the “+x” direction the electron motion started to induce electron spin rotation around the axis parallel to the direction of the electron motion. The measurement of an electron spin in this proposal has thus a destructive character. Since the electron’s trajectory strongly depends on its initial spin the proposed read out scheme is very precise. The proposed nanodevices can naturally be integrated with the nanodevices capable to realize basic quantum gates on single electron spin qubits as presented in Ref. [127].

2.2 Article A2, *Spin accumulation and spin read out without magnetic field*

A continuation of the research on the design of nanodevices for electron spin qubit read out and set up [A1] is presented in article [A2]. As mentioned in the introduction, all-electrical magnetic free control of electron or hole spins seems to be a very appealing method to address individual qubits in a quantum register without disturbing the state of other qubits, which is essential for realizing a scalable quantum computer architecture. In the original article [126], such an all-electrical control of the electron spin was proposed and appropriate nanodevices were designed and simulated. If one wants to apply such nanodevices for quantum computation purposes, the electron spin initialization as well as the read out have also to be realized without application of a magnetic field. In the article [A2] we propose such devices which are new and improved in comparison to nanodevices from the previous proposal [A1]. They can be naturally integrated with devices from Ref. [126]. One of the currently proposed devices [A2] is capable of the realization of a magnetic free electron spin accumulation for electron spin qubit initialization purposes. The second one is suitable for a nondestructive read out of the electron spin in the sense that it can answer the following question “is the electron in the spin up state?”. The proposed method is unique since, as far as we know, there are no experiments and even theoretical proposals where the single electron spin can be initialized or read out completely without application of a magnetic field in semiconductor quantum dot systems. Which is also very important

and desired is the fact that the read out is realized in a nondestructive manner (i.e. a projective type measurement). Furthermore, electron spin initialization and read out is realized in an ultrafast manner (sub nanosecond) and with very high fidelity reaching 99%.

In order to avoid interaction with non zero nuclear spins of the host material which leads to an electron spin dephasing ⁶ [105, 106, 107, 108] we replace ZnTe by Si which can be prepared in a form with more than 99% from nuclear spin free isotopes (i.e. ²⁸Si). Therefore, the coherence time of the electron spin qubit confined in a Si quantum well is significantly prolonged.

Since we are dealing now with Si as host material (with a cubic diamond crystal structure) Dresselhaus coupling is no longer present in the system. In the current proposal [A2] we employ instead the RSOI. The RSOI interaction couples the spin and charge degree of freedom of an electron in such a way that when the electron moves, its spin is rotated around the axis perpendicular to the direction of motion. Furthermore, in presence of RSOI spin dependent transport can also be realized and the straight motion of an electron along x axis is only possible if its spins is oriented up or down. Such a motion does not affect the electron spin. We use the system of coordinates where the quantum well is placed in the y direction.

The spin preparation process as well as the spin read out realized by the proposed nanodevices is divided into two main steps. In both proposed devices the first step of the accumulation as well as read out process is almost identical as in the previous proposal [A1], but because this time the Rashba SOI is employed, electrons are moving initially along the path in the “+x” direction (not in “+z”) and electrons whose spin was not oriented exactly in “+z” or “-z” direction due to the presence of RSOI are altered either in plus or minus z direction. Thus this part of the nanodevice plays the role of the spin filter where only electrons with spin up or down can be selected and pass through.

In the next step of the spin set up and spin read out process, the spin up and spin down electrons are distinguished and are directed to different parts of the nanodevice. In order to realize electron spin accumulation we use a nanodevice where the electrodes which cover the nanodevice are designed in such a way that after passing the first filtering part the electron reflects from the cut corner electrode, turns by 90° and then starts to move in the “+z” direction. Just after reflection its momentum vector points exactly in the “+z” direction. Then, due to the presence of RSOI, the trajectory of a spin up electron

⁶As a consequence if no special effort is made the electron spin loses its coherence in a ns timescale

is curved to the right (“+x”) while a spin down electron is directed to the left (“-x”). After the reflection, the electron motion starts to induce electron spin rotation. Fortunately, after traveling a distance λ_{SO} the electron spin is restored (a full 2π angle rotation is realized) and the electron trajectory becomes parallel to the “z” axis again while the spin up and spin down electrons are now separated spatially. Then the electron is reflected from the 45° cut corner edge of the electrode. (Thanks to the fact that just before the reflection the electron momentum \vec{p} points exactly in the “+z” direction, it is possible to obtain a smooth 90° reflection.) The electron with spin down orientation reflects in the “-x” direction while a spin up electron is reflected in the “+x” direction. Then both move straight. Since now the electron spin is oriented either up or down it does not precess during its motion (precession around the “z” axis). Thus at the end, an electron with spin up will accumulate in one part of the nanodevice and move in the “+x” direction while an electron with spin down will move in the opposite “-x” direction in another region of the proposed nanostructure. Electrons with such a prepared spin state can be transported to nanodevices that act as quantum gates on single electron spin states [126].

The second nanodevice is capable to measure the spin state of the electron without affecting its spin state after the read out process. The measurement is performed in such a way that the answer to the following question is provided ”is the initial electron spin oriented up?” The measurement is based on the idea of checking the presence of the electron under “a control quantum dot”. The nanodevice acts as follows. After the first step of the filtering process, the electron is reflected. Depending on its spin orientation it will follow two different trajectories. If the electron spin was initially oriented up it travels along a certain path (omitting the region with “the control quantum dot”) and then returns to its initial position. Consequently, there is an absence of the electron in the controlling quantum dot. Thus by measuring the presence or the absence of the electron in the region of the control quantum dot (i.e. by the QPC method) one can indicate what was the initial value of the electron spin. The presence of the electron means that initially the electron spin was oriented down and the answer to the asked question is negative and the electron spin state is destroyed. Such a method does not require application of an external magnetic field. Proposed devices can be naturally integrated with the quantum gates proposed in a recent article [126]. Moreover, the proposed nanodevices are also suitable for acting on the spin state of a single valence hole confined in zinc blende semiconductors in which the DSOI is present. The difference will be in nanodevice size which is determined by the λ_{SO} , and the electrodes’ arrangement which have be rotated by the 90° with respect to

the current orientation.

2.3 Article A3, *Spin-Orbit-Mediated Manipulation of Heavy-Hole Spin Qubits in Gated Semiconductor Nanodevices*

Many experiments [112, 149, 150, 151] have shown that the interaction between a hole spin and nuclear spins of the host material is significantly weaker than for the electron spin, thus making a spin of a valence hole confined in semiconductor nanostructures an attractive candidate for a robust solid state spin qubit, and a promising alternative for the electron spin qubit. However, there are only few theoretical proposals on how to control HH spin qubits [152, 153, 154, 155, 156]. Several experiments exist based mainly on optical methods, in which the hole spin states in quantum dots [157, 158, 159, 160, 161, 162, 163, 164] are controlled. Most of them require the application of a magnetic field. Very recently, all-electric hole spin manipulation in gated semiconductor nanowires has also been demonstrated [165]. Within the work [A3] we present a new and promising method for controlling HH spin qubits in semiconductor nanostructures without application of a magnetic field. In particular we show that the motion of a hole along an induced quantum wire [125] in presence of DSOI can induce coherent rotations of the HH spin (more precisely of the pseudo spin $1/2$) state. We further exploit this observation to realize an all electrical-control scheme for the HH spin qubit. The motion of the hole along a certain direction is equivalent to the application of an effective magnetic field which cause the heavy-hole spin to rotate in a coherent manner. This method seems to be more suitable for the coherent manipulation of a HH spin than the application of a real magnetic field which, due to the small hole in plane g factor, has to be very high (several Teslas) in order to rotate the hole spin. The application of such a high external magnetic field is possible but still very challenging in experiments. The proposed all-electrical HH spin control circumvents this problem. We make calculations within the k-p HH-LH multiband model and show that in the investigated systems the hole occupies mostly the HH band which is caused due to the strong confinement in the quantum well growth direction. This is an important result which allows to encode the qubit in HH spin basis states. As suggested, only in systems with negligible HH/LH band mixing the coherence of a hole spin state is significantly (about ten times) prolonged compared to the electron spin coherence time [114, 115, 116, 117, 118, 119, 120]. By analyzing HH spin rotations in the investigated

system, we numerically estimate the λ_{SO} ⁷ parameter for different materials: GaAs, CdTe, ZnTe. Moreover the form of rotation operators which act on a HH spin while the hole is moving are provided.

Based on these results we put forward a proposal of a GaAs nanodevice which can realize a quantum NOT gate on a HH spin qubit. In order to realize this operation, the hole is transported around a closed rectangular loop which is determined by the geometry of specially designed top metal electrodes. During the realization of the proposed gate, the hole passes each segment of the loop and an appropriate set of π and $\pi/2$ rotations is made. Finally, the quantum NOT logic operation is performed. Since the hole is transported to the initial position, the required quantum operation is performed exclusively on its spin state. The quantum NOT logic operation is realized within sub nanoseconds ($\tau_{OP}^{GaAs} \sim 250$ picoseconds). If the hole spin coherence time reaches $T_2 = 100$ picoseconds, as suggested by the experiment [112] it is potentially possible to reach the threshold for application of quantum error correction codes (defined by the ratio of coherence time and gate operation $\frac{\tau_{coh}}{\tau_{op}}$), which typically varies between 10^{-5} and 10^{-3} [15, 16, 17, 18, 19].

2.4 Article A4, *All-electrical control of quantum gates for single heavy-hole spin qubits*

The all-electrical concept of manipulating the spin states of a hole via controlling its motion introduced in previous article [A3] is extended in the current proposal [A4].

The design of a set of nanodevices which can realize basic quantum logic gates on a single HH spin qubit is put forward [A4]. In particular, we propose nanodevices which can realize Pauli X, Y and Z gates suitable for the realization of π angle rotations of a HH spin qubit around the x, y, and z axis, respectively. We also design a nanodevice which can realize an operation which we call the U_S gate: $\pi/2$ angle rotation of the HH spin and at the same time the operation is capable to create (or destroy) a balanced superposition of the basis states of the qubit. Moreover we design a nanodevice covered by a system of metal gates which can realize an arbitrary sequence of all previously proposed quantum logic gates. Each quantum gate is realized by transporting the hole along a special trajectory - a closed rectangular loop - determined by the shape of the surface electrodes. During the motion along the loop a certain sequence of π and $\pi/2$ HH spin rotations are performed, which results in the realization of the desired quantum gate. Motion of the hole along

⁷Distance which has to be traveled by the hole in order to realize full 2π HH spin rotation.

certain directions induces HH spin rotations and special operators can be associated with this process which were introduced in [A3]. The topology of the metal gates is deduced from the form of these operators.

Since the proposed all-electric HH spin control method allows for addressing individual qubits we also show how such a device can be arranged in a quantum register to form a scalable architecture for quantum computation applications.

The presented nanodevices in [A4] are now based on CdTe, while the proposals in [A3] were based on GaAs. This allows to obtain smaller and faster devices as well as potentially longer coherence times of the hole spin confined in it. Furthermore, the proposed gates are characterized by a very high fidelity reaching 99%.

3 Nanodevice for High Precision Readout of Electron Spin

Nanodevice for High Precision Readout of Electron Spin

P. SZUMNIAK, S. BEDNAREK, B. SZAFRAN AND P. GRYNKIEWICZ

Faculty of Physics and Applied Computer Science, AGH University of Science and Technology
al. Mickiewicza 30, 30-059 Kraków, Poland

In this paper we propose and simulate operation of a nanodevice, which enables the electron spin accumulation and very precise read-out of its final value. We exploit the dependence of the electron trajectory on its spin state due to the spin-orbit coupling in order to distinguish between different spin orientations.

PACS: 73.21.La, 73.63.Nm, 03.67.Lx, 05.45.Yv

1. Introduction

The essential components of a quantum computer are quantum bits (qubits) and an appropriate set of quantum gates. The spin state of electron confined in a semiconductor heterostructure is well suited for physical realization of a quantum bit [1, 2]. There has been widespread search for nanodevices, which could perform logical operations on such states [3–5]. So far the majority of proposed solutions for achieving transitions between different spin states require the application of external microwaves. It is the simplest method of processing information stored in an isolated qubit, but applying it to perform selective operations on single qubit, being part of a many-qubit register is not possible. In order to overcome this problem, we recently proposed the realization of one-qubit logical gates, without the usage of microwaves [6, 7].

The main idea of our method is to obtain the spin rotation by the spin-orbit coupling during electron's motion in closed trajectories, which are determined by the metal electrodes deposited on top of a semiconductor heterostructure. The operations are triggered by applying low voltages to the gates. We have simulated operation of the basic one-qubit quantum gates: negation, Hadamard and phase shift [6, 7]. Two of the problems that remain to be solved are: setting electron's spin in the desired orientation before the logical operation and precise read-out of the quantum computation results.

In this paper we put forward the design of a nanodevice which could serve as an electron spin filter to accumulate electrons in a given spin state in order to set the initial value of qubit and its read-out after quantum computation.

2. Experimental

The proposed nanodevice is based on the planar heterostructure described in the previous paper [6]. Its vertical cross-section is depicted in Fig. 1. The nanostruc-

ture consists of a quantum well 10 nm high sandwiched between two tunnel barriers of the same height. The quantum well is separated from strongly doped substrate by 50 nm thick dopant-free buffer. Metal electrodes are deposited on top of the upper barrier. If one places, in the quantum well, an electron forming a charge cloud, it will induce an opposite charge on the surface of the conductor above. The induced charge attracts the electron and the electric field has a component directed to the center of the cloud. The self-focusing effect of the wave function occurs [8]. As the result the electron is trapped beneath the metal electrode forming a stable wave packet, which exhibits finite spatial extent and conserves its shape as it travels along the path determined by the electrode [9]. Such wave packet shows features unique for a quantum particle to have, as it reflects from a potential barrier or tunnels through it with probability of 1 like a classical object. This fact makes it possible to transfer the electron between different sites of the nanodevice in a controllable manner.

3. Model

Despite its classical behavior the electron time evolution is described in the framework of quantum mechanics using time-dependent Schrödinger equation. We also describe electron spin quantum mechanically. The electron is set in motion by voltages applied to the electrodes. We choose the coordinates x and z in the quantum well plane and y pointed in the direction of layer growth. The motion in the y direction is forbidden due to trapping in the quantum well. In the description of the motion in the (x, z) plane we use the following Hamiltonian:

$$H(x, z, t) = -\frac{\hbar^2}{2m} \left(\frac{\partial^2}{\partial x^2} + \frac{\partial^2}{\partial z^2} \right) - e\varphi(x, y_0, z, t) + H_D, \quad (1)$$

where y_0 denotes the center of the quantum well, $\varphi(\mathbf{r}, t)$ is the electrostatic potential being the result of solving the

Poisson equation in a box containing entire nanodevice using methods described in our previous papers [5, 8]. The method we use in computation enables us to determine the electron time evolution with the self-focusing effect during its motion. The last term in (1) denotes the Dresselhaus spin-orbit coupling in the quantum well and has the following form:

$$H_D = \frac{\hbar k_{so}}{m} (p_x \sigma_x - p_z \sigma_z), \quad (2)$$

where σ_x and σ_z are the Pauli matrices and k_{so} is the characteristic wave vector dependent on the quantum well width, effective electron mass m and the coupling constant in bulk γ :

$$k_{so} = \frac{m}{\hbar} \left(\frac{\pi}{d} \right)^2 \gamma.$$

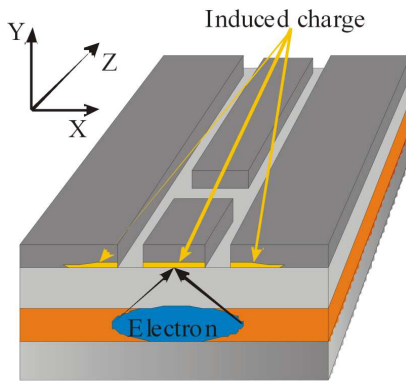


Fig. 1. The layout of the considered nanostructure with electrodes deposited on its surface, wave packet and the induced charge on the lower surface of the electrode.

We denote the wave function as a column matrix

$$\Psi(x, z, t) = \begin{pmatrix} \psi_1(x, z, t) \\ \psi_2(x, z, t) \end{pmatrix}. \quad (3)$$

The simulation described in this paper are the solutions of the time-dependent Schrödinger equation with Hamiltonian (1):

$$\Psi(t + dt) = \Psi(t - dt) - \frac{2i}{\hbar} H(t) \Psi(t) dt. \quad (4)$$

As the electron charge distribution varies in time, the electrostatic potential $\varphi(\mathbf{r}, t)$ has to be computed at each time step. This leads to the time dependence of Hamiltonian (1) introduced in (4). In all simulations the initial wave function is the solution of the time-independent Schrödinger equation:

$$H(x, z, 0) \Psi(x, z, 0) = E \Psi(x, z, 0) \quad (5)$$

with potential distribution valid for electron confined beneath particular metal electrode. In our computation we use the material parameters of ZnTe in which the Dresselhaus coupling constant is $\gamma = 13.3 \text{ eV \AA}^3$, the effective

mass $m = 0.2m_e$ and the dielectric constant $\epsilon = 7.4$. Due to large effective mass and small dielectric constant, the self-focusing effect is relatively strong in this material. During electron motion along a straight line the Dresselhaus coupling results in the electron spin rotation around the axis parallel to the movement direction. If it is not forced to move along a straight line, electron trajectory is spin-dependent.

4. Results and discussion

Figure 2 depicts trajectories of electrons with different initial spin orientation. The simulation was carried out with the initial wave function obtained for electron trapped beneath the e_1 electrode. After starting the iteration of time-dependent Schrödinger equation, the voltage on e_2 is increased by 0.1 mV, resulting in electron gaining velocity in the z direction. Only the electrons with their spin parallel or anti-parallel to the z axis move along the straight line. In any other case the trajectory drifts in the x direction. Such perturbation of the motion can be used to filter out electrons in undesired spin states.

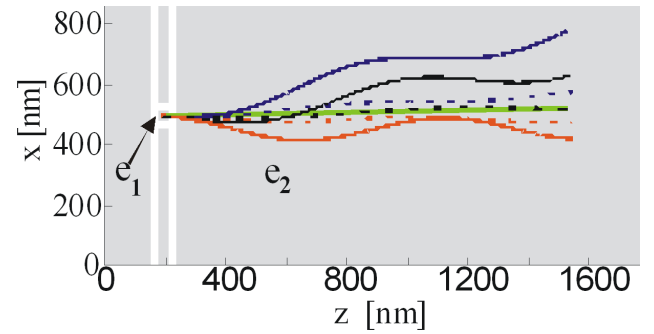


Fig. 2. Trajectories of electrons with diverse initial spin orientation. Continuous lines: blue, red and black for electrons with spin parallel to the axis: x , y and xy (bisector of the angle between x and y axis). Dashed lines for electrons in spin states composed of 90% of state parallel to the z axis and 10% of state parallel to axis x , y or xy . The straight yellow line stands for electrons with spin precisely parallel or anti-parallel to the z axis (direction of motion).

We put forward the device able to perform such an operation depicted in Fig. 3. Single electron is initially confined beneath e_1 electrode. After lowering the voltages on e_1 and e_2 the particle is forced to move along e_3 . The width of e_3 and the distances between e_3 and the neighboring electrodes are chosen in such a way that the electron cloud centered beneath e_3 extends under e_4 and e_5 . Then, the slightest lateral perturbation of electron trajectory causes electron to be intercepted by either e_4 or e_5 . Only the electrons with spin parallel or anti-parallel to the z axis are capable of traveling along the entire track beneath e_6 . One last step of the process remaining is telling between spin up and spin down states.

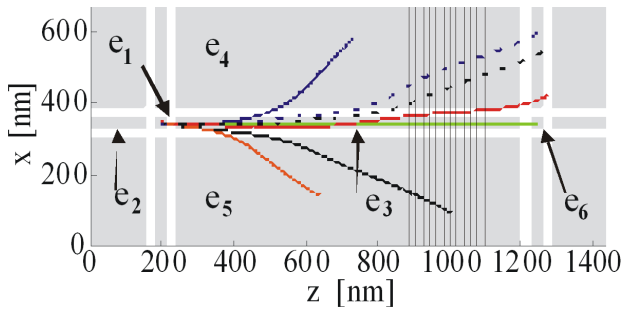


Fig. 3. The layout of electrodes in a nanodevice filtering-out electrons in spin state having any x or y component. The trajectories of electrons with different spins are marked as in Fig. 2. The area marked with vertical lines contains the semimagnetic semiconductor and is used to distinguish between spin parallel to z axis from anti-parallel one.

We propose two possible structures for reaching this goal. First one is based on placing the e_3 electrode above the quantum well containing semimagnetic semiconductor (an area in which part of Zn ions is replaced by Mn ions). If the spins of Mn ions are polarized by the external magnetic field applied parallel to the z axis, this area is a barrier for electrons with spin anti-parallel to Mn ion spins.

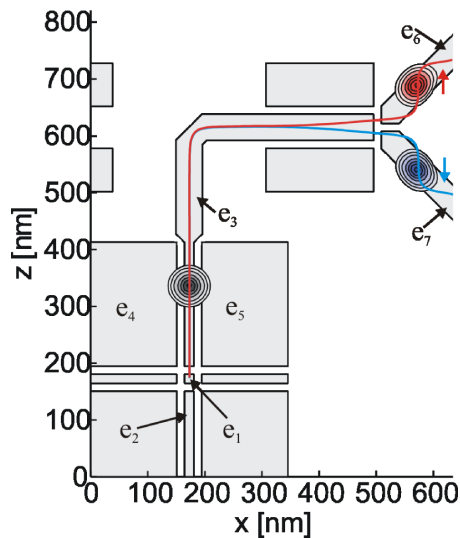


Fig. 4. The nanodevice in which the initial electron spin orientation is measured without applying external magnetic field.

Electrons with spin precisely parallel to Mn ion spins, encounter and cross only a shallow potential cavity, and are the only ones that could reach the e_6 electrode. Presented nanodevice can serve to spin accumulation or to spin readout. Unfortunately, in order to polarize Mn

ions one has to apply external magnetic field, which is a certain disadvantage, because it leads to persistent spin precession around the direction of the magnetic field.

In alternative structure one manages to measure spin orientation without the necessity of applying external magnetic field. The geometry of this nanodevice and electron trajectories are depicted in Fig. 4. In order to distinguish between spin up and spin down states, we change the direction of electron motion by 90° forcing it to run in direction of the x axis. The spin-orbit interaction directs the electron in spin-up (spin down) state under e_6 (e_7) electrode. This nanodevice is able to perform spin read-out. Its main flaw is the destruction of the initial spin state caused by the measurement.

5. Conclusion

We put forward and simulated the operating of two alternate nanodevices based on the induced quantum dots and wires, which could be used both to spin accumulation and to perform spin read-out.

Acknowledgments

This work was supported by the grant No. N N202 128337 from the Ministry of Science and Higher Education, as well as by the “Kraków Interdisciplinary PhD-Project in Nanoscience and Advances Nanostructures” operated within Foundation for Polish Science MPD Programme co-financed by European Regional Development Fund.

References

- [1] D. Loss, D.P. DiVincenzo, *Phys. Rev. A* **57**, 120 (1998).
- [2] R. Hanson, L.P. Kouwenhoven, J.R. Petta, S. Tarucha, L.M.K. Vandersypen, *Rev. Mod. Phys.* **79**, 1217 (2007).
- [3] J.R. Petta, A.C. Johnson, J.M. Taylor, E.A. Laird, A. Yacoby, M.D. Lukin, C.M. Marcus, M.P. Hanson, A.C. Gossard, *Science* **309**, 2180 (2005).
- [4] J.M. Elzermann, R. Hanson, L.H.W. van Beveren, B. Witkamp, L.M.K. Vandersypen, L.P. Kouwenhoven, *Nature* **430**, 431 (2004).
- [5] K.C. Nowack, F.H.L. Koppens, Yu.V. Nazarov, L.M.K. Vandersypen, *Science* **318**, 1430 (2007).
- [6] S. Bednarek, B. Szafran, *Phys. Rev. Lett.* **101**, 216805 (2008).
- [7] S. Bednarek, B. Szafran, *Nanotechnology* **20**, 065402 (2009).
- [8] S. Bednarek, B. Szafran, K. Lis, *Phys. Rev. B* **72**, 075319 (2005).
- [9] S. Bednarek, B. Szafran, R.J. Dudek, K. Lis, *Phys. Rev. Lett.* **100**, 126805 (2008).

4 Spin accumulation and spin read out without magnetic field

Spin accumulation and spin read out without magnetic field

S. Bednarek, P. Szumniak, and B. Szafran

Faculty of Physics and Applied Computer Science, AGH University of Science and Technology, al. Mickiewicza 30, 30-059 Kraków, Poland

(Received 21 October 2010; published 16 December 2010)

An idea for construction of two spintronic single-electron nanodevices is presented and supported by a quantum-mechanical simulation of their operation. The first device selects electrons of a given spin orientation and the other performs the spin read out. The operation of proposed devices exploits the spin-dependent deflection of electron trajectories induced by the spin-orbit Rashba coupling and does not require application of an external magnetic field. The operation of the nanodevice requires application of weak voltages applied to the electrodes only.

DOI: [10.1103/PhysRevB.82.235319](https://doi.org/10.1103/PhysRevB.82.235319)

PACS number(s): 73.63.Nm, 72.25.-b, 03.67.Lx

I. INTRODUCTION

Many extensive efforts have been conducted for fabrication of a quantum computer based on the semiconductor nanostructures. The quantum bit of information is supposed to be stored in the electron spin confined in a quantum dot.¹⁻³ Electrostatic quantum dots⁴⁻⁸ are considered particularly promising for quantum logic processing including the storage of single separate electrons and operations on their spins. In most of the devices constructed so far the modification of the electron spin state is induced by absorption of microwave radiation in high magnetic field that energetically separates the spin-up and spin-down states. This is the most direct method for rotation of a single-electron spin. However, the microwave radiation is not suitable for addressing a single spin in a register of several qubits contained within the same nanostructure. The use of the external microwave radiation was avoided in a device of Ref. 8 in which the spin rotation is accomplished due to the spin-orbit (SO) coupling. This device⁸ still requires application of an external magnetic field, which induces a continuous precession of spins of all the confined electrons. The inhomogeneities of this field result in dephasing of the precession of separate spins. A device that could operate without an external magnetic field would be free of this source of decoherence. Recently, we proposed a couple of devices rotating the electron spins without the external magnetic field.^{9,10} We introduced an idea and simulated the operation of nanodevices that perform the single-qubit Haddamard, negation and phase change quantum gate operations. The nanodevices exploit the self-focusing of electron wave function due to interaction with the electron gas of the electrodes.¹¹ The interaction allows for formation of a stable electron wave packet that can be put in motion by low voltages applied to the electrodes. The motion of the electron along any desired trajectory combined with the spin-orbit coupling allows for arbitrary spin rotations. In this work we present an idea for construction of spin filters that do without the external magnetic field. A first variant of the nanodevice can be used for selection of an electron of a desired spin orientation for the purpose of the initial state set up. The second variant is suitable for the spin read out on the final state.

II. DEVICE AND NUMERICAL METHOD

The proposed device is based on a planar heterostructure similar to the one previously used in Ref. 9 with a schematic cross section given in Fig. 1. The nanostructure contains a quantum well 10 nm wide sandwiched between two barriers each of 10 nm width. The quantum well is separated from the substrate by a 50 nm thick undoped layer. On top of the upper blocking layer the metal electrodes are deposited. Electron confined in the quantum well forms a charge “cloud” distribution that induces an appearance of positive charge on the lower surface of the metal electrodes. The electric field stemming from the positive induced charge possesses an in-plane component directed to the center of the electron charge distribution. The wave function of the electron that is formed in this way becomes a stable packet that can move within the quantum well with a constant shape. When the self-focusing effect is strong enough (the quantum well is close to the electrodes and the dielectric constant is not too large) the scattering properties of the wave packet become classical, i.e., the electron backscatters or transfers through a potential defect with a 0% or 100% probability.¹¹ The electron with classical scattering properties is still described by the time-dependent Schrödinger equation. The electron spin is also described in a standard way as two-row

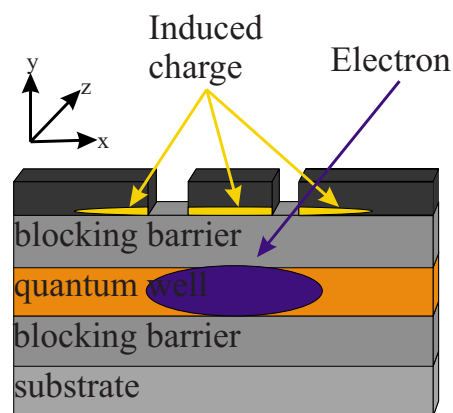


FIG. 1. (Color online) Schematics of the considered nanodevice with electrodes deposited on top, the electron wave packet, and the charge induced on the lower surface of the electrode.

single-column vectors. We choose the system of coordinates in which the y axis is oriented parallel to the growth direction. The electron motion in this direction is frozen. The electron is free to move in the x and z directions within the quantum well. Its wave function

$$\Psi(x, z, t) = \begin{pmatrix} \Psi_1(x, z, t) \\ \Psi_2(x, z, t) \end{pmatrix} \quad (1)$$

depends on two spatial coordinates and time. The time dependence is described by the Schrödinger equation

$$\Psi(x, z, t + dt) = \Psi(x, z, t - dt) - \frac{2i}{\hbar} \hat{H} \Psi(x, z, t) dt \quad (2)$$

with Hamiltonian

$$\hat{H}(x, z, t) = -\frac{\hbar^2}{2m} \left(\frac{\partial^2}{\partial x^2} + \frac{\partial^2}{\partial z^2} \right) - e\phi(x, y_0, z, t) + H_R, \quad (3)$$

where y_0 is the center of the quantum well and $\phi(x, y_0, z, t)$ is the electrostatic potential due to the electrodes and the charges induced on them. The potential is found by solution of the Poisson equation in a three-dimensional box that contains the entire nanodevice. The Poisson equation needs to be solved in every time step due to the motion of the wave packet. The description of the method is given in Refs. 9 and 12. The Poisson equation gives the classical potential distribution. Quantum calculations¹³ indicate that this is a good approximation of the actual response potential of the electron gas. The applied approach allows correctly describes the self-focusing mechanism and allows for investigation of the motion of the electron packet. The last term of Hamiltonian (3) accounts for the Rashba spin-orbit interaction¹⁴

$$H_R = \alpha(p_z \sigma_x - p_x \sigma_z), \quad (4)$$

where p 's are the momentum operators and σ 's are the Pauli matrices. In the initial moment of each simulation the wave function was assumed as a solution to the time-independent Schrödinger equation with the electron cloud distribution corresponding to the bound state confined under one of the electrodes,

$$H(x, z, 0)\Psi(x, z, 0) = E\Psi(x, z, 0). \quad (5)$$

In the calculations we adopted Si material parameters with $m=0.19m_0$, the dielectric constant $\epsilon=13$, and the Rashba coupling constant $\alpha=7.2 \times 10^{-13}$ eV m.

III. RESULTS AND DISCUSSION

The trajectory of an electron that is put in motion within a quantum well, in which the Rashba coupling is present, depends on the direction of its spin. The results of the simulation for various initial states of the spin are given in Fig. 2. For the initial condition we took the ground state of the electron confined in an induced quantum dot under electrode e_1 . The simulation is started by raising the potential of e_2 electrode by 0.1 mV, which extracts the electron from under electrode e_1 to under electrode e_2 . The electron acquires an initial velocity that is parallel to the x axis. The electron

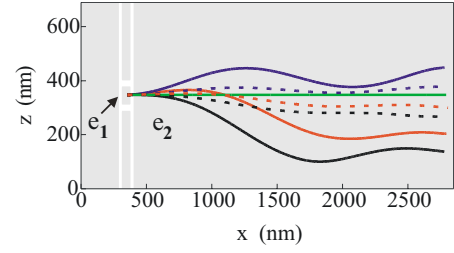


FIG. 2. (Color online) Electron trajectories for opposite orientations of the spin. The solid lines—black, dark gray (blue online), and light gray (red online) correspond to the spin orientation parallel to x , y , and xy (a bisector of the angle formed by x and y axes). The dotted lines correspond to spin state containing a 95% of the spin parallel to the z axis and 5% of the state parallel to the x , y , and xy axes. The straight green line shows the electron trajectory for the initial spin orientation parallel or antiparallel to the z axis.

whose spin is parallel or antiparallel to the z axis moves along a straight line that is parallel to the x axis. This trajectory is marked in Fig. 2 by the light gray straight line (green online). The Rashba coupling induces rotation of the electron spin moving along the x axis around the z axis, hence for both considered spin orientations they remain unchanged as the electron moves. However, when the electron wave function contains a contribution of any other spin component the electron trajectory is no longer a straight line. This effect can be used to filter out the electrons with spins that are not parallel to the z axis. This operation can be performed using the nanodevice presented in Fig. 3. The electron is initially confined under electrode e_1 in the lowest energy state for a given spin orientation. Then, the voltage on electrodes e_1 and e_2 is lowered by 0.1 mV and we start the iteration of Eq. (2). The electron is ejected under electrode e_3 and acquires a velocity parallel to the x axis. The width of e_3 electrode and the distance to the lateral electrodes e_4 and e_5 is adjusted in a way that the center of the packet is localized under electrode e_3 and the tails of the packet reach the lateral e_4 and e_5 electrodes. On electrodes e_4 and e_5 we put a voltage 0.1 mV higher than the one applied to the e_3 . Hence the straight motion is only weakly stabilized and any deviation of the electron direction leads to its extraction to one of the lateral electrodes. In consequence only electrons with spin parallel or antiparallel to the z axis cross the entire length of the e_3 electrode. Even a small admixture of the spin that is neither parallel not antiparallel to the z axis leads to the electron escape to the area below the lateral electrodes (e_4, e_5).

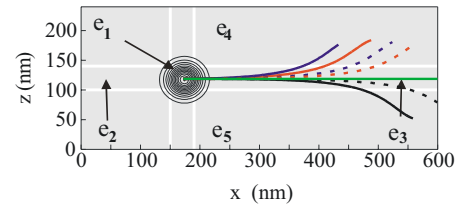


FIG. 3. (Color online) The system of electrodes in the nanodevice that filters out the electrons with spin that is not parallel to the z axis. Electron trajectories of various initial spin orientations are marked as in Fig. 2.

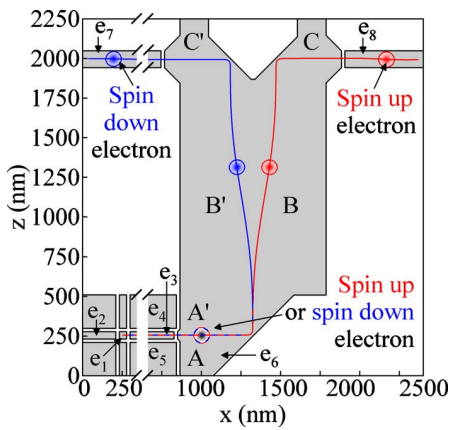


FIG. 4. (Color online) Nanodevice for the spin accumulation. The system of electrodes (gray color) and electron trajectories of spin up (down) marked in gray (red online) [dark gray (blue on-line)]. The trajectory is defined by mean positions of the electron packet.

We use the idea of the spin filter of Fig. 3 for a larger nanodevice dedicated to spin accumulation (see Fig. 4). The spin filter is placed at the lower left corner of the plot. Only the electrons of spins parallel or antiparallel to the z axis pass through this filter and get to the area below the large electrode e_6 . The proposed device separates the electrons with the spin oriented up from the spin-down electrons. The electron trajectory turns by 90° upon reflection on a 45° cut of the e_6 electrode for $x \approx 1300$ nm. After the electrons trajectory is changed, the spin-up and spin-down electrons follow different trajectories: the spin-down electron is deflected to the left (blue curve in Fig. 4) and the spin-up electron to the right (red curve in Fig. 4). Figures 5(a) and 5(b) shows the time dependence of the mean values of the electron positions $x(t)=\langle x \rangle$, $z(t)=\langle z \rangle$ (solid lines), and the mean value of the spin components $s_{x,y,z}(t)=\langle s_{x,y,z} \rangle$ (dashed lines) for the spin oriented initially “up” and “down,” respectively. The $z(t)$ is the same for both initial spin orientations, the $x(t)$ curves overlap only at the first part of the trajectory when the electron moves ideally parallel to the x axis. The electron spin undergoes precession when it follows a curved trajectory. Thus one needs to allow the electron to cross a distance equal to SO length (for the applied material parameters $\lambda_{SO}=1750$ nm) after which the initial electron spin orientation is restored and the trajectory becomes parallel to the z axis again (see Figs. 4 and 5). Then, the electron is reflected for the second time from a properly cut top edge of the e_6 electrode. It starts to move parallel to the x axis and the spin precession is terminated. The electrons with spin oriented initially up (down) get under electrode e_8 (e_7). The electrons can be stored therein or taken away to other locations within the nanodevice.

Figure 6 contains a schematic drawing of a nanodevice which is supposed to read the electron spin after completion of a quantum computation. Since the quantum algorithms account for limitations set for a possible measurement outcome due to the quantum nature of the system, our device is designed to answer the question: “is the electron spin oriented up?” The measurement is of a projective type, which

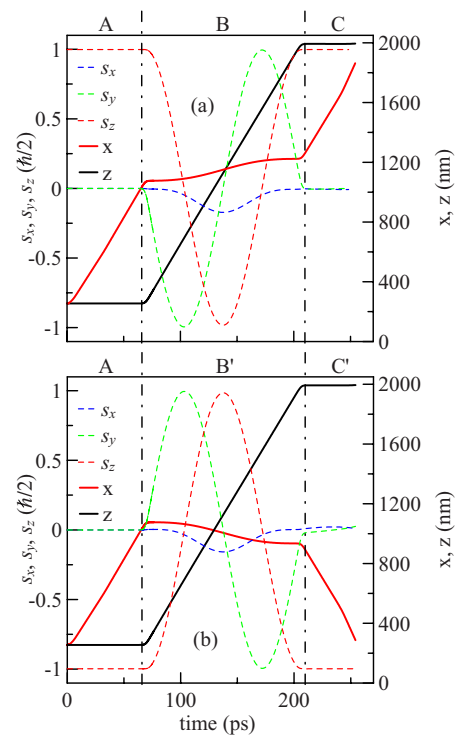


FIG. 5. (Color online) Average position and spin components of the electron following the trajectories depicted in Fig. 4. Solid lines shows the mean values of the position of the electron packet in z direction (black) and in x direction [gray (red online)], dashed lines shows the average components of the spin (a) for the electron spin oriented initially up and (b) for initial spin down.

means that in case of positive answer the spin state is unaffected. Otherwise the state may be changed.

The electron whose spin state we want to test is localized under electrode e_1 (Fig. 6). We lower the voltage applied to electrode e_2 , the electron is ejected out under electrode e_3 and moves beneath in the z direction till it reaches the ample

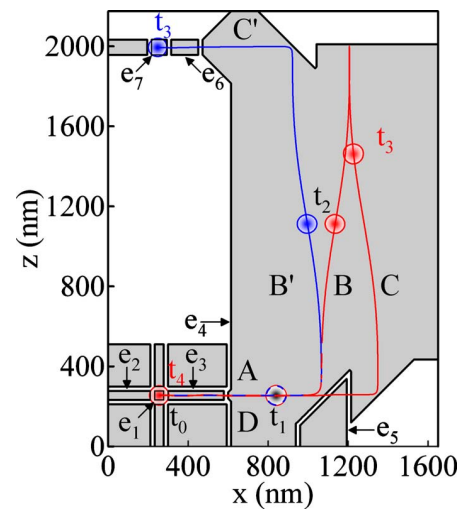


FIG. 6. (Color online) Nanodevice for the spin read out and trajectories of electrons with spins initially oriented up [gray (red online) curve] and down [dark gray (blue online)].

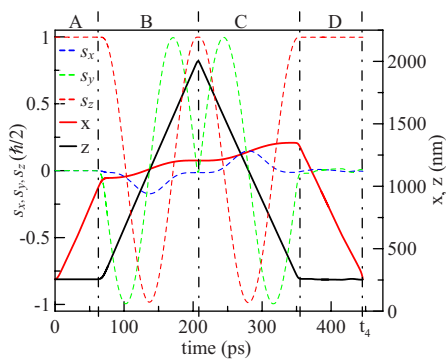


FIG. 7. (Color online) Same as Fig. 5(a) for the spin-up electron following the red trajectory in the spin read out device of Fig. 6.

electrode e_4 , where the direction of its motion is changed by 90° , this time by reflection off the edge of electrode e_5 set at 45° angle, to which a (repulsive) voltage is applied by 1.5 mV lower than the one applied to e_4 . After the direction of electron motion is changed to z , the electron trajectory is no longer a straight line. If the electron spin was initially parallel to the z axis (oriented up) it chooses the trajectory that turns right and is marked in Fig. 6 by the red color. For this specific case in Fig. 7 we plotted the mean values of position and spin components in function of time. As long as the electron moves parallel to the x axis the spin is constant $s_z = \hbar/2$, $s_x = s_y = 0$. After the direction of motion is changed the spin starts to precess: s_z is changed and nonzero s_x , s_y components appear. After passing a distance of λ_{SO} in the z direction s_z component returns to its initial value and the others components vanish. The device is designed in such a way that at this very moment the electron hits the top edge of the electrode that is in this place perpendicular to the electron velocity. Upon reflection the electron does not follow the precedent trajectory when moving in the $-z$ direction but is deflected to the left. After passing a distance of λ_{SO} in the $-z$ direction the electron is reflected from the edge of e_4 electrode and change its direction to $-x$. The electron goes under electrode e_5 whose voltage was in the meantime set equal to the voltage of e_4 electrode, hence the region under e_5 is transparent for the electron motion. The electron is finally recaptured under e_1 electrode. On its way back the electron spin rotates by a full angle, its initial state is restored and the spin can be recycled for the quantum computation. For the electron spin oriented initially antiparallel to the z axis, the electron after reflection by the e_5 electrode is deflected to the left (see the blue trajectory in Fig. 6). After passing the λ_{SO} distance in the z direction the electron is reflected by the edge of e_4 electrode and starts to move in the $-x$ direction. Eventually, the electron gets beneath electrode e_6 and it is taken away to under electrode e_7 where it is

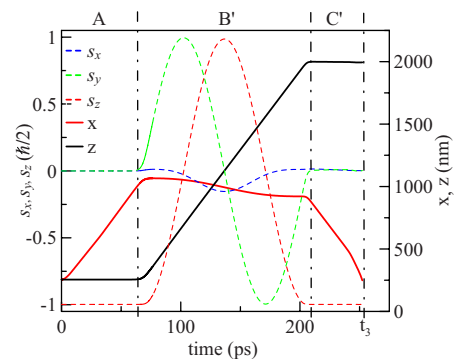


FIG. 8. (Color online) Same as Fig. 5(b) for the spin-down electron following the blue trajectory in the spin read out device of Fig. 6.

trapped. The presence of the electron under e_7 electrode can be verified by any method, including the ones that destroy its spin, since the mere presence of the electron in this location implies a negative answer for the question that was asked. The mean values of position and spin components in function of time are plotted in Fig. 8. In Fig. 6 on the electron trajectories we marked the electron positions in subsequent moments in time $t_0 - t_4$. The duration of the entire cycle is 0.43 ns, which is lower enough than the decoherence time in Si.¹⁵

IV. SUMMARY AND CONCLUSIONS

We have proposed and simulated operation of two nanodevices. One of them can be used to extract from the electron gas single electrons of a well-defined spin state or to spin accumulation, i.e., storage of electrons of opposite spin orientations in two separate regions of the nanodevice. The second device serves for the spin read out. It performs a projective measurement which for a positive answer leaves the spin in the identified state. The spin read out has the “interaction free measurement” character since the electron whose state could be perturbed implies a negative answer to the question asked. The nanodevices work without the external magnetic field. Its operation is controlled by low dc voltages applied to gates.

ACKNOWLEDGMENTS

This work was supported by the Grant No. N N202 12837 from the Ministry of Science and Higher Education, as well as by the “Krakow Interdisciplinary Ph.D.-Project in Nanoscience and Advances Nanostructures” operated within Foundation for Polish Science MPD Programme cofinanced by European Regional Development Fund.

- ¹D. Loss and D. P. DiVincenzo, *Phys. Rev. A* **57**, 120 (1998).
- ²D. Awschalom, D. Loss, and N. Samarth, *Semiconductor Spintronics and Quantum Computation* (Springer-Verlag, Berlin, 2002).
- ³R. Hanson, L. P. Kouwenhoven, J. R. Petta, S. Tarucha, and L. M. Vandersypen, *Rev. Mod. Phys.* **79**, 1217 (2007).
- ⁴J. R. Petta, A. C. Johnson, J. M. Taylor, E. A. Laird, A. Yacoby, M. D. Lukin, C. M. Marcus, M. P. Hanson, and A. C. Gossard, *Science* **309**, 2180 (2005).
- ⁵J. M. Elzerman, R. Hanson, L. H. Willems van Beveren, B. Witkamp, L. M. K. Vandersypen, and L. P. Kouwenhoven, *Nature (London)* **430**, 431 (2004).
- ⁶T. Meunier, I. T. Vink, L. H. Willems van Beveren, F. H. L. Koppens, H. P. Tranitz, W. Wegscheider, L. P. Kouwenhoven, and L. M. K. Vandersypen, *Phys. Rev. B* **74**, 195303 (2006).
- ⁷F. H. L. Koppens, C. Buizert, K. J. Tielrooij, I. T. Vink, K. C. Nowack, T. Meunier, L. P. Kouwenhoven, and L. M. K. Vandersypen, *Nature (London)* **442**, 766 (2006).
- ⁸K. C. Nowack, F. H. L. Koppens, Yu. V. Nazarov, and L. M. K. Vandersypen, *Science* **318**, 1430 (2007).
- ⁹S. Bednarek and B. Szafran, *Phys. Rev. Lett.* **101**, 216805 (2008).
- ¹⁰S. Bednarek and B. Szafran, *Nanotechnology* **20**, 065402 (2009).
- ¹¹S. Bednarek, B. Szafran, and K. Lis, *Phys. Rev. B* **72**, 075319 (2005).
- ¹²S. Bednarek, B. Szafran, R. J. Dudek, and K. Lis, *Phys. Rev. Lett.* **100**, 126805 (2008).
- ¹³S. Bednarek and B. Szafran, *Phys. Rev. B* **73**, 155318 (2006).
- ¹⁴E. I. Rashba, *Sov. Phys. Solid State* **2**, 1109 (1960); Y. Bychkov and E. I. Rashba, *J. Phys. C* **17**, 6039 (1984).
- ¹⁵J. P. Gordon and K. D. Bowers, *Phys. Rev. Lett.* **1**, 368 (1958).

5 Spin-Orbit-Mediated Manipulation of Heavy-Hole Spin Qubits in Gated Semiconductor Nanodevices

Spin-Orbit-Mediated Manipulation of Heavy-Hole Spin Qubits in Gated Semiconductor Nanodevices

P. Szumniak,^{1,2} S. Bednarek,¹ B. Partoens,² and F. M. Peeters²

¹*Faculty of Physics and Applied Computer Science, AGH University of Science and Technology, al. Mickiewicza 30, 30-059 Kraków, Poland*

²*Departement Fysica, Universiteit Antwerpen, Groenenborgerlaan 171, B-2020 Antwerpen, Belgium*
(Received 10 February 2012; published 4 September 2012)

A novel spintronic nanodevice is proposed that is able to manipulate the single heavy-hole spin state in a coherent manner. It can act as a single quantum logic gate. The heavy-hole spin transformations are realized by transporting the hole around closed loops defined by metal gates deposited on top of the nanodevice. The device exploits Dresselhaus spin-orbit interaction, which translates the spatial motion of the hole into a rotation of the spin. The proposed quantum gate operates on subnanosecond time scales and requires only the application of a weak static voltage which allows for addressing heavy-hole spin qubits individually. Our results are supported by quantum mechanical time-dependent calculations within the four-band Luttinger-Kohn model.

DOI: [10.1103/PhysRevLett.109.107201](https://doi.org/10.1103/PhysRevLett.109.107201)

PACS numbers: 75.76.+j, 03.67.Lx, 71.70.Ej, 85.75.-d

There is currently great interest in studying spin related phenomena in semiconductors. On the one hand there is novel fundamental physics at the nanoscale and on the other hand one expects applications in terms of spin based quantum information processing [1,2]. Physical realization of quantum computers requires fulfillment of a number of challenging criteria [3]. A fragile quantum state has to be coherent for sufficient long time which usually requires its isolation from the environment. On the other hand it has to be externally manipulated. For these purposes, the electron spin in semiconductor quantum dots was suggested as a promising candidate [4]. There are a number of experiments in which the electron spin is initialized, manipulated, stored, and read out [5–11].

Usually spin-state manipulation requires the application of microwave radiation, radio-frequency electric fields as well as magnetic fields. These methods strongly limits the possibility to address spins qubits individually. The first step towards selective control of individual single electron spins was demonstrated in recent state of the art experiments [12,13]. Electron spin manipulation was realized by means of electric fields which can be generated locally quite easily and indirectly via spin orbit interaction which couples charge and spin degrees of freedom. Electron spin control based on spin orbit effect was also proposed in some theoretical papers [14–18].

Unfortunately, in most semiconductor quantum dots the electron spin is exposed to hyperfine interaction with nuclear spins which are present in the host material. This interaction is then the main source of electron spin decoherence in quantum dots putting a severe restriction on the possibility to realize a highly coherent electron spin qubit [19,20]. There are several appealing ideas how to deal with this type of decoherence in quantum dot systems [21]. Very promising way to eliminate or reduce the contact hyperfine interaction with the nuclear spin lattice is to use the spin state of the valence holes—a missing electron in the

valence band—as a carrier of quantum information instead of electrons. Holes are described by the p orbitals that vanish at a nuclear site, which strongly suppresses the Fermi hyperfine contact interaction. Thus one can expect longer coherence times for hole spin states [22,23]. Some experiments seem to confirm this statement reporting long relaxation (\sim ms) and coherence (\sim μ s) times [24–27] for hole spins while others reported a very short hole spin dephasing time (\sim ns) [28]. Recent theoretical investigations [29,30] and experiments [31] seem to resolve this mismatch of coherence times in different experiments suggesting that the absence of mixing between the heavy-hole (HH) and the light-hole (LH) state is crucial for a long hole spin coherence time. Not only long coherence times but also the possibility to initialize the hole spin state even without a magnetic field [25], and the recent realization of a coherent control of a hole spin state in single and double coupled quantum dots [32–34] has promoted the hole as a very good candidate as carrier of quantum bit information. There are also a few appealing theoretical proposals how the HH spin state can be manipulated [35–39].

In this Letter, we demonstrate by using a four-band HH-LH model that the motion of the valence hole in gated semiconductor nanostructures can induce the rotation of the HH spin in the presence of the Dresselhaus spin-orbit interaction (DSOI). Supported by these results we present an efficient scheme which can be used to realize any rotation of the HH spin and propose a nanodevice which acts as a quantum logic NOT gate on a HH spin qubit. The spin rotations are realized by transporting the hole along a closed loop which is defined by metal gates. This method is more suitable for controlling the hole spin than the application of a magnetic field, because the in-plane hole g factor is very small. Therefore, one would need a magnetic field of several Teslas, which is still experimentally challenging. Application of the multiband model allows us to study mixing between HH and LH states. We found that

in the considered nanostructures the HH-LH mixing is negligible so we can expect long coherence times for a qubit stored in the HH spin state [29–31].

We consider a planar heterostructure covered by nanostructured metal gates. The system consist of a 10-nm thick (unstrained) zinc-blende quantum well structure sandwiched between two 10-nm blocking barriers (Fig. 1) in which the single valence hole is confined. The hole which forms a charge distribution in this quantum well induces a response potential of the electron gas in the metallic gate which in turns leads to a self-focusing mechanism of the confined charged particle wave function [40]. Thus interaction of the hole with the metal is a source of additional lateral confinement. As a result the hole is self-trapped under the metal in the form of a stable Gaussian like wave packet. It has the unique property for a quantum particle, that it reflects from a barrier or tunnels through it with 100% probability while conserving its shape, which is rather a characteristic of classical objects. This property can be used to transfer a charged particle in the form of a stable wave packet (soliton) between different locations within the nanodevice by applying static weak voltages to the electrodes only [41]. We use a system of coordinates in which the quantum well is oriented in the z [001] (growth) direction and the hole can move only in the x [100] – y [010] plane. We consider the two dimensional four-band HH ($J_z = \pm 3/2$), LH ($J_z = \pm 1/2$) Hamiltonian:

$$\hat{H} = \hat{H}_{\text{LK}} - |e|\phi(x, y, z_0)\hat{I} + \hat{H}_{\text{BIA}}^{2\text{D}}. \quad (1)$$

The first term is the Luttinger-Kohn Hamiltonian [42] describing the kinetic energy of the 2D hole, which for unstrained zinc blende materials can be written in the effective mass approximation as

$$\hat{H}_{\text{LK}} = \begin{pmatrix} \hat{P}_+ & 0 & \hat{R} & 0 \\ 0 & \hat{P}_- & 0 & \hat{R} \\ \hat{R}^\dagger & 0 & \hat{P}_- & 0 \\ 0 & \hat{R}^\dagger & 0 & \hat{P}_+ \end{pmatrix}, \quad (2)$$

where $\hat{P}_\pm = \frac{2}{2m_0}(\gamma_1 \pm \gamma_2)(k_x^2 + k_y^2) + E_0^\pm$ and $\hat{R} = \frac{2}{2m_0}\sqrt{3}[\gamma_2(k_x^2 - k_y^2) - 2i\gamma_3k_xk_y]$. We denote $E_0^\pm = \frac{2}{2m_0}(\gamma_1 \mp 2\gamma_2)\langle k_z^2 \rangle$ as the first subband energy in the z direction ($E_0^- = E_{\text{LH}}^{\text{LH}}$, $E_0^+ = E_{\text{HH}}^{\text{HH}}$) with $\langle k_z^2 \rangle = \pi^2/d^2$, where d is the quantum well height, $\gamma_1, \gamma_2, \gamma_3$ are the Luttinger parameters and m_0 is the free electron mass. Momentum operators are $k_q = -i\frac{\partial}{\partial q}$ where $q = x, y$. We use the representation where the projections of Bloch angular momentum on

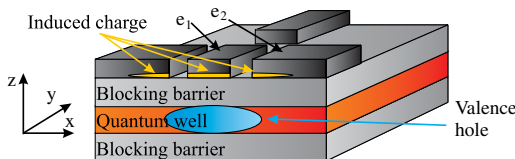


FIG. 1 (color online). Cross section of the nanodevice.

the z axis are arranged in the following order $J_z = \frac{3}{2}, \frac{1}{2}, -\frac{1}{2}, -\frac{3}{2}$. Consistently with this convention, the state vector can be written as

$$\Psi(x, y, t) = (\psi_{\text{HH}}^\dagger(x, y, t), \psi_{\text{LH}}^\dagger(x, y, t), \psi_{\text{LH}}^\dagger(x, y, t), \psi_{\text{HH}}^\dagger(x, y, t))^T. \quad (3)$$

The electrostatic potential $\phi(x, y, z_0, t)$, which is “felt” by the hole, is the source of the self-trapping potential. Its origin is due to charges induced on the metal electrodes. The potential is found by solving the Poisson equation in a three dimensional computational box containing the entire nanodevice. The detailed method was described in Refs. [17,41]. Quantum calculations [43] indicate that this is a good approximation of the actual response potential of the electron gas. The \hat{I} is the unit operator, e is the elementary charge and z_0 is the center of the quantum well. The \hat{H}_{BIA} term accounts for the DSOI [44] which is caused by the lack of inversion symmetry of the crystal—a characteristic feature for zinc blende materials—and (including two main contributions) takes the following form for bulk [45]

$$\hat{H}_{\text{BIA}} = -\beta_0\mathbf{k} \cdot \boldsymbol{\Omega}_J - \beta\boldsymbol{\Omega}_k \cdot \mathbf{J}, \quad (4)$$

where $\mathbf{k} = (k_x, k_y, k_z)$ is the momentum vector and $\mathbf{J} = (J_x, J_y, J_z)$ is the vector of the 4×4 spin $3/2$ matrices. The x component of $\boldsymbol{\Omega}_O$ is the $\Omega_O^x = \{O_x, O_y^2 - O_z^2\}$ and Ω_O^y, Ω_O^z can be obtained by cyclic permutations, $\{A, B\} = \frac{1}{2}(AB + BA)$ and the operator $O = k, J$. Going from bulk to 2D systems and neglecting cubic k terms [46], the bulk DSOI can be directly transformed into

$$\hat{H}_{\text{BIA}}^{2\text{D}} = -\beta_0(k_x\Omega_j^x + k_y\Omega_j^y) + \beta\langle k_z^2 \rangle(k_xJ_x - k_yJ_y), \quad (5)$$

where β_0 and β can be found in Refs. [45,47]. The time evolution of the system is described by the time-dependent Schrödinger equation which is solved numerically self-consistently with the Poisson equation. Due to the motion of the hole wave packet, the Poisson equation has to be solved in every time step of the iteration procedure. The initial condition is the ground state of the hole confined under the metal due to the self-focusing effect and is calculated by solving the stationary Schrödinger equation $\hat{H}\Psi_0(x, y) = E\Psi_0(x, y)$.

Let us consider the heterostructure from Fig. 1: an unstrained GaAs quantum well of 10-nm height sandwiched between two blocking barriers of 10-nm height, covered by a 65×65 nm square electrode (called e_1) and an approximately 4000-nm long electrode (called e_2), as also depicted in Figs. 2(d) and 2(d'). The distance between both electrodes is chosen to be 10 nm. This distance should be small enough so that when the hole wave function is located under electrode e_1 , there is a small overlap with the area under electrode e_2 . In the initial state, the hole is confined in the ground state under e_1 , which can be

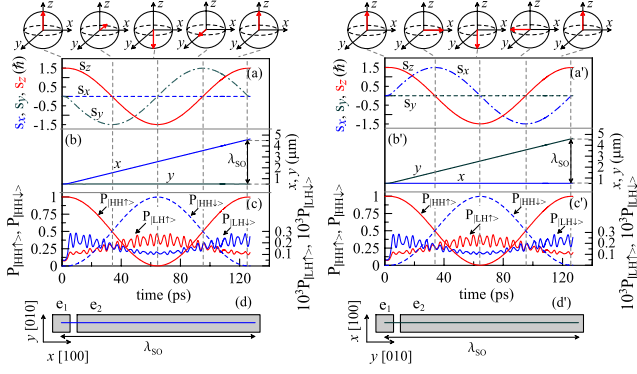


FIG. 2 (color online). Time evolution of the HH spin components (a), average position of the hole wave packet (b), and probability of occupying the following hole basis states (c): $|\text{HH}\uparrow\rangle$, $|\text{HH}\downarrow\rangle$, $|\text{LH}\uparrow\rangle$, $|\text{LH}\downarrow\rangle$, for a hole moving along the wire covered by the electrodes e_1 , e_2 from figure (d). In (c) left (right) axis corresponds to probability of finding the hole in the HH (LH) spin states. Results for hole moving along the wire placed in y (x') direction are depicted in (a'), (b'), and (c'). Above each plot, there are Bloch spheres representing the qubit after each $\pi/2$ rotation.

achieved by applying a voltage $V_1 = -0.3$ mV and $V_2 = 0$ to the electrodes e_1 and e_2 , respectively [48]. We assume that the hole is in the initial state $\Psi(x, y, t_0) = (\psi_{\text{HH}}^{\uparrow}(x, y, t_0), 0, 0, 0)^T$ [49]. The preparation of such a spin state—as well as its read-out—can be achieved without the application of a magnetic field by using the experimentally demonstrated high fidelity (99%) optical methods [25] or by using an analogous device, as proposed theoretically in Ref. [18], which acts on the HH spin. The hole is forced to move along the path under the electrode e_2 by changing the voltage configuration to $V_1 = 0$, $V_2 = -0.7$ mV. We plot the probability of finding the hole in the possible basis states $P_{J_z}(t) = \int |\psi_{J_z}(x, y, t)|^2 dx dy$ in Figs. 2(c) and 2(c') where $J_z = 3/2, 1/2, -1/2, -3/2$. We observe that during the motion as well as in the ground state, the probability of finding the hole in the LH state is very small ($\sim 10^{-4}$). It shows that the mixing between HH and LH states is negligible in our system. By decreasing the quantum well height further, the HH-LH splitting energy $\Delta_{\text{HL}} = E_{\perp}^{\text{LH}} - E_{\perp}^{\text{HH}}$ would increase and the probability of finding the system in the LH state would be reduced further.

Because of the fact that the hole is mainly composed of the HH state in the considered nanostructures, we can calculate expectation values of the HH pseudospin 1/2 operator $\vec{s} = \langle \frac{3}{2} \vec{\sigma} \rangle_{\Psi_{\text{HH}}}$ for the HH state defined as $\Psi_{\text{HH}}(x, y, t) = (\psi_{\text{HH}}^{\uparrow}(x, y, t), \psi_{\text{HH}}^{\downarrow}(x, y, t))^T$ where $\vec{\sigma}$ are the Pauli spin 1/2 matrices. For a hole occupying only the HH band, the expectation values of total angular momentum $J = 3/2$ matrices are $\langle J_x \rangle = \langle J_y \rangle = 0$ and $\langle J_z \rangle = s_z$. The time dependence of the HH average spin components are given in Figs. 2(a) and 2(a'). During the motion of a hole along the x (y) axis, the s_x (s_y) spin component is preserved and

s_y (s_x), s_z components oscillate: the HH spin is rotated around the axis parallel to the direction of motion. This behavior can be understood by analyzing an approximated $\hat{H}_{\text{BIA}}^{\text{HH}}$ Hamiltonian for the HH band only [50]

$$\hat{H}_{\text{BIA}}^{\text{HH}} = -\frac{\tilde{\beta}}{3} [(p_x^3 + p_x p_y^2) \sigma_x + (p_y^3 + p_x^2 p_y) \sigma_y]. \quad (6)$$

For quantum wires placed along the q direction, the above Hamiltonian can be approximated by $\hat{H}_{\text{BIA},q}^{\text{HH}} = -\frac{\tilde{\beta}}{3} (p_q^3 + p_q \langle p_{q\perp}^2 \rangle) \sigma_q$, where $q = x, y$, q_{\perp} axis is perpendicular to q and the $\tilde{\beta}$ is an effective DSOI coupling strength given in [50]. From the fact that the momentum operators p_q and p_q^3 are multiplied by the HH spin operator σ_q , one can expect that the hole motion with p_q momentum will generate a spin rotation around the q axis according to the time evolution operator $\hat{U}_q(t) = e^{-i\hat{H}_{\text{BIA},q}^{\text{HH}} t}$.

After traveling a certain distance $\lambda(t)$, the spin is rotated by the angle $\phi(t) = 2\pi \frac{\lambda(t)}{\lambda_{SO}}$. Thus, one can say that a unitary operation was performed on the HH spin state. One can derive the corresponding unitary spin rotation operator for a hole moving in the wire placed along the x axis:

$$\hat{R}_x(\phi) = \frac{1}{\sqrt{2}} \begin{pmatrix} i\sqrt{1 + \cos(\phi)} & \frac{\sin(\phi)}{\sqrt{1 + \cos(\phi)}} \\ \frac{\sin(\phi)}{\sqrt{1 + \cos(\phi)}} & i\sqrt{1 + \cos(\phi)} \end{pmatrix} \quad (7)$$

and for a hole moving in the wire which is placed along the y direction:

$$\hat{R}_y(\phi) = \frac{1}{\sqrt{2}} \begin{pmatrix} \sqrt{1 + \cos(\phi)} & -\frac{\sin(\phi)}{\sqrt{1 + \cos(\phi)}} \\ \frac{\sin(\phi)}{\sqrt{1 + \cos(\phi)}} & \sqrt{1 + \cos(\phi)} \end{pmatrix}. \quad (8)$$

The hole restores its initial spin after passing the distance λ_{SO} which depends on the DSOI coupling strengths and the effective mass (Luttinger parameters). The presented results are obtained for a GaAs quantum well and taking into account the full DSOI Hamiltonian (5). We also performed calculations for other materials ZnSe, and CdTe and estimated the λ_{SO} length: $\lambda_{SO}^{\text{GaAs}} \approx 4.05 \mu\text{m}$, $\lambda_{SO}^{\text{ZnSe}} \approx 0.86 \mu\text{m}$, $\lambda_{SO}^{\text{CdTe}} \approx 0.74 \mu\text{m}$ [51]. It is worth mentioning that the “on-demand” single electron transport on such distances (μm), and even much larger, was recently realized experimentally using surface acoustic waves [52,53].

Taking advantage of the fact that the hole motion generates HH spin rotations, one can design a gated semiconductor nanodevice that will act on the HH spin qubit as a quantum gate. We propose a nanodevice covered by the system of electrodes from Fig. 3(d) which act as a quantum NOT gate. The hole whose spin we want to transform is initially confined under the 65×65 nm electrode e_1 , where a constant $V_1 = -0.2$ mV voltage is applied while the voltage on the other electrodes is set to zero. Electrodes are separated by a distance of 10 nm. Let us assume that the

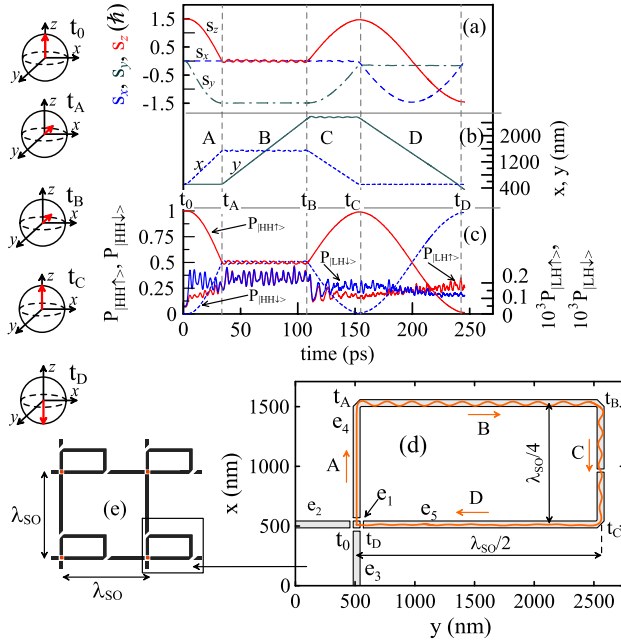


FIG. 3 (color online). (a),(b) and (c) same as Figs. 2(a)–2(c), but for the quantum NOT gate which is covered by the system of electrodes e_1 – e_5 presented in (d). In (d) the solid orange line represents the hole trajectory (orange arrow represents direction of motion of the hole). Hole initially confined under e_1 goes to the $+x$ direction passing A, B, C, and D segments of the loop. Vector state is depicted on the Bloch spheres in the subsequent moments of time: t_0 – t_D . Scheme in figure (e) illustrates the scalability of the nanodevice. Spins of the different holes confined under the red electrodes form a quantum register, and on each qubit quantum logic gate can be separately applied by means of small electric fields.

hole is in the ground state with its initial spin state prepared to the HH spin up state. By changing the voltage applied to e_1 to $V_1 = 0$ and switching the voltage on e_4 to $V_4 = -0.7$ mV the hole starts to move in the $+x$ direction under electrode e_4 . After passing a $\lambda_{SO}/4$ distance of segment A, the HH spin is rotated around the x axis by an angle $\pi/2$, and the $\hat{R}_x(\pi/2)$ operation is performed. At the end of segment A, the hole wave packet turns right and starts to move parallel to the y axis. During the reflection the hole wave packet does not scatter due to the self-focusing effect. The hole passes the B segment whose length is $\lambda_{SO}/2$ performing the $\hat{R}_y(\pi)$ operation and turns right. Then hole goes under electrode e_5 whose voltage was in the meantime set to the voltage of the e_4 electrode. The hole moves in $-x$ and $-y$ directions performing the $\hat{R}_x(-\pi/2)$ and $\hat{R}_y(-\pi)$ operation. Finally, the hole returns to its initial position under the e_1 electrode, where it is captured by applying the $V_1 = -1.0$ mV voltage. After passing the whole loop, a set of HH spin transformations is performed resulting in a NOT gate operation $\hat{U}_{\text{NOT}} = \hat{R}_y(-\pi)\hat{R}_x(-\pi/2)\hat{R}_y(\pi)\hat{R}_x(\pi/2) = -i\sigma_x$. Since the hole after completing the set of transformations returns to its

initial position, the gate operation is performed on the HH spin exclusively, not on the spatial part of the wave function. The size of the gate depends only on the λ_{SO} length for the considered material.

The gate operation time for GaAs and applied starting voltage configuration is $t_{\text{NOT}}^{\text{GaAs}} \approx 250$ ps. As the time is proportional to λ_{SO} the gate operation time for other materials is significantly improved reaching $t_{\text{NOT}}^{\text{CdTe}} \approx 60$ ps and $t_{\text{NOT}}^{\text{ZnSe}} \approx 80$ ps.

The dipolar hyperfine interaction could affect the fidelity of the proposed gate. But, as demonstrated, the HH/LH mixing can be neglected and the dipolar hyperfine interaction for pure HH spin states is of the Ising type [29,30], leading to a HH spin coherence time which was experimentally determined to be at least 100 ns [26]. Thus, the proposed gate can be applied about $\sim 10^3$ times until the HH spin coherence will be lost. Our proposal can also be extended to a larger number of qubits that can be integrated in a single nanodevice. This scalability is shown in Fig. 3(e). Furthermore, the proposed device is suitable for coherent transport of a hole wave packet and thus allows for transferring quantum information between different locations in this nanodevice.

In conclusion, we showed that the motion of the hole in gated semiconductor heterostructures can induce a coherent rotation of the HH spin where the DSOI is the mediator of this process. An important result is that during the motion in the presence of the DSOI, the mixing between HH and LH states is negligible from which we can expect that the proposed HH spin qubit should be robust to decoherence coming from the interaction with the nuclear spins. We proposed a quantum NOT gate which operates in subnanoseconds, and it is controlled only by means of small static local electric fields generated by the top gates. It allows us to address the HH spin qubit individually, making our proposal scalable.

This work was supported by the Grant No. N N202 128337 from the Ministry of Science and Higher Education, as well as by the “Krakow Interdisciplinary PhD-Project in Nanoscience and Advances Nanostructures” operated within the Foundation for Polish Science MPD Programme and cofinanced by European Regional Development Fund, the Belgian Science Policy (IAP), and the Flemish Science Foundation (FWO-V1).

- [1] D. Awschalom, D. Loss, and N. Samarth, *Semiconductor Spintronics and Quantum Computation* (Springer Verlag, Berlin, 2002).
- [2] I. Zutic, J. Fabian, and S. Das Sarma, *Rev. Mod. Phys.* **76**, 323 (2004).
- [3] D. P. DiVincenzo, *Fortschr. Phys.* **48**, 771 (2000).
- [4] D. Loss and D. P. DiVincenzo, *Phys. Rev. A* **57**, 120 (1998).
- [5] R. Hanson, L. P. Kouwenhoven, J. R. Petta, S. Tarucha, and L. M. K. Vandersypen, *Rev. Mod. Phys.* **79**, 1217 (2007).

- [6] S. Amasha, K. MacLean, I. P. Radu, D. M. Zumbühl, M. A. Kastner, M. P. Hanson, and A. C. Gossard, *Phys. Rev. Lett.* **100**, 046803 (2008).
- [7] J. R. Petta, A. C. Johnson, J. M. Taylor, E. A. Laird, A. Yacoby, M. D. Lukin, C. M. Marcus, M. P. Hanson, and A. C. Gossard, *Science* **309**, 2180 (2005).
- [8] J. M. Elzerman, R. Hanson, L. H. Willems van Beveren, B. Witkamp, L. M. K. Vandersypen, and L. P. Kouwenhoven, *Nature (London)* **430**, 431 (2004).
- [9] T. Meunier, I. T. Vink, L. H. Willems van Beveren, F. H. L. Koppens, H. P. Tranitz, W. Wegscheider, L. P. Kouwenhoven, and L. M. K. Vandersypen, *Phys. Rev. B* **74**, 195303 (2006).
- [10] F. H. L. Koppens, C. Buizert, K. J. Tielrooij, I. T. Vink, K. C. Nowack, T. Meunier, L. P. Kouwenhoven, and L. M. K. Vandersypen, *Nature (London)* **442**, 766 (2006).
- [11] A. Morello, J. J. Pla, F. A. Zwanenburg, K. W. Chan, K. Y. Tan, H. Huebl, M. Möttönen, C. D. Nugroho, C. Yang, J. A. van Donkelaar, A. D. C. Alves, D. N. Jamieson, C. C. Escott, L. C. L. Hollenberg, R. G. Clark, and A. S. Dzurak, *Nature (London)* **467**, 687 (2010).
- [12] K. C. Nowack, F. H. L. Koppens, Yu. V. Nazarov, and L. M. K. Vandersypen, *Science* **318**, 1430 (2007).
- [13] S. Nadj-Perge, S. M. Frolov, E. P. A. M. Bakkers, and L. P. Kouwenhoven, *Nature (London)* **468**, 1084 (2010).
- [14] V. N. Golovach, M. Borhani, and D. Loss, *Phys. Rev. B* **74**, 165319 (2006).
- [15] S. Debal and C. Emary, *Phys. Rev. Lett.* **94**, 226803 (2005).
- [16] C. Flindt, A. S. Sorensen, and K. Flensberg, *Phys. Rev. Lett.* **97**, 240501 (2006).
- [17] S. Bednarek and B. Szafran, *Phys. Rev. Lett.* **101**, 216805 (2008).
- [18] S. Bednarek, P. Szumniak, and B. Szafran, *Phys. Rev. B* **82**, 235319 (2010).
- [19] I. A. Merkulov, A. L. Efros, and M. Rosen, *Phys. Rev. B* **65**, 205309 (2002).
- [20] A. V. Khaetskii, D. Loss, and L. Glazman, *Phys. Rev. Lett.* **88**, 186802 (2002).
- [21] J. Fischer and D. Loss, *Science* **324**, 1277 (2009).
- [22] G. Burkard, *Nature Mater.* **7**, 100 (2008).
- [23] M. H. Kolodrubetz and J. R. Petta, *Science* **325**, 42 (2009).
- [24] D. Heiss, S. Schaeck, H. Huebl, M. Bichler, G. Abstreiter, J. J. Finley, D. V. Bulaev, and D. Loss, *Phys. Rev. B* **76**, 241306 (2007).
- [25] B. D. Gerardot, D. Brunner, P. A. Dalgarno, P. Öhberg, S. Seidl, M. Kroner, K. Karrai, N. G. Stoltz, P. M. Petroff, and R. J. Warburton, *Nature (London)* **451**, 441 (2008).
- [26] D. Brunner, B. D. Gerardot, P. A. Dalgarno, G. Wüst, K. Karrai, N. G. Stoltz, P. M. Petroff, and R. J. Warburton, *Science* **325**, 70 (2009).
- [27] F. Fras, B. Eble, P. Desfonds, F. Bernardot, C. Testelin, M. Chamarro, A. Miard, and A. Lemaître, *Phys. Rev. B* **84**, 125431 (2011).
- [28] B. Eble, C. Testelin, P. Desfonds, F. Bernardot, A. Balocchi, T. Amand, A. Miard, A. Lemaître, X. Marie, and M. Chamarro, *Phys. Rev. Lett.* **102**, 146601 (2009).
- [29] C. Testelin, F. Bernardot, B. Eble, and M. Chamarro, *Phys. Rev. B* **79**, 195440 (2009).
- [30] J. Fischer, W. A. Coish, D. V. Bulaev, and D. Loss, *Phys. Rev. B* **78**, 155329 (2008).
- [31] E. A. Chekhovich, A. B. Krysa, M. S. Skolnick, and A. I. Tartakovskii, *Phys. Rev. Lett.* **106**, 027402 (2011).
- [32] K. De Greve, P. L. McMahon, D. Press, T. D. Ladd, D. Bisping, C. Schneider, M. Kamp, L. Worschech, S. Höfling, A. Forchel, and Y. Yamamoto, *Nature Phys.* **7**, 872 (2011).
- [33] A. Greilich, S. G. Carter, D. Kim, A. S. Bracker, and D. Gammon, *Nature Photon.* **5**, 702 (2011).
- [34] T. M. Godden, J. H. Quilter, A. J. Ramsay, Yanwen Wu, P. Brereton, S. J. Boyle, I. J. Luxmoore, J. Puebla-Nunez, A. M. Fox, and M. S. Skolnick, *Phys. Rev. Lett.* **108**, 017402 (2012).
- [35] D. V. Bulaev and D. Loss, *Phys. Rev. Lett.* **98**, 097202 (2007).
- [36] C. Y. Hsieh, R. Cheriton, M. Korkusinski, and P. Hawrylak, *Phys. Rev. B* **80**, 235320 (2009).
- [37] J. C. Budich, D. G. Rothe, E. M. Hankiewicz, and B. Trauzettel, *Phys. Rev. B* **85**, 205425 (2012).
- [38] T. Andlauer and P. Vogl, *Phys. Rev. B* **79**, 045307 (2009).
- [39] R. Roloff, T. Eissfeller, P. Vogl, and W. Pötz, *New J. Phys.* **12**, 093012 (2010).
- [40] S. Bednarek, B. Szafran, and K. Lis, *Phys. Rev. B* **72**, 075319 (2005).
- [41] S. Bednarek, B. Szafran, R. J. Dudek, and K. Lis, *Phys. Rev. Lett.* **100**, 126805 (2008).
- [42] J. M. Luttinger and W. Kohn, *Phys. Rev.* **97**, 869 (1955).
- [43] S. Bednarek and B. Szafran, *Phys. Rev. B* **73**, 155318 (2006).
- [44] G. Dresselhaus, *Phys. Rev.* **100**, 580 (1955).
- [45] R. Winkler, *Spin-Orbit Coupling Effects in Two Dimensional Electron and Hole Systems* (Springer, Berlin, 2003).
- [46] We can neglect the cubic Dresselhaus term since in the proposed device the lateral size ($l \approx 65$ nm) of the induced quantum dot is larger than the quantum well height ($d = 10$ nm). Therefore, the cubic Dresselhaus term is smaller than the linear one by a factor of $(d/l)^2$, which is of the order of ~ 0.01 .
- [47] M. Cardona, N. E. Christensen, and G. Fasol, *Phys. Rev. B* **38**, 1806 (1988).
- [48] Since the metal gate is in contact with an undoped semiconductor, the Schottky barrier V_B should be taken into account with mV accuracy. Therefore, the potential applied to the gates is equal to $V_i \rightarrow V_i - V_B$. V_B should be determined experimentally for a certain structure.
- [49] In fact due to lateral confinement ground state of the hole in induced quantum dot has some small amount ($< 0.1\%$) of LH states Fig. 2(c).
- [50] D. V. Bulaev and D. Loss, *Phys. Rev. Lett.* **95**, 076805 (2005).
- [51] We use Luttinger parameters ($\gamma_1, \gamma_2, \gamma_3$) and dielectric constant (ϵ): $\gamma_1^{\text{GaAs}} = 6.85$, $\gamma_2^{\text{GaAs}} = 2.1$, $\gamma_3^{\text{GaAs}} = 2.9$, $\epsilon^{\text{GaAs}} = 12.4$, $\gamma_1^{\text{CdTe}} = 5.3$, $\gamma_2^{\text{CdTe}} = 1.7$, $\gamma_3^{\text{CdTe}} = 2.$, $\epsilon^{\text{CdTe}} = 10.125$, $\gamma_1^{\text{ZnSe}} = 4.3$, $\gamma_2^{\text{ZnSe}} = 1.14$, $\gamma_3^{\text{ZnSe}} = 1.84$, $\epsilon^{\text{ZnSe}} = 9.14$ taken from Table D.1 from Ref. [45].
- [52] S. Hermelin, S. Takada, M. Yamamoto, S. Tarucha, A. D. Wieck, L. Saminadayar, C. Bäuerle, and T. Meunier, *Nature (London)* **477**, 435 (2011).
- [53] R. P. G. McNeil, M. Kataoka, C. J. B. Ford, C. H. W. Barnes, D. Anderson, G. A. C. Jones, I. Farrer, and D. A. Ritchie, *Nature (London)* **477**, 439 (2011).

6 All-electrical control of quantum gates for single heavy-hole spin qubits

All-electrical control of quantum gates for single heavy-hole spin qubitsP. Szumniak,^{1,*} S. Bednarek,¹ J. Pawłowski,¹ and B. Partoens²¹*AGH University of Science and Technology, Faculty of Physics and Applied Computer Science, al. Mickiewicza 30, 30-059 Kraków, Poland*²*Department of Physics, University of Antwerp, Groenenborgerlaan 171, 2020 Antwerp, Belgium*

(Received 4 March 2013; published 20 May 2013)

In this paper several nanodevices which realize basic single heavy-hole qubit operations are proposed and supported by time-dependent self-consistent Poisson-Schrödinger calculations using a four band heavy-hole–light-hole model. In particular we propose a set of nanodevices which can act as Pauli X , Y , Z quantum gates and as a gate that acts similar to a Hadamard gate (i.e., it creates a balanced superposition of basis states but with an additional phase factor) on the heavy-hole spin qubit. We also present the design and simulation of a gated semiconductor nanodevice which can realize an arbitrary sequence of all these proposed single quantum logic gates. The proposed devices exploit the self-focusing effect of the hole wave function which allows for guiding the hole along a given path in the form of a stable solitonlike wave packet. Thanks to the presence of the Dresselhaus spin-orbit coupling, the motion of the hole along a certain direction is equivalent to the application of an effective magnetic field which induces in turn a coherent rotation of the heavy-hole spin. The hole motion and consequently the quantum logic operation is initialized only by weak static voltages applied to the electrodes which cover the nanodevice. The proposed gates allow for an all electric and ultrafast (tens of picoseconds) heavy-hole spin manipulation and give the possibility to implement a scalable architecture of heavy-hole spin qubits for quantum computation applications.

DOI: [10.1103/PhysRevB.87.195307](https://doi.org/10.1103/PhysRevB.87.195307)

PACS number(s): 73.21.La, 03.67.Lx, 73.63.Nm

I. INTRODUCTION

The idea to realize quantum computers has attracted enormous attention and effort of theoreticians and experimentalists in the last years. Among the many appealing proposals for the physical realization of quantum computation, solid state spin based implementations seem to be particularly interesting and promising.^{1,2} The spin state of an electron which is confined in a semiconductor nanostructure like a quantum dot or a quantum wire is considered to be a perfect candidate as carrier of a quantum bit of information.³ The realization of many state of the art experiments where an electron spin qubit can be prepared in a certain spin state, stored, manipulated, and read out^{4–14} show the enormous progress that has been made in the field in the last decade.

Very challenging demands for the physical realization of quantum computation¹⁵ are to obtain long living qubits which are immune to decoherence and to develop control methods which allow for a high fidelity and ultrafast qubit manipulation. Furthermore, the scalability requirement of the physical implementation of quantum computation imposes that one has to be able to control each qubit in the quantum register in an individual, selective manner as well as to couple long distant qubits so that also two-qubit gates can be realized.

The main difficulty related to the use of the electron spin as a qubit is its relatively short coherence time. In most quantum dot structures the spin of the confined electron experiences a contact hyperfine interaction with a large number of nonzero nuclear spins of the host material. This results in electron spin decoherence,^{16–19} and if no special effort is made an electron spin qubit loses its coherence in nanoseconds.

Several appealing ideas have been proposed and successfully applied to overcome the fast electron spin decoherence process,²⁰ such as the application of spin echo techniques^{21–23} or the preparation of the nuclear spins of the host material

in a special narrow state.^{19,24–27} A straightforward approach to avoid the interaction with nuclear spins is to confine the electron in a nuclear-spin free material such as silicon,^{28,29} carbon nanotubes,^{30,31} or graphene quantum dots,³² or to store the quantum bit in a spin state of the nitrogen vacancy center in diamond.^{33–36}

Recently the spin state of the hole emerged as an alternative and very promising candidate for the realization of a qubit^{37–39} in semiconductor solid state systems. Its main advantage over the electron spin is the fact that the hole is less sensitive to the interaction with the nuclear spin of the surrounding material. Since the hole is described by a p -type orbital in many semiconductors, its wave function vanishes at the nuclear site and thus the contact hyperfine interaction between hole spin and nuclear spin is canceled. Even though holes still experience interaction with nuclear spins with dipolar character, it is about ten times weaker than the contact interaction for electrons.^{40–46} Consequently, the coherence time of the spin state of the hole is longer than for the electron spin. The coherence time also depends on the heavy-hole (HH)–light-hole (LH) mixing. For pure HH states, the coherence time of the hole reaches its maximum because the interaction between hole spin and nuclear spins has an Ising type character.^{40,42}

Despite the fact that many experimental and theoretical investigations have been done on hole spin related phenomena including relaxation and decoherence mechanisms,^{40–59} HH-LH mixing,^{60–62} spin-orbit effect,^{63–68} Kondo effect,⁶⁹ and even Majorana fermions physics,⁷⁰ so far hole spin dynamics in semiconductor nanostructures is still largely unexplored and needs deeper understanding. However, the fact that holes are alternative long living qubits has stimulated progress in the experimental realization of hole spin preparation, manipulation, and read out.^{44,71–78} It is quite remarkable that it is even possible to initialize hole spin states with very high fidelity (99%) without the application of an external

magnetic field.⁴⁸ Very recently electrical control of a single hole spin in a gated InSb nanowire has been realized.⁷⁹ Other theoretical proposals for hole spin control are EDSR (electron dipole spin resonance) techniques for heavy holes,⁸⁰ non-Abelian geometric phases,⁸¹ the application of a static magnetic field applied in quantum dots,⁸² and an electric g tensor manipulation,^{83,84} and are waiting for their experimental realization.

Another important and indispensable aspect for the realization of a quantum computer architecture is scalability. Recently, scalable architectures were proposed where long distant qubit coupling might be obtained via floating gates.⁸⁵ Furthermore, coupling between spin qubits defined in a semiconductor InAs nanowire and a superconducting cavity⁸⁶ was experimentally realized, which is particularly promising for future realizations of scalable networks of spin qubits. A scalable architecture for optically controlled hole spin qubits confined in quantum dot molecules was also proposed.⁸⁷

Recently we have shown that the motion of a hole in gated semiconductor nanodevices can induce heavy-hole spin rotations in the presence of the Dresselhaus spin-orbit coupling (DSOI).⁸⁸ We proposed a nanodevice based on GaAs which can act as a quantum NOT (Pauli X) gate. In this paper we propose a couple of nanodevices capable to realize other single quantum logic gates: Pauli Y and Z gates and a U_S gate which can realize a balanced superposition of qubit basis states. The required quantum logic operation is realized by transporting the hole around a rectangular loop which is defined by metal electrodes which cover the semiconductor nanostructure. The geometry of the metal gates determines the hole trajectory and consequently the type of quantum operation which we want to perform. Moreover, we propose a so called combo nanodevice in which each of the proposed quantum logic gates (Pauli X , Y , Z and U_S) can be applied in an arbitrary sequence on a HH spin qubit. We give a full theoretical description of the nanodevices and present the results of time-dependent simulations. The description of the all electrical control scheme which has to be applied in order to perform the desired quantum gate by the proposed nanodevice is provided. Moreover, thanks to the fact that the proposed gates are only controlled by weak static voltages applied to the local top electrodes, it is possible to realize a scalable quantum architecture in which each qubit can be addressed individually without disturbing the state of other qubits in the quantum register.

In this paper we perform our simulations for CdTe, and not GaAs as in Ref. 88 for several reasons. Due to the smaller dielectric constant and higher in-plane effective mass, the binding energy of a self-trapped hole under a metal gate in a CdTe quantum well is larger and consequently the hole soliton effect is more pronounced than in the previously used GaAs material. Since the Cd and Te isotopes are characterized by a nuclear spin $I = \frac{1}{2}$, the dipolar hyperfine interaction between the hole spin and the nuclear spin of the host material is weaker than for GaAs, which nuclei have spin $I = \frac{3}{2}$. Furthermore, the dephasing time of an electron or a hole confined in a quantum dot made from II-VI group compounds is a few times longer than for III-V compounds because of the significantly lower natural concentration of isotopes with nonzero nuclear magnetic moment (Ga 100%, As 100%, Cd 25%, Te 7.8%).^{16,42,89}

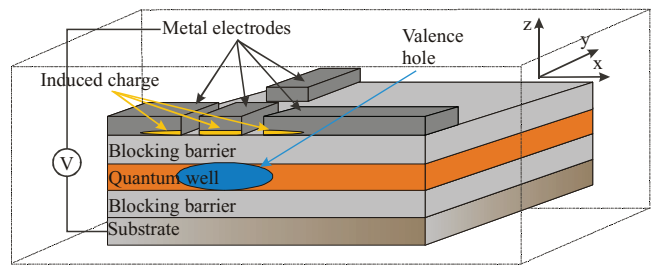


FIG. 1. (Color online) Cross section of the nanodevice.

The lateral size of proposed nanodevices is determined by the λ_{SO} length: The distance which has to be traveled by the hole in order to perform a full 2π HH spin rotation. Since $\lambda_{SO}^{\text{GaAs}} \approx 4000$ nm and $\lambda_{SO}^{\text{CdTe}} \approx 700$ nm the proposed nanodevices which are based on CdTe are significantly smaller than those based on GaAs.

The proposed devices can also be realized in other zinc-blende semiconductors, but due to different material parameters they will differ in size and gate operation time.⁸⁸

This paper is further organized as follows. Section II describes the general device layout and discusses the applied theoretical model, i.e., our self-consistent Poisson-Schrödinger approach with the Luttinger-Kohn Hamiltonian. The ground state wave functions are presented in Sec. III. In Sec. IV we present and describe the separate nanodevices acting as quantum logic gates on heavy-hole spin states, together with the results of our time-dependent simulations. The combo nanodevice in which an arbitrary sequence of single quantum logic gates can be performed on a HH spin state is described in Sec. V as well as the proposal of a scalable architecture. Section VI summarizes the obtained results.

II. DEVICE AND THEORETICAL MODEL

Let us consider a planar semiconductor heterostructure covered by nanostructured metal gates. The system contains a zinc-blende semiconductor quantum well (QW) which is sandwiched between two 10 nm blocking barriers (Fig. 1). The single valence hole is confined in the quantum well region which is oriented in the $z[001]$ (growth) direction and thus the hole can only move in the $x[100]$ - $y[010]$ plane. In such a structure the hole induces a response potential in the electron gas in the metallic gate which in turn leads to a lateral self-confinement of the hole wave function.^{90,91} This self-trapped hole has solitonlike properties: It can be transported as a stable wave packet which maintains its shape during motion. Furthermore, it can reflect or pass through obstacles (potential barriers or wells) with 100% probability while conserving its shape. This property can be used to realize on demand transfer of a hole between different locations within the nanodevice (in the area of the quantum well which is under the metal electrodes) by applying static weak voltages to the electrodes only.⁹²

In order to describe the presented system we rely on the two-dimensional four band HH-LH Hamiltonian:

$$\hat{H} = \hat{H}_{LK}^{2D} + |e|\phi(x, y, z_0)\hat{I} + \hat{H}_{BIA}^{2D}. \quad (1)$$

The HH (LH) states are characterized by the $J_z = \pm 3/2$ ($J_z = \pm 1/2$) projections of total angular momentum on the z axis. The first term is the Luttinger-Kohn Hamiltonian⁹³ describing the kinetic energy of the two-dimensional hole, which for unstrained zinc-blende structures can be written in the effective mass approximation as

$$\hat{H}_{\text{LK}}^{2\text{D}} = \begin{pmatrix} \hat{P}_h & 0 & \hat{R} & 0 \\ 0 & \hat{P}_l & 0 & \hat{R} \\ \hat{R}^\dagger & 0 & \hat{P}_l & 0 \\ 0 & \hat{R}^\dagger & 0 & \hat{P}_h \end{pmatrix}, \quad (2)$$

where

$$\begin{aligned} \hat{P}_h &= \frac{\hbar^2}{2m_0}(\gamma_1 + \gamma_2)(k_x^2 + k_y^2) + E_0^+, \\ \hat{P}_l &= \frac{\hbar^2}{2m_0}(\gamma_1 - \gamma_2)(k_x^2 + k_y^2) + E_0^-, \\ \hat{R} &= \frac{\hbar^2}{2m_0}\sqrt{3}[\gamma_2(k_x^2 - k_y^2) - 2i\gamma_3k_xk_y]. \end{aligned} \quad (3)$$

We denote $E_0^\pm = \frac{\hbar^2}{2m_0}(\gamma_1 \mp 2\gamma_2)\langle k_z^2 \rangle$ as the first subband energy in the z direction ($E_0^- = E_{\perp}^{\text{LH}}, E_0^+ = E_{\perp}^{\text{HH}}$) with $\langle k_z^2 \rangle = \pi^2/d^2$, where d is the quantum well width, $\gamma_1, \gamma_2, \gamma_3$ are the Luttinger parameters, and m_0 is the free electron mass. The momentum operators are defined as $\hbar k_q = -i\hbar \frac{\partial}{\partial q}$, where $q = x, y$. \hat{I} is the unit operator, e is the elementary charge, and z_0 is the center of the quantum well. We use the representation where the projections of the Bloch angular momentum on the z axis are arranged in the following order: $J_z = \frac{3}{2}, \frac{1}{2}, -\frac{1}{2}, -\frac{3}{2}$ ($|\text{HH}\uparrow\rangle, |\text{LH}\uparrow\rangle, |\text{LH}\downarrow\rangle, |\text{HH}\downarrow\rangle$). Consistently with this convention the state vector can be written as

$$\Psi(x, y, t) = \begin{pmatrix} \psi_{\text{HH}\uparrow}^\uparrow(x, y, t) \\ \psi_{\text{LH}\uparrow}^\uparrow(x, y, t) \\ \psi_{\text{LH}\downarrow}^\downarrow(x, y, t) \\ \psi_{\text{HH}\downarrow}^\downarrow(x, y, t) \end{pmatrix}. \quad (4)$$

The electrostatic potential $\phi(x, y, z_0, t)$ which is ‘‘felt’’ by the hole is the source of the self-trapping potential. Its origin is due to charges induced on the metal electrodes. The electrostatic potential $\phi(x, y, z_0, t)$ can be calculated according to the superposition principle and it is the difference between the total electrostatic potential and the self-interaction potential $\phi(x, y, z_0, t) = \Phi_{\text{tot}}(x, y, z_0, t) - \phi_{\text{si}}(x, y, z_0, t)$. The total electrostatic potential distribution within the considered system is found by solving the Poisson equation in a three-dimensional computational box containing the entire nanodevice:

$$\nabla^2 \Phi_{\text{tot}}(x, y, z, t) = -\frac{1}{\epsilon \epsilon_0} \rho_{\text{tot}}(x, y, z, t). \quad (5)$$

The charge density of a single hole is described by the two-dimensional distribution $\rho_{\text{tot}}(x, y, z, t) = \rho(x, y, t)\delta(z - z_0)$, where

$$\begin{aligned} \rho(x, y, t) &= |e| [|\psi_{\text{HH}\uparrow}^\uparrow(x, y, t)|^2 + |\psi_{\text{LH}\uparrow}^\uparrow(x, y, t)|^2 \\ &\quad + |\psi_{\text{LH}\downarrow}^\downarrow(x, y, t)|^2 + |\psi_{\text{HH}\downarrow}^\downarrow(x, y, t)|^2]. \end{aligned} \quad (6)$$

The self-interaction potential $\phi_{\text{si}}(x, y, z_0, t)$ is directly connected to the total wave packet charge density distribution and

can be calculated straightforwardly as follows:

$$\phi_{\text{si}}(\mathbf{r}, t) = \frac{1}{4\pi\epsilon \epsilon_0} \int d\mathbf{r}' \frac{\rho(\mathbf{r}', t)}{|\mathbf{r} - \mathbf{r}'|}. \quad (7)$$

Quantum calculations⁹⁴ indicate that the electrostatic approach described above is a good approximation of the actual response potential of the electron gas.

Since in the considered system the hole is confined in the zinc-blende semiconductor (thus lacking crystal inversion symmetry) quantum well we have to take into account the DSOI⁹⁵ described by the \hat{H}_{BIA} Hamiltonian which for holes in bulk (including the two leading contributions) can be written as⁶³

$$\begin{aligned} \hat{H}_{\text{BIA}} &= -\beta_0 [k_x \{J_x, J_y^2 - J_z^2\} + k_y \{J_y, J_z^2 - J_x^2\} \\ &\quad + k_z \{J_z, J_x^2 - J_y^2\}] - \beta [\{k_x, k_y^2 - k_z^2\} J_x \\ &\quad + \{k_y, k_z^2 - k_x^2\} J_y + \{k_z, k_x^2 - k_y^2\} J_z], \end{aligned} \quad (8)$$

where $\mathbf{k} = (k_x, k_y, k_z)$ is the momentum vector and $\mathbf{J} = (J_x, J_y, J_z)$ is the vector of the 4×4 spin 3/2 matrices. We denote half of the anticommutator as $\{A, B\} = \frac{1}{2}(AB + BA)$. Going from bulk to two-dimensional systems and neglecting cubic k terms⁹⁶ the bulk DSOI can be directly transformed and expressed in the matrix form as

$$\begin{aligned} \hat{H}_{\text{BIA}}^{2\text{D}} &= -\beta_0 [k_x \{J_x, J_y^2 - J_z^2\} + k_y \{J_y, J_z^2 - J_x^2\}] \\ &\quad + \beta \langle k_z^2 \rangle (k_x J_x - k_y J_y) \\ &= \frac{\beta_0}{4} \begin{pmatrix} 0 & \sqrt{3}k_+ & 0 & 3k_- \\ \sqrt{3}k_- & 0 & -3k_+ & 0 \\ 0 & -3k_- & 0 & \sqrt{3}k_+ \\ 3k_+ & 0 & \sqrt{3}k_- & 0 \end{pmatrix} \\ &\quad + \frac{\beta \langle k_z^2 \rangle}{2} \begin{pmatrix} 0 & \sqrt{3}k_+ & 0 & 0 \\ \sqrt{3}k_- & 0 & 2k_+ & 0 \\ 0 & 2k_- & 0 & \sqrt{3}k_+ \\ 0 & 0 & \sqrt{3}k_- & 0 \end{pmatrix}, \end{aligned} \quad (9)$$

where $k_\pm = k_x \pm ik_y$. Similar as in the Luttinger-Kohn Hamiltonian, one has $\hbar k_q = -i\hbar \frac{\partial}{\partial q}$, where $q = x, y$. Numerical estimates of the DSOI coupling constants β_0 and β for different materials can be found in Refs. 63 and 97. We assume that the CdTe quantum well is symmetric in the z direction, thus Rashba spin-orbit interaction is absent in the investigated systems.

The time evolution of the system is described by the time-dependent Schrödinger equation which is solved numerically in an iterative manner:

$$\Psi(x, y, t + dt) = \Psi(x, y, t - dt) - \frac{2idt}{\hbar} \hat{H} \Psi(x, y, t), \quad (10)$$

which is solved self-consistently with the Poisson equation (5) and the self-interaction potential (7). Since the hole wave packet is moving, the Poisson equation has to be solved in every time step of the iteration procedure. We take the ground state wave function $\Psi_0(x, y) = \Psi(x, y, t_0)$ of the self-confined hole under the metal electrode as the initial condition for the time evolution numerical scheme (10). This ground state wave function is found by solving the stationary Schrödinger

equation

$$\hat{H}\Psi_0(x,y) = E\Psi_0(x,y) \quad (11)$$

using the imaginary time propagation (ITP) method.⁹⁸

III. GROUND STATE WAVE FUNCTION

It is important to know the contribution of different basis states in the ground state of the self-confined hole under the metal electrodes, i.e., the mixing of HH and LH states. We consider the system from Fig. 1: The hole is confined in the CdTe quantum well and covered by the system of electrodes. The center of the QW is 15 nm distant from the top metal electrodes (the QW layer and blocking layers are 10 nm thick). We perform calculations for CdTe with the following Luttinger parameters: $\gamma_1^{\text{CdTe}} = 5.3$, $\gamma_2^{\text{CdTe}} = 1.7$, $\gamma_3^{\text{CdTe}} = 2$, dielectric constant $\epsilon^{\text{CdTe}} = 10.125$, and the DSOI coupling constants $\beta_0 = 0.027 \text{ eV \AA}$, $\beta = 76.93 \text{ eV \AA}^3$. The hole is initially “prepared” in the $|\text{HH}\uparrow\rangle$ state. After the ITP procedure, the system relaxes to the “real” hole ground state. Let us now consider two situations, when the DSOI is present and when it is absent in the system.

For nonzero DSOI coupling constants we obtain the following probabilities to occupy the different basis hole states:

$$\begin{aligned} P_{|\text{HH}\uparrow\rangle} &= \int dx dy |\psi_{\text{HH}}^\uparrow(x,y,t_0)|^2 \approx 0.99, \\ P_{|\text{HH}\downarrow\rangle} &= \int dx dy |\psi_{\text{HH}}^\downarrow(x,y,t_0)|^2 \approx 0.01, \\ P_{|\text{LH}\uparrow\rangle} &= \int dx dy |\psi_{\text{LH}}^\uparrow(x,y,t_0)|^2 \approx 8.6 \times 10^{-5}, \\ P_{|\text{LH}\downarrow\rangle} &= \int dx dy |\psi_{\text{LH}}^\downarrow(x,y,t_0)|^2 \approx 1.1 \times 10^{-4}. \end{aligned}$$

The modulus square of the components of the Luttinger spinor ground state wave function $\Psi(x,y,t_0)$ are plotted in Fig. 2. When the DSOI is absent only the $|\text{HH}\uparrow\rangle$ and $|\text{HH}\downarrow\rangle$ are occupied with following probabilities: $P_{|\text{HH}\uparrow\rangle} \approx 1$, $P_{|\text{LH}\downarrow\rangle} \approx 8.7 \times 10^{-5}$. The obtained results show that the mixing between HH and LH states is negligible, the DSOI induces only a very small mixing into the HH state. This is an important result because in systems in which the hole occupies only the HH band, the hole spin coherence time is significantly longer than for electron spin.^{40,42} Furthermore, we can say that in the considered system the hole spin qubit is well defined with 99% probability in the subspace of the HH spin basis states.

IV. QUANTUM GATES

Recently we have shown that the motion of the hole along an induced quantum wire in the presence of DSOI can induce HH spin rotations.⁸⁸ In particular, during the motion of the hole along x ([100]) and y ([010]) direction, its spin rotates (precesses) around the axis parallel to the direction of motion and this process can be associated with following operations: $\hat{R}_x(\phi)$ and $\hat{R}_y(\phi)$. Their explicit form is⁹⁹

$$\hat{R}_x(\phi) = \frac{1}{\sqrt{2}} \begin{pmatrix} i\sqrt{1+\cos(\phi)} & \frac{\sin(\phi)}{\sqrt{1+\cos(\phi)}} \\ \frac{\sin(\phi)}{\sqrt{1+\cos(\phi)}} & i\sqrt{1+\cos(\phi)} \end{pmatrix}, \quad (12)$$

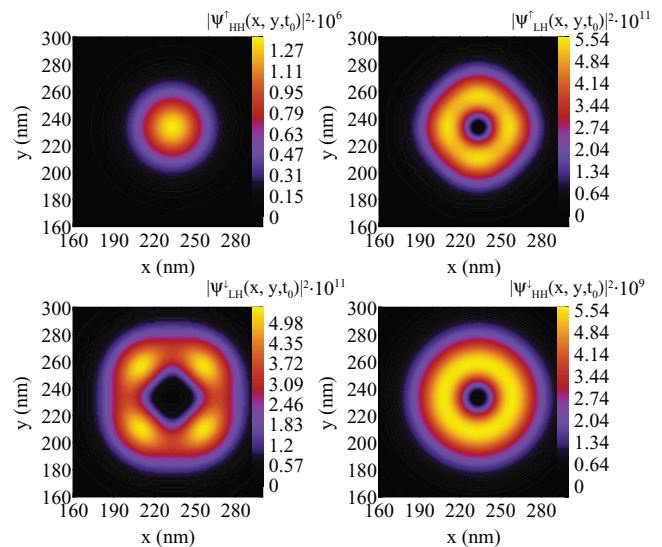


FIG. 2. (Color online) Modulus square of the components of the hole Luttinger spinor wave function: $|\psi_{\text{HH}}^\uparrow(x,y,t_0)|^2$, $|\psi_{\text{LH}}^\uparrow(x,y,t_0)|^2$, $|\psi_{\text{LH}}^\downarrow(x,y,t_0)|^2$, and $|\psi_{\text{HH}}^\downarrow(x,y,t_0)|^2$ in the spin up ground state in the presence of the DSOI interaction. It can be noticed that $\psi_{\text{HH}}^\uparrow(x,y,t_0)$ has the biggest contribution to the total wave function $\Psi(x,y,t_0)$, while the LH components $\psi_{\text{LH}}^\uparrow(x,y,t_0)$, $\psi_{\text{LH}}^\downarrow(x,y,t_0)$ are about 4 orders of magnitude smaller. In case of absence of the DSOI there are only two nonzero components $\psi_{\text{HH}}^\uparrow(x,y,t_0)$, $\psi_{\text{LH}}^\downarrow(x,y,t_0)$ and their modulus square looks identical as for those in the presence of DSOI as depicted in the above figure.

$$\hat{R}_y(\phi) = \frac{1}{\sqrt{2}} \begin{pmatrix} \sqrt{1+\cos(\phi)} & -\frac{\sin(\phi)}{\sqrt{1+\cos(\phi)}} \\ \frac{\sin(\phi)}{\sqrt{1+\cos(\phi)}} & \sqrt{1+\cos(\phi)} \end{pmatrix}, \quad (13)$$

where $\phi(t) = 2\pi \frac{\lambda(t)}{\lambda_{\text{SO}}}$ is the rotation angle, while $\lambda(t)$ is the distance traveled by the hole after time t , $q = x, y$ is the direction of motion as well as the axis around which the HH spin is rotated. After passing the distance λ_{SO} , the HH spin makes a full 2π rotation. The above operators [Eqs. (12) and (13)] act on the following wave function:

$$\Psi_{\text{HH}}(x,y,t) = \begin{pmatrix} \psi_{\text{HH}}^\uparrow(x,y,t) \\ \psi_{\text{HH}}^\downarrow(x,y,t) \end{pmatrix}, \quad (14)$$

which is defined in the subspace of HH basis states. For such a wave function we define the expectation value of the HH pseudospin $\frac{1}{2}$ as $s_i(t) = \frac{3}{2}\hbar \langle \Psi_{\text{HH}}(x,y,t) | \sigma_i | \Psi_{\text{HH}}(x,y,t) \rangle$, where the σ_i is a Pauli matrix, $i = x, y, z$.

Taking advantage of the fact that hole motion induces HH spin rotations, we can design nanodevices which are able to realize various single quantum logic gates. We use operators (12) and (13) to determine the topology of the metal electrodes that cover the nanodevice and in this way determine the hole trajectory which is passed by the hole during the realization of a certain quantum gate on a HH spin qubit. We propose nanodevices which can act as a quantum Pauli X, Y , and Z gate:

$$\hat{\sigma}_x = \begin{pmatrix} 0 & 1 \\ 1 & 0 \end{pmatrix}, \quad \hat{\sigma}_y = \begin{pmatrix} 0 & -i \\ i & 0 \end{pmatrix}, \quad \hat{\sigma}_z = \begin{pmatrix} 1 & 0 \\ 0 & -1 \end{pmatrix}. \quad (15)$$

Furthermore, we propose a nanodevice which is able to perform a quantum logic operation similar to the Hadamard gate, which we call the U_S gate:

$$\hat{U}_S = \frac{1}{\sqrt{2}} \begin{pmatrix} -1 & i \\ 1 & i \end{pmatrix}, \quad \hat{U}_S^{-1} = \frac{1}{\sqrt{2}} \begin{pmatrix} 1 & -1 \\ i & i \end{pmatrix}. \quad (16)$$

The Pauli Q gate performs the HH spin rotation about an angle π around the Q axis where $Q = X, Y, Z$. The $s_k = \frac{3}{2}\hbar$ HH spin state can be transformed into the $s_k = -\frac{3}{2}\hbar$ state using the σ_i or σ_j gate, where i, j, k can take x, y, z values while $i \neq j \neq k$.

The easiest to design and to implement (within the proposed nanostructure) quantum gates that transform one basis state into a balanced superposition of two basis states of the qubit are the U_S and U_S^{-1} gates. Their functionality is similar to the Hadamard gate but since $U_S^2 \neq I_{2 \times 2}$ ($U_S^3 = I_{2 \times 2}$) U_S is not exactly a Hadamard gate. Application of the U_S gate is equivalent to the rotation of the $s_x = \pm \frac{3}{2}\hbar$, $s_z = \pm \frac{3}{2}\hbar$ ($s_y = \pm \frac{3}{2}\hbar$) HH spin states around the $z, y, (x)$ axis about an angle $\pi/2, \pi/2$ ($-\pi/2$), respectively, such that the states $s_y = \mp \frac{3}{2}\hbar$, $s_x = \mp \frac{3}{2}\hbar$ ($s_z = \pm \frac{3}{2}\hbar$) are produced. The reverse process can be obtained by applying the U_S^{-1} gate.

In order to demonstrate how quantum logic operations are realized, we make a precise numerical time-dependent simulation. We depict the time evolution of the expectation value of the HH spin $s_x(t), s_y(t), s_z(t)$, the average position of the hole $x(t), y(t)$, and the probability of occupying the hole basis states $|\text{HH}\uparrow\rangle, |\text{LH}\uparrow\rangle, |\text{LH}\downarrow\rangle, |\text{HH}\downarrow\rangle$ in parts (a), (b), and (c) of Figs. 3–6 for each quantum operation process. The nanodevices are covered by a specially designed system of electrodes which define the path—a closed rectangular loop—which has to be traveled by the hole in order to realize the desired quantum logic operation. The scheme of metal electrodes labeled by e_1 – e_5 which cover the nanodevices, the hole trajectory, and the contour plots of the hole charge density at a few moments of time are depicted in part (d) of Figs. 3–6.

In the initial step of each quantum operation process, the hole is confined under electrode e_1 with dimensions 50×50 nm on which a constant $V_1 = -0.3$ mV voltage is applied. The voltage applied to the other electrodes $e_{2,3,4,5}$ is set to $V_{2,3,4,5} = 0$. The distance between e_1 and the neighbor $e_{2,3,4,5}$ electrodes is about 7 nm. It should be mentioned that due to the Schotky contact, the Schotky voltage V_{Schotky} has to be taken into account with mV accuracy and the “real” voltage applied to the metal gates is $V_i \rightarrow V_i - V_{\text{Schotky}}$. V_{Schotky} should be determined experimentally for a particular structure. In case of the Pauli X (NOT) gate we assume that the hole is initially prepared in the HH spin $s_y = \frac{3}{2}\hbar$ state:

$$\Psi(x, y, t_0) = \frac{1}{\sqrt{2}} \begin{pmatrix} \psi_{\text{HH}}^\uparrow(x, y, t_0) \\ 0 \\ 0 \\ i\psi_{\text{HH}}^\downarrow(x, y, t_0) \end{pmatrix}, \quad (17)$$

while the “magnetic free” preparation of the hole spin states can be achieved using experimentally demonstrated methods⁴⁸ or by utilizing an analogous device to those which we recently proposed¹⁰⁰ to prepare the electron spin in a certain state without application of a magnetic field.

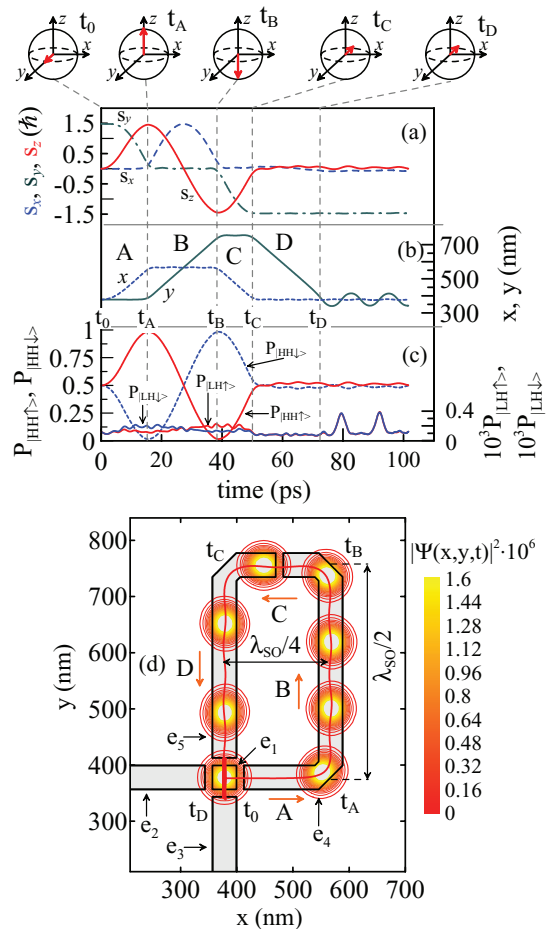


FIG. 3. (Color online) The time evolution of the expectation value of the HH spin components $s_x(t), s_y(t), s_z(t)$ (a), average position $x(t), y(t)$ of the hole wave packet (b), and the occupation probabilities $P_{|\text{HH}\uparrow\rangle}(t), P_{|\text{HH}\downarrow\rangle}(t), P_{|\text{LH}\uparrow\rangle}(t), P_{|\text{LH}\downarrow\rangle}(t)$ of the hole basis states (c), for the quantum Pauli X (NOT) gate which is covered by the system of electrodes e_1 – e_5 presented in (d). (c) The left (right) axis corresponds to the probability of finding the hole in the HH (LH) spin states. (d) The solid red line represents the hole trajectory (the orange arrow represents the direction of motion of the hole). The hole is initially confined under electrode e_1 and moves in the $+x$ direction. The HH spin qubit state is depicted on the Bloch spheres at times t_0, t_A, t_B, t_C, t_D of the quantum gate operation cycle. The contour plots represent the charge density $\rho(x, y, t)$ at a few selected moments in time.

The hole is forced to move in the $+x$ direction by changing the voltage applied on e_1 to $V_1 = 0$ and switching the voltage on e_4 to $V_4 = -0.3$ mV. In our numerical scheme the voltage is changed linearly in time in a duration of $t_{\text{rise}} = 0.1$ ps. (For a longer $t_{\text{rise}} = 1$ ps the gate operation time is identical, while for $t_{\text{rise}} = 5$ ps the gate operation time is about 2.5 ps longer. It is caused by the slightly smaller initial hole momentum.) After traveling the $\lambda_{\text{SO}}/4$ long segment A of the loop the $\hat{R}_x(\pi/2)$ operation is performed on the HH spin. At the end of segment A, the hole wave packet reflects from the potential barrier at the corner of electrode e_4 and changes its direction of motion into the $+y$ direction. Next the hole passes the segment B whose length is $\lambda_{\text{SO}}/2$ and realizes a $\hat{R}_y(\pi)$ rotation. In the meantime the voltage applied to electrode e_5 was set to the voltage of

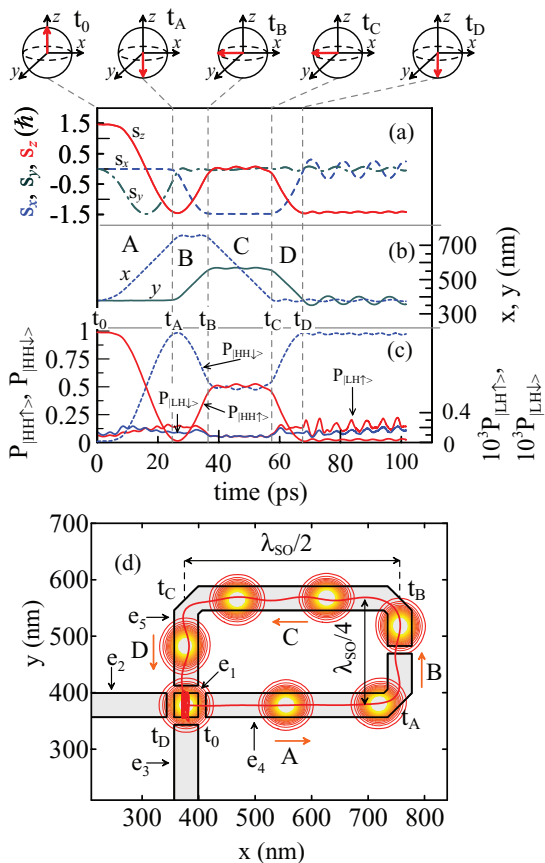


FIG. 4. (Color online) The same as Fig. 3, but for the quantum Pauli Y gate which is covered by the system of electrodes e_1 – e_5 presented in (d).

the e_4 electrode so that the hole can enter easily under e_5 . Then the hole passes segments C and D, realizing $\hat{R}_x(-\pi/2)$ and $\hat{R}_y(-\pi)$ operations, respectively, and finally returns under electrode e_1 whose voltage is set to $V_1 = -0.3$ mV, while the voltage on the neighbor electrodes e_2 – e_5 is set to $V_{2,3,4,5} = 0.6$ mV. After passing the whole loop, a set of HH spin rotations is performed resulting in the Pauli X operation:

$$\hat{R}_y(-\pi)\hat{R}_x(-\pi/2)\hat{R}_y(\pi)\hat{R}_x(\pi/2) = e^{i3\pi/2}\hat{\sigma}_x. \quad (18)$$

The Pauli Y gate is realized by the nanodevice covered by the system of electrodes shown in Fig. 4(d). In this case, as initial condition in our simulation, we take a HH spin up state $s_z = \frac{3}{2}\hbar$:

$$\Psi(x, y, t_0) = \begin{pmatrix} \psi_{\text{HH}}^\uparrow(x, y, t_0) \\ 0 \\ 0 \\ 0 \end{pmatrix}. \quad (19)$$

At the beginning of the gate operation process the hole is forced to move in the $+x$ direction and follows the trajectory defined by the metal gates deposited on top of the nanodevice. The hole passes the A, B, C, and D segments, realizing appropriate rotations and finally the Pauli Y gate is performed:

$$\hat{R}_y(-\pi/2)\hat{R}_x(-\pi)\hat{R}_y(\pi/2)\hat{R}_x(\pi) = e^{i\pi/2}\hat{\sigma}_y. \quad (20)$$

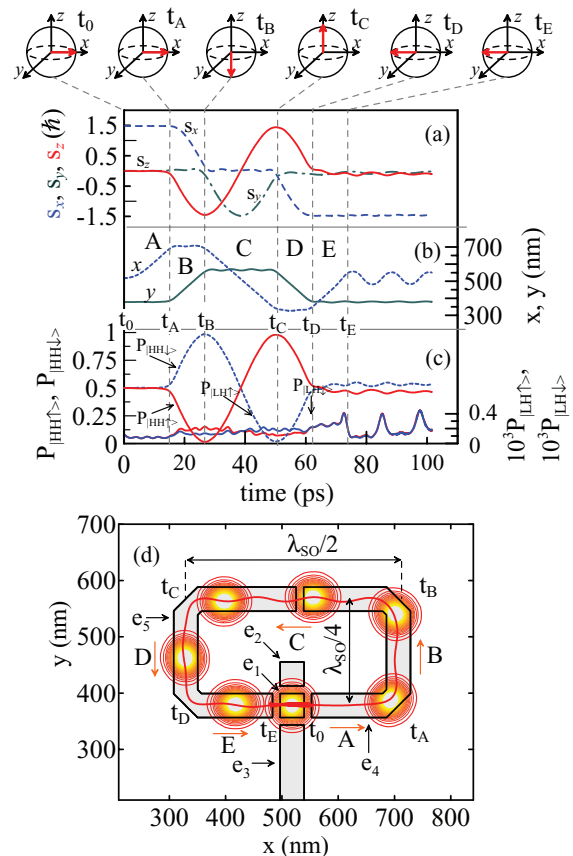


FIG. 5. (Color online) The same as Fig. 3, but for the quantum Pauli Z gate which is covered by the system of electrodes e_1 – e_5 presented in (d).

The scheme of the electrodes which cover the nanodevice that acts as a Pauli Z (a phase π flip) gate is depicted in Fig. 5(d). Let us assume that initially the hole is prepared in the HH spin $s_x = 3/2\hbar$ state:

$$\Psi(x, y, t_0) = \frac{1}{\sqrt{2}} \begin{pmatrix} \psi_{\text{HH}}^\uparrow(x, y, t_0) \\ 0 \\ 0 \\ \psi_{\text{HH}}^\downarrow(x, y, t_0) \end{pmatrix}. \quad (21)$$

After changing gate the voltage configuration to $V_4 = -0.3$ mV the hole starts to move in the $+x$ direction and subsequently passes A, B, C, D, and E segments of the loop and eventually realizes the quantum logic operation

$$\hat{R}_x(\pi/2)\hat{R}_y(-\pi/2)\hat{R}_x(-\pi)\hat{R}_y(\pi/2)\hat{R}_x(\pi/2) = \hat{\sigma}_z. \quad (22)$$

The last proposed gate U_S can be realized by the nanodevice which is covered by the system of metal gates shown in Fig. 6(d). We make a numerical simulation starting with a HH spin up state. In the first step of this proposal, the hole is injected under the electrode e_4 in the $+x$ direction. Then the hole moves along the loop which consist of the segments A, B, C, and D and carries out certain HH spin rotations. Finally, the hole returns to its initial position and the U_S operation is

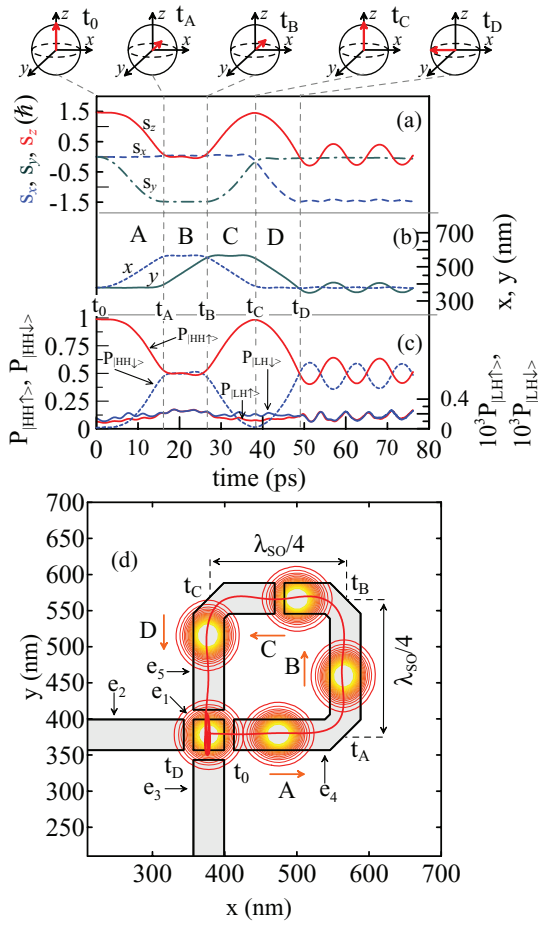


FIG. 6. (Color online) The same as Fig. 3, but for the quantum U_S gate which is covered by the system of electrodes e_1 – e_5 presented in (d).

accomplished:

$$\hat{R}_y(-\pi/2)\hat{R}_x(-\pi/2)\hat{R}_y(\pi/2)\hat{R}_x(\pi/2) = e^{i\pi/4}\hat{U}_S. \quad (23)$$

The inverse operation U_S^{-1} ,

$$\hat{R}_x(-\pi/2)\hat{R}_y(-\pi/2)\hat{R}_x(\pi/2)\hat{R}_y(\pi/2) = e^{i3\pi/4}\hat{U}_S^{-1}, \quad (24)$$

can be obtained by transporting the hole in the same loop but in the opposite direction.

In all proposed gates the hole returns to its initial position after completing the set of transformations and consequently the quantum logic operation is performed exclusively on the HH spin state. The hole is trapped when it reaches the area under the e_1 electrode which can be achieved by applying the following voltage configuration scheme: $e_1 = -0.3$ mV and $e_{2,3,4,5} = +0.6$ mV. Since there is no energy dissipation term in the Hamiltonian (1), the kinetic energy of the hole (which was transferred to it at the initial time step of the gate operation process) is still present in the system after its trapping. This is the reason why the position of the hole wave packet and the expectation value of its spin oscillate after trapping under the e_1 electrode. In general, due to interactions with phonons kinetic energy can be lost and eventually the hole will stop as well as its spin will end its oscillation. The presence of an additional quantum well may also lead to the energy

dissipation of the soliton⁹⁴ caused by the retardation effect. Thus in the presented setup energy dissipation (which does not lead to spin dephasing) is rather a desired effect.

Despite the fact that after trapping the hole position still oscillates, in certain cases it may practically not affect the final value of the spin. This can be achieved if in the last step of the gate operation process the hole spin is parallel to its direction of motion like in the case of Pauli X and Pauli Z gates acting on $s_y = \pm\frac{3}{2}\hbar$ and $s_x = \pm\frac{3}{2}\hbar$, respectively.

It should be noticed that in order to achieve a straight hole trajectory after reflection from a corner in the loop, the initial hole velocity (controlled by the magnitude of the voltages) should be properly adjusted. If the voltage is not properly adjusted, the trajectory is oscillating but fortunately it only slightly affects the final value of the spin. This deviation from the perfect gate result is a measure for the gate fidelity $\mathcal{F}_{\text{gate}} = |\langle\Psi|U_{\text{perfect}}^\dagger U_{\text{simulated}}|\Psi\rangle|^2$. The fidelity of the proposed gates ($\mathcal{F}_{\text{gate}}$) which is slightly affected by these oscillations takes the following values: $98.6\% < \mathcal{F}_{\text{Pauli X}} < 99.4\%$, $99.3\% < \mathcal{F}_{\text{Pauli Y}} < 99.8\%$, $99.7\% < \mathcal{F}_{\text{Pauli Z}} < 99.9\%$, $97.8\% < \mathcal{F}_{U_S} < 99.9\%$. The easiest factor to tune which affects the hole

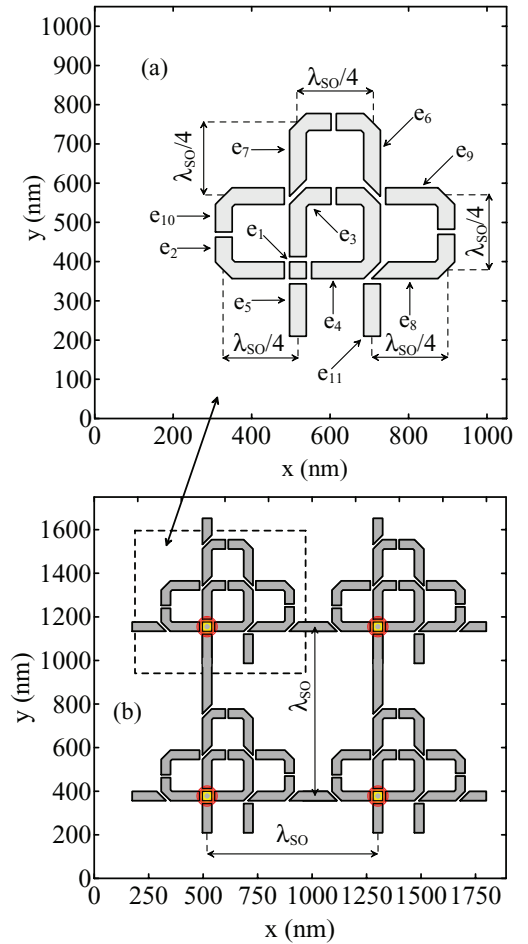


FIG. 7. (Color online) The system of electrodes which covers the combo nanodevice (a). The electrodes are labeled with e_1 – e_{11} . The interelectrode distance is about 7 nm. Fragment of the scalable architecture (b) consisting of four HH spin qubits on which the proposed quantum gates can be applied one by one and in an arbitrary sequence.

TABLE I. Proposed voltage configuration scheme which has to be applied to the electrodes that cover the gated combo nanodevice in order to realize a Pauli X, Y, Z and U_S quantum logic operation. In the presented simulation we take $V_0 = -0.4$ mV.

Gate label \ time	Pauli X gate				Pauli Y gate				Pauli Z gate				U_S gate			
	t_0	t_{start}	t_{change}	t_{stop}	t_0	t_{start}	t_{change}	t_{stop}	t_0	t_{start}	t_{change}	t_{stop}	t_0	t_{start}	t_{change}	t_{stop}
V_1	V_0	0	V_0	V_0	V_0	0	V_0	V_0	V_0	0	V_0	V_0	V_0	0	V_0	V_0
V_2	0	0	V_0	$-2V_0$	0	0	V_0	$-2V_0$	0	0	V_0	$-2V_0$	0	0	V_0	$-2V_0$
V_3	0	0	V_0	$-2V_0$	0	0	V_0	$-2V_0$	0	0	V_0	$-2V_0$	0	0	V_0	$-2V_0$
V_4	0	V_0	V_0	$-2V_0$	0	V_0	V_0	$-2V_0$	0	V_0	V_0	$-2V_0$	0	V_0	V_0	$-2V_0$
V_5	0	0	0	$-2V_0$	0	0	0	$-2V_0$	0	0	V_0	$-2V_0$	0	0	0	$-2V_0$
V_6	0	V_0	V_0	V_0	0	V_0	V_0	V_0	0	$-V_0$	$-V_0$	$-V_0$	0	$-V_0$	$-V_0$	$-V_0$
V_7	0	V_0	V_0	V_0	0	$-V_0$	$-V_0$	$-V_0$	0	V_0	V_0	V_0	0	$-V_0$	$-V_0$	$-V_0$
V_8	0	$-V_0$	$-V_0$	$-V_0$	0	V_0	V_0	V_0	0	$-V_0$	$-V_0$	$-V_0$	0	$-V_0$	$-V_0$	$-V_0$
V_9	0	V_0	V_0	V_0	0	V_0	V_0	V_0	0	$-V_0$	$-V_0$	$-V_0$	0	$-V_0$	$-V_0$	$-V_0$
V_{10}	0	V_0	V_0	V_0	0	$-V_0$	$-V_0$	$-V_0$	0	V_0	V_0	V_0	0	$-V_0$	$-V_0$	$-V_0$
V_{11}	0	$-V_0$	$-V_0$	$-V_0$	0	V_0	V_0	V_0	0	$-V_0$	$-V_0$	$-V_0$	0	$-V_0$	$-V_0$	$-V_0$

trajectory is the initial gate voltage. By properly adjusting this voltage, one can get a straight hole trajectory. On the other hand, with higher voltages the hole moves faster and one can get faster gates but with a slightly smaller gate fidelity.

V. GATED COMBO NANODEVICE

All of the previously proposed nanodevices which realize HH qubit quantum gates can be integrated into a single so called gated combo nanodevice. This device is capable of realizing Pauli X, Y, Z and U_S quantum logic operations in an arbitrary sequence. The nanodevice is covered by 11 electrodes labeled by e_1-e_{11} which are depicted in Fig. 7(a). In order to realize a certain quantum logic gate in this nanodevice a special scheme of voltages V_1-V_{11} has to be applied to the electrodes e_1-e_{11} . The voltages have to be switched several times during the gate operation process. We denote t_0 as the initial time step at which the hole is confined under electrode e_1 , which can be achieved by application of the following voltage configuration $V_1 = V_0$ (in numerical simulation we take $V_0 = -0.4$ mV) and $V_{2,3,4,5} = 0$, respectively, to electrode e_1 and its neighbor electrodes $e_{2,3,4,5}$. The time t_{start} corresponds to the moment the hole is forced to move. In all proposed gates (except the U_S^{-1} gate) the hole is initially injected from under e_1 to under

e_4 (e_3) which is realized by switching the voltage to $V_1 = 0$ and $V_4 = V_0$ ($V_3 = V_0$). During the gate operation process the voltage on some electrodes has to be changed at time t_{change} so the hole can enter the appropriate area of the nanodevice. At the end of the gate operation cycle the hole returns to its initial position under e_1 . At t_{stop} it is captured again by using the following voltage configuration scheme: $V_1 = V_0$ and $V_{2,3,4,5} = -2V_0$. The voltage configuration scheme which has to be applied to the electrodes in order to realize a particular quantum logic gate is shown in Table I.

We performed time-dependent simulations of each quantum gate that can be realized by this nanodevice taking $V_0 = -0.4$ mV, which is slightly larger than for the separate nanodevices (-0.3 mV) from the previous section. The larger voltage and thus hole momentum is necessary in this case to allow the hole to pass easily through the regions between electrodes (depending on the gate we want to realize): e_4 and e_6 , e_4 and e_8 , e_3 and e_{10} , respectively, for Pauli X, Y , and Z gates. This larger initial momentum as well as the presence of additional electrodes which induce some asymmetry in the electrostatic potential distribution (lateral confinement potential) result in a “wavy” hole trajectory which is depicted in Fig. 9 (a_j), where j denotes the certain quantum gate. Fortunately, a hole trajectory that is not perfectly straight only affects the final spin

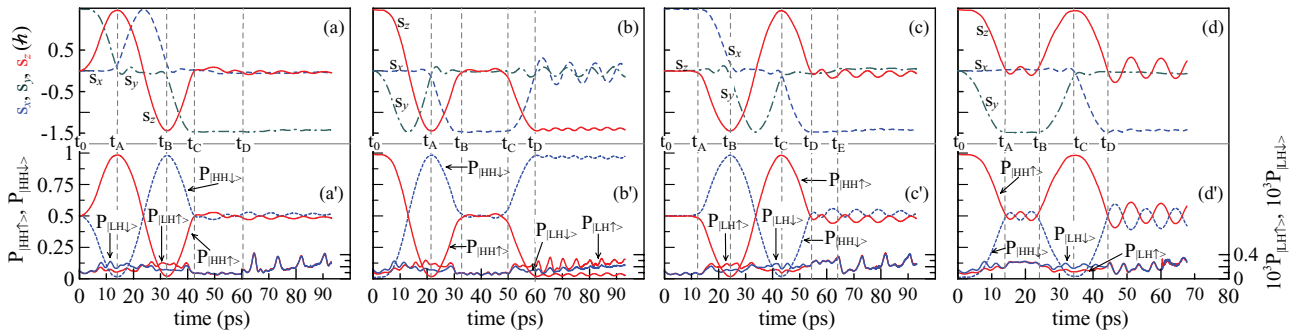


FIG. 8. (Color online) Time evolution of the HH spin components for the Pauli X (a), Y (b), Z (c), and U_S gate (d) realized by the gated combo nanodevice which is covered by the system of electrodes shown in Fig. 7(a). The electrode voltage scheme which is responsible for initialization and control of a particular quantum logic operation can be found in Table I. The corresponding occupation probabilities for the HH and LH spin states are depicted in (a'), (b'), (c'), and (d'). The hole trajectory for each quantum gate realized by the combo nanodevice can be found in Fig. 9 (a_j), where j denotes the quantum gate.

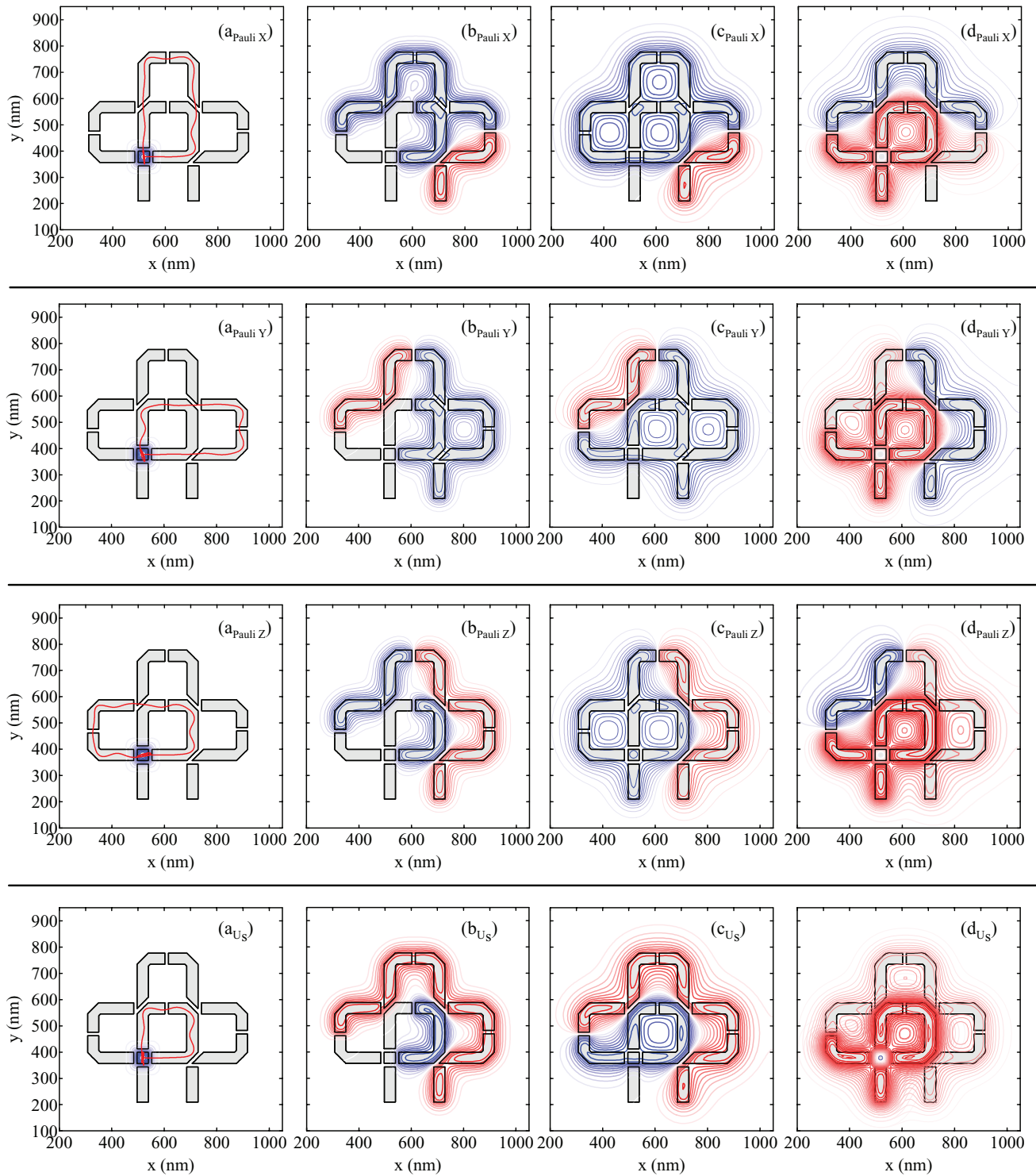


FIG. 9. (Color online) The electrostatic potential distribution $\phi_0(x, y, z_0)$ in the quantum well layer (z_0) which comes from the presence of the electrodes to which a certain voltage V_i is applied according to the scheme from Table I, where $i = 1, \dots, 11$. The $\phi_0(x, y, z_0)$ is plotted for four crucial moments of time of the quantum gate operation process: (a_j) $t \leq t_0$, (b_j) $t_{\text{start}} < t < t_{\text{change}}$, (c_j) $t_{\text{change}} < t < t_{\text{stop}}$, (d_j) $t_{\text{stop}} < t$. The hole trajectory is depicted in (a_j), where j denotes a particular quantum gate. The red isolines denote a positive electrostatic potential distribution while the blue lines a negative one.

state slightly. In this case the fidelity of proposed gates takes the following values: $96.8\% < \mathcal{F}_{\text{Pauli } X} < 99.1\%$, $98.5\% < \mathcal{F}_{\text{Pauli } Y} < 99.6\%$, $99.7\% < \mathcal{F}_{\text{Pauli } Z} < 99.9\%$, $99.1\% < \mathcal{F}_{U_s} <$

99.9% . We plot the time evolution of average HH pseudospin components $s_x(t)$, $s_y(t)$, $s_z(t)$ in Figs. 8(a)–8(d) and the occupation probability of the different hole spin basis

states: $P_{|\text{HH}\uparrow\rangle}(t), P_{|\text{HH}\downarrow\rangle}(t), P_{|\text{LH}\uparrow\rangle}(t), P_{|\text{LH}\downarrow\rangle}(t)$ can be found in Figs. 8(a')–8(d') for each quantum gate cycle (Pauli X , Y , Z and U_S) realized by the proposed combo nanodevice. Application of the gate voltages as well as its geometry define the path which is passed by the hole. The area under a positively charged electrode forms a barrier for the moving hole while a negatively charged electrode forms a potential well within which the hole can be transported. In order to illustrate how the gate voltage influences the hole trajectory, we plot the electrostatic potential distribution $\phi_0(x, y, z_0)$ in the quantum well region which comes from the presence of the electrodes and gate voltages applied to them at four crucial moments $t < t_0$, $t_{\text{start}} < t < t_{\text{change}}$, $t_{\text{change}} < t < t_{\text{stop}}$, $t_{\text{stop}} < t$ for each (Pauli X , Y , Z and U_S) gate cycle. The electrostatic potential $\phi_0(x, y, z_0)$ is the solution of Laplace equation in the quantum well (z_0) region

$$\nabla^2 \phi_0(x, y, z) = 0, \quad (25)$$

with boundary conditions determined by the presence of the electrodes $\phi_0(x, y, z_{\text{electrodes}}) = V_{1-11}$. We have plotted $\phi_0(x, y, z_0)$ in Fig. 9.

In the presence of the hole there is an additional dip in the electrostatic distribution localized in the center of the hole wave packet and as the hole moves this dip follows the hole (self-trapping mechanism). The total potential which is felt by the hole in the quantum well region was defined in Sec. II as $\Phi(x, y, z_0, t)$.

For the presented electric control scheme t_{change} corresponds to a different moment of time for each quantum logic gate. In case of the Pauli X gate it is reasonable to change the voltage when the hole is in the area between the e_6 and e_7 electrode and it is done in the numerical simulation at $t_{\text{change}} \approx 35$ ps. For the Pauli Y gate process it is convenient to choose $t_{\text{change}} \approx 35$ ps, when the hole is between the electrodes e_8 and e_9 . When the nanodevice realizes the Pauli Z or U_S (U_S^{-1}) gate, the voltage is changed at $t_{\text{change}} \approx 15$ ps when the hole is under electrode e_4 (it is in the middle of e_3 at $t_{\text{change}} \approx 10$ ps) just after the reflection from the first corner. The hole is stopped at $t_{\text{stop}} \approx 60$ ps, $t_{\text{stop}} \approx 60$ ps, $t_{\text{stop}} \approx 63$ ps, and $t_{\text{stop}} \approx 44$ ps for Pauli X , Y , Z and U_S gates, respectively.

The fact that in the proposed device the quantum operations are controlled only by the weak constant voltages applied to locally defined electrodes allows for the realization of a scalable architecture. In Fig. 7(b) we plot the systems of electrodes for a scalable system of HH qubits on which each of the proposed gates can be applied in an individual, selective manner.

Furthermore, the proposed device is suitable for coherent transport of a hole wave packet and thus allows for transferring quantum information between different locations within the nanodevice. Thanks to this property two qubit gates can be

realized by transporting a hole from one induced quantum dot to another one so that the two holes can occupy the same region (the hole wave functions can overlap), for example under electrode e_1 , for a certain time t . Thanks to the exchange interaction their spins can swap according to the Heisenberg exchange Hamiltonian $H_s(t) = J(t)\vec{S}_1 \cdot \vec{S}_2$ similar as two electron qubit gates are realized in two electron double quantum dots. More details about two electron and hole soliton dynamics as well as two qubit gate implementation in induced quantum dots and wires will be published in a forthcoming paper.

VI. SUMMARY

In conclusion, we proposed a set of nanodevices which can act as single quantum logic gates (Pauli X , Y , Z and U_S) and a combo nanodevice which is capable to perform any of the Pauli X , Y , Z and U_S gate operations in an arbitrary sequence on a HH spin qubit. Quantum logic operations can be realized all electrically and ultrafast, i.e., within 70 ps. The proposed devices are based on induced quantum dots and wires which allow for transporting the hole in the form of a stable solitonlike wave packet, while the hole trajectory is determined by the geometry and voltages applied to the top electrodes. The motion of the hole along specially designed paths in the presence of the Dresselhaus spin-orbit field is equivalent to the sequential application of static magnetic fields which rotate the HH spin qubit. This control method allows us to avoid the application of real magnetic fields which, because of the very small hole in-plane g factor, have to be of the order of several Teslas, which is still experimentally challenging to achieve.

Since quantum gates are controlled only by low static electric fields generated by the local top electrodes, our proposal can be extended to a larger number of qubits stored in the quantum register as in Fig. 7(b) where each qubit can be manipulated individually. Therefore, a scalable architecture can be realized. Furthermore, the proposed device is suitable for coherent transport of a hole wave packet, and thus allows for transferring quantum information between different locations in the nanodevice which gives perspective to couple long distant HH spin qubits and realize two qubit quantum gates in this proposed scalable system.

ACKNOWLEDGMENTS

This work was supported by the Polish National Science Center (Grant No. DEC-2011/03/N/ST3/02963), as well as by the ‘‘Krakow Interdisciplinary PhD-Project in Nanoscience and Advanced Nanostructures’’ operated within the Foundation for Polish Science MPD Programme, co-financed by the European Regional Development Fund. This research was supported in part by PL-Grid Infrastructure.

*pawel.szumniak@gmail.com

¹D. Awszalom, D. Loss, and N. Samarth, *Semiconductor Spintronics and Quantum Computation* (Springer, Berlin, 2002).

²I. Zutic, J. Fabian, and S. Das Sarma, *Rev. Mod. Phys.* **76**, 323 (2004).

³D. Loss and D. P. DiVincenzo, *Phys. Rev. A* **57**, 120 (1998).

⁴R. Hanson, L. P. Kouwenhoven, J. R. Petta, S. Tarucha, and L. M. K. Vandersypen, *Rev. Mod. Phys.* **79**, 1217 (2007).

- ⁵S. Amasha, K. MacLean, I. P. Radu, D. M. Zumbuhl, M. A. Kastner, M. P. Hanson, and A. C. Gossard, *Phys. Rev. Lett.* **100**, 046803 (2008).
- ⁶J. R. Petta, A. C. Johnson, J. M. Taylor, E. A. Laird, A. Yacoby, M. D. Lukin, C. M. Marcus, M. P. Hanson, and A. C. Gossard, *Science* **309**, 2180 (2005).
- ⁷J. M. Elzerman, R. Hanson, L. H. Willem van Beveren, B. Witkamp, L. M. K. Vandersypen, and L. P. Kouwenhoven, *Nature (London)* **430**, 431 (2004).
- ⁸T. Meunier, I. T. Vink, L. H. W. van Beveren, F. H. L. Koppens, H. P. Tranitz, W. Wegscheider, L. P. Kouwenhoven, and L. M. K. Vandersypen, *Phys. Rev. B* **74**, 195303 (2006).
- ⁹F. H. L. Koppens, C. Buizert, K. J. Tielrooij, I. T. Vink, K. C. Nowack, T. Meunier, L. P. Kouwenhoven, and L. M. K. Vandersypen, *Nature (London)* **442**, 766 (2006).
- ¹⁰A. Morello, J. J. Pla, F. A. Zwanenburg, K. W. Chan, K. Y. Tan, H. Huebl, M. Möttönen, C. D. Nugroho, C. Yang, J. A. van Donkelaar, A. D. C. Alves, D. N. Jamieson, C. C. Escott, L. C. L. Hollenberg, R. G. Clark, and A. S. Dzurak, *Nature (London)* **467**, 687 (2010).
- ¹¹K. C. Nowack, F. H. L. Koppens, Yu. V. Nazarov, and L. M. K. Vandersypen, *Science* **318**, 1430 (2007).
- ¹²S. Nadj-Perge, S. M. Frolov, E. P. A. M. Bakkers and L. P. Kouwenhoven, *Nature (London)* **468**, 1084 (2010).
- ¹³S. Nadj-Perge, V. S. Pribiag, J. W. G. van den Berg, K. Zuo, S. R. Plissard, E. P. A. M. Bakkers, S. M. Frolov, and L. P. Kouwenhoven, *Phys. Rev. Lett.* **108**, 166801 (2012).
- ¹⁴R. Hanson and D. D. Awschalom, *Nature (London)* **453**, 1043 (2008).
- ¹⁵D. P. DiVincenzo, *Fortschr. Phys.* **48**, 771 (2000).
- ¹⁶I. A. Merkulov, A. L. Efros, and M. Rosen, *Phys. Rev. B* **65**, 205309 (2002).
- ¹⁷A. V. Khaetskii, D. Loss, and L. Glazman, *Phys. Rev. Lett.* **88**, 186802 (2002).
- ¹⁸L. Cywiński, W. M. Witzel, and S. Das Sarma, *Phys. Rev. Lett.* **102**, 057601 (2009).
- ¹⁹W. A. Coish and J. Baugh, *Phys. Status Solidi B* **246**, 2203 (2009).
- ²⁰J. Fischer and D. Loss, *Science* **324**, 1277 (2009).
- ²¹A. Abragam, *The Principles of Nuclear Magnetism* (Oxford University Press, New York, 1983).
- ²²F. H. L. Koppens, K. C. Nowack, and L. M. K. Vandersypen, *Phys. Rev. Lett.* **100**, 236802 (2008).
- ²³H. Bluhm, S. Foletti, I. Neder, M. Rudner, D. Mahalu, V. Umansky, and A. Yacoby, *Nat. Phys.* **7**, 109 (2010).
- ²⁴W. A. Coish, *Nat. Phys.* **5**, 710 (2009).
- ²⁵C. Latta, A. Högele, Y. Zhao, A. N. Vamivakas, P. Maletinsky, M. Kroner, J. Dreiser, I. Carusotto, A. Badolato, D. Schuh, W. Wegscheider, M. Atature, and A. Imamoglu, *Nat. Phys.* **5**, 758 (2009).
- ²⁶D. J. Reilly, J. M. Taylor, J. R. Petta, C. M. Marcus, M. P. Hanson, and A. C. Gossard, *Science* **321**, 817 (2008).
- ²⁷A. Greilich, A. Shabaev, D. R. Yakovlev, A. L. Efros, I. A. Yugova, D. Reuter, A. D. Wieck, and M. Bayer, *Science* **317**, 1896 (2007).
- ²⁸J. J. Pla, K. Y. Tan, J. P. Dehollain, W. H. Lim, J. J. L. Morton, D. N. Jamieson, A. S. Dzurak and Andrea Morello, *Nature (London)* **489**, 541 (2012).
- ²⁹B. M. Maune, M. G. Borselli, B. Huang, T. D. Ladd, P. W. Deelman, K. S. Holabird, A. A. Kiselev, I. Alvarado-Rodriguez, R. S. Ross, A. E. Schmitz, M. Sokolich, C. A. Watson, M. F. Gyure, and A. T. Hunter, *Nature (London)* **481**, 344 (2012).
- ³⁰D. V. Bulaev, B. Trauzettel, and D. Loss, *Phys. Rev. B* **77**, 235301 (2008).
- ³¹F. Pei, E. A. Laird, G. A. Steele, and L. P. Kouwenhoven, *Nat. Nanotechnol.* **7**, 630 (2012).
- ³²B. Trauzettel, D. V. Bulaev, D. Loss, and G. Burkard, *Nat. Phys.* **3**, 192 (2007).
- ³³J. R. Maze, J. M. Taylor, and M. D. Lukin, *Phys. Rev. B* **78**, 094303 (2008).
- ³⁴G. D. Fuchs, V. V. Dobrovitski, D. M. Toyli, F. J. Heremans, C. D. Weis, T. Schenkel, and D. D. Awschalom, *Nat. Phys.* **6**, 668 (2010).
- ³⁵G. D. Fuchs, G. Burkard, P. V. Klimov, and D. D. Awschalom, *Nat. Phys.* **7**, 789 (2011).
- ³⁶D. M. Toyli, D. J. Christle, A. Alkauskas, B. B. Buckley, C. G. Van de Walle, and D. D. Awschalom, *Phys. Rev. X* **2**, 031001 (2012).
- ³⁷G. Burkard, *Nat. Mater.* **7**, 100 (2008).
- ³⁸M. H. Kolodrubetz and J. R. Petta, *Science* **325**, 42 (2009).
- ³⁹A. Tartakovskii, *Nat. Photon.* **5**, 647 (2011).
- ⁴⁰J. Fischer, W. A. Coish, D. V. Bulaev, and D. Loss, *Phys. Rev. B* **78**, 155329 (2008).
- ⁴¹B. Eble, C. Testelin, P. Desfonds, F. Bernardot, A. Balocchi, T. Amand, A. Miard, A. Lemaître, X. Marie, and M. Chamarro, *Phys. Rev. Lett.* **102**, 146601 (2009).
- ⁴²C. Testelin, F. Bernardot, B. Eble, and M. Chamarro, *Phys. Rev. B* **79**, 195440 (2009).
- ⁴³P. Fallahi, S. T. Yilmaz, and A. Imamoglu, *Phys. Rev. Lett.* **105**, 257402 (2010).
- ⁴⁴P. Desfonds, B. Eble, F. Fras, C. Testelin, F. Bernardot, M. Chamarro, B. Urbaszek, T. Amand, X. Marie, J.-M. Gérard, V. Thierry-Mieg, A. Miard, and A. Lemaître, *Appl. Phys. Lett.* **96**, 172108 (2010).
- ⁴⁵E. A. Chekhovich, A. B. Krysa, M. S. Skolnick, and A. I. Tartakovskii, *Phys. Rev. Lett.* **106**, 027402 (2011).
- ⁴⁶Z. K. Keane, M. C. Godfrey, J. C. H. Chen, S. Fricke, O. Klochan, A. M. Burke, A. P. Micolich, H. E. Beere, D. A. Ritchie, K. V. Trunov, D. Reuter, A. D. Wieck, and A. R. Hamilton, *Nano Lett.* **11**, 3147 (2011).
- ⁴⁷D. Heiss, S. Schaeck, H. Huebl, M. Bichler, G. Abstreiter, J. J. Finley, D. V. Bulaev, and D. Loss, *Phys. Rev. B* **76**, 241306 (2007).
- ⁴⁸B. D. Gerardot, D. Brunner, P. A. Dalgarno, P. Öhberg, S. Seidl, M. Kroner, K. Karrai, N. G. Stoltz, P. M. Petroff, and R. J. Warburton, *Nature (London)* **451**, 441 (2008).
- ⁴⁹D. Brunner, B. D. Gerardot, P. A. Dalgarno, G. Wüst, K. Karrai, N. G. Stoltz, P. M. Petroff, and R. J. Warburton, *Science* **325**, 70 (2009).
- ⁵⁰F. Fras, B. Eble, P. Desfonds, F. Bernardot, C. Testelin, M. Chamarro, A. Miard, and A. Lemaître, *Phys. Rev. B* **84**, 125431 (2011).
- ⁵¹D. V. Bulaev and D. Loss, *Phys. Rev. Lett.* **95**, 076805 (2005).
- ⁵²K. Gawarecki and P. Machnikowski, *Phys. Rev. B* **85**, 041305 (2012).
- ⁵³N. A. Sinitsyn, Yan Li, S. A. Crooker, A. Saxena, and D. L. Smith, *Phys. Rev. Lett.* **109**, 166605 (2012).
- ⁵⁴Yan Li, N. Sinitsyn, D. L. Smith, D. Reuter, A. D. Wieck, D. R. Yakovlev, M. Bayer, and S. A. Crooker, *Phys. Rev. Lett.* **108**, 186603 (2012).
- ⁵⁵Y. Hu, F. Kueemeth, C. M. Lieber, and C. M. Marcus, *Nat. Nanotechnol.* **7**, 47 (2012).
- ⁵⁶F. Fras, B. Eble, B. Siarry, F. Bernardot, A. Miard, A. Lemaître, C. Testelin, and M. Chamarro, *Phys. Rev. B* **86**, 161303(R) (2012).

- ⁵⁷X. J. Wang, S. Chesi, and W. A. Coish, *Phys. Rev. Lett.* **109**, 237601 (2012).
- ⁵⁸M. Trif, P. Simon, and D. Loss, *Phys. Rev. Lett.* **103**, 106601 (2009).
- ⁵⁹J. I. Climente, C. Segarra, and J. Planelles, arXiv:1301.4381.
- ⁶⁰D. Csontos, P. Brusheim, U. Zülicke, and H. Q. Xu, *Phys. Rev. B* **79**, 155323 (2009).
- ⁶¹T. Belhadj, T. Amand, A. Kunold, C.-M. Simon, T. Kuroda, M. Abbarchi, T. Mano, K. Sakoda, S. Kunz, X. Marie, and B. Urbaszek, *Appl. Phys. Lett.* **97**, 051111 (2010).
- ⁶²F. Maier and D. Loss, *Phys. Rev. B* **85**, 195323 (2012).
- ⁶³R. Winkler, *Spin-Orbit Coupling Effects in Two Dimensional Electron and Hole Systems* (Springer, Berlin, 2003).
- ⁶⁴B. Habib, M. Shayegan, and R. Winkler, *Semicond. Sci. Technol.* **24**, 064002 (2009).
- ⁶⁵B. Habib, J. Shabani, E. P. De Poortere, M. Shayegan, and R. Winkler, *Phys. Rev. B* **75**, 153304 (2007).
- ⁶⁶G. Katsaros, V. N. Golovach, P. Spathis, N. Ares, M. Stoffel, F. Fourmel, O. G. Schmidt, L. I. Glazman, and S. De Franceschi, *Phys. Rev. Lett.* **107**, 246601 (2011).
- ⁶⁷C. Kloeffel, M. Trif, and D. Loss, *Phys. Rev. B* **84**, 195314 (2011).
- ⁶⁸S. Chesi, G. F. Giuliani, L. P. Rokhinson, L. N. Pfeiffer, and K. W. West, *Phys. Rev. Lett.* **106**, 236601 (2011).
- ⁶⁹O. Klochan, A. P. Micolich, A. R. Hamilton, K. Trunov, D. Reuter, and A. D. Wieck, *Phys. Rev. Lett.* **107**, 076805 (2011).
- ⁷⁰L. Mao, M. Gong, E. Dumitrescu, S. Tewari, and C. Zhang, *Phys. Rev. Lett.* **108**, 177001 (2012).
- ⁷¹K. De Greve, P. L. McMahon, D. Press, T. D. Ladd, D. Bisping, C. Schneider, M. Kamp, L. Worschech, S. Höfling, A. Forchel, and Y. Yamamoto, *Nat. Phys.* **7**, 872 (2011).
- ⁷²A. Greilich, S. G. Carter, D. Kim, A. S. Bracker, and D. Gammon, *Nat. Photon.* **5**, 702 (2011).
- ⁷³T. M. Godden, J. H. Quilter, A. J. Ramsay, Yanwen Wu, P. Brereton, S. J. Boyle, I. J. Luxmoore, J. Puebla-Nunez, A. M. Fox, and M. S. Skolnick, *Phys. Rev. Lett.* **108**, 017402 (2012).
- ⁷⁴K. Müller, A. Bechtold, C. Ruppert, C. Hautmann, J. S. Wildmann, T. Kaldewey, M. Bichler, H. J. Krenner, G. Abstreiter, M. Betz, and J. J. Finley, *Phys. Rev. B* **85**, 241306 (2012).
- ⁷⁵B. Eble, P. Desfonds, F. Fras, F. Bernardot, C. Testelin, M. Chamarro, A. Miard, and A. Lemaître, *Phys. Rev. B* **81**, 045322 (2010).
- ⁷⁶F. Fras, B. Eble, F. Bernardot, C. Testelin, M. Chamarro, A. Miard, and A. Lemaître, *Appl. Phys. Lett.* **100**, 012104 (2012).
- ⁷⁷A. J. Ramsay, S. J. Boyle, R. S. Kolodka, J. B. B. Oliveira, J. Skiba-Szymanska, H. Y. Liu, M. Hopkinson, A. M. Fox, and M. S. Skolnick, *Phys. Rev. Lett.* **100**, 197401 (2008).
- ⁷⁸T. M. Godden, J. H. Quilter, A. J. Ramsay, Y. W. Wu, P. Brereton, I. J. Luxmoore, J. Puebla, A. M. Fox, and M. S. Skolnick, *Phys. Rev. B* **85**, 155310 (2012).
- ⁷⁹V. S. Pribiag, S. Nadj-Perge, S. M. Frolov, J. W. G. van den Berg, I. van Weperen, S. R. Plissard, E. P. A. M. Bakkers, and L. P. Kouwenhoven, *Nat. Nanotechnol.* **8**, 170 (2013).
- ⁸⁰D. V. Bulaev and D. Loss, *Phys. Rev. Lett.* **98**, 097202 (2007).
- ⁸¹J. C. Budich, D. G. Rothe, E. M. Hankiewicz, and B. Trauzettel, *Phys. Rev. B* **85**, 205425 (2012).
- ⁸²C. Y. Hsieh, R. Cheriton, M. Korkusinski, and P. Hawrylak, *Phys. Rev. B* **80**, 235320 (2009).
- ⁸³T. Andlauer and P. Vogl, *Phys. Rev. B* **79**, 045307 (2009).
- ⁸⁴R. Roloff, T. Eissfeller, P. Vogl, and W. Pötz, *New J. Phys.* **12**, 093012 (2010).
- ⁸⁵L. Trifunovic, O. Dial, M. Trif, J. R. Wootton, R. Abebe, A. Yacoby, and D. Loss, *Phys. Rev. X* **2**, 011006 (2012).
- ⁸⁶K. D. Petersson, L. W. McFaul, M. D. Schroer, M. Jung, J. M. Taylor, A. A. Houck, and J. R. Petta, *Nature (London)* **490**, 380 (2012).
- ⁸⁷S. E. Economou, J. I. Climente, A. Badolato, A. S. Bracker, D. Gammon, and M. F. Doty, *Phys. Rev. B* **86**, 085319 (2012).
- ⁸⁸P. Szumniak, S. Bednarek, B. Partoens, and F. M. Peeters, *Phys. Rev. Lett.* **109**, 107201 (2012).
- ⁸⁹C. Le Gall, A. Brunetti, H. Boukari, and L. Besombes, *Phys. Rev. B* **85**, 195312 (2012).
- ⁹⁰S. Bednarek, B. Szafran, and K. Lis, *Phys. Rev. B* **72**, 075319 (2005).
- ⁹¹K. Yano and D. K. Ferry, *Superlattices Microstruct.* **11**, 61 (1991).
- ⁹²S. Bednarek, B. Szafran, R. J. Dudek, and K. Lis, *Phys. Rev. Lett.* **100**, 126805 (2008).
- ⁹³J. M. Luttinger and W. Kohn, *Phys. Rev.* **97**, 869 (1955).
- ⁹⁴S. Bednarek and B. Szafran, *Phys. Rev. B* **73**, 155318 (2006).
- ⁹⁵G. Dresselhaus, *Phys. Rev.* **100**, 580 (1955).
- ⁹⁶The lateral size of CdTe induced quantum dot is about $l \approx 50$ nm which is greater than quantum well height $d = 10$ nm in the z direction. Cubic Dresselhaus terms can be thus neglected since its contribution is about $(d/l)^2 \sim 0.04$ smaller than those of linear DSOI terms.
- ⁹⁷M. Cardona, N. E. Christensen, and G. Fasol, *Phys. Rev. B* **38**, 1806 (1988).
- ⁹⁸K. T. R. Davies, H. Flocard, S. Krieger, and M. S. Weiss, *Nucl. Phys. A* **342**, 111 (1980).
- ⁹⁹The operators are accurate when the hole is purely in HH states and when the hole is moving exactly straight with constant velocity along the quantum wire placed in x or y direction. Simulation shows that hole trajectory is not exactly straight especially after reflection from cut corner electrodes thus the operators have only approximated character. The operators are used to deduce the topology of metal gates which covers certain quantum gate.
- ¹⁰⁰S. Bednarek, P. Szumniak, and B. Szafran, *Phys. Rev. B* **82**, 235319 (2010).

Summary

In this thesis we design, model and present results of time dependent simulations of semiconductor nanodevices which can be utilized as basic building blocks of a future quantum computer. In the designed nanodevices, the basic unit of quantum information - a qubit - is encoded in the spin (intrinsic angular momentum) of a single electron or hole confined in the semiconductor nanostructure in which induced quantum dots and wires are formed.

The proposed nanodevices are designed in such a way that they fulfill the basic criteria of physical implementation of quantum computation: the ability to initialize and read out (possibly in nondestructive or projective type manner) the state of a qubit respectively before and after realization of a certain quantum algorithm, the capability to realize fully controllable manipulation on a qubit, i.e. the realization of one and two qubit quantum logic gates. Furthermore, the qubit should be characterized by a long coherence time. The whole quantum computer architecture should fulfill the scalability requirement which means that it should be possible to build quantum registers composed of many qubits, which one can control individually without disturbing the state of other qubits in the register.

In particular we have designed and simulated nanodevices which are capable to initialize and read out the spin state of the electron, and devices which are able to manipulate the spin state of a single hole by the application of single quantum logic gates. We have also designed a so called "combo" nanodevice in which arbitrary sequence of proposed single quantum logic gates can be realized as well as a fragment of a scalable architecture composed from such "combo" nanodevices, containing four hole spin qubits.

The fact that spin manipulation, initialization and read out realized by the proposed nanodevices does not require the application of a magnetic field (except one nanodevice from Chapter 3) makes our proposals particularly interesting and unique among other proposals based on electron and hole spin qubits in semiconductor nanostructures. The proposed devices operate on spin qubits using exclusively weak static electric fields, which are locally generated by the voltages applied to the metal electrodes deposited on top of the investigated nanostructure. It allows to control individual qubits in the quantum register without disturbing the state of other qubits, which is very important for the realization of a scalable architecture.

Control of electron (hole) spin qubits without a magnetic field is possible thanks to

the interplay between the spin-orbit interaction and the self-focusing effect of an electron (hole) wave function which is present in induced quantum dots and wires. The former effect couples the motional and spin degree of freedom of an electron (hole) enabling motion induced spin rotation of a single charge carrier or vice versa, resulting in a spin dependent particle trajectory. While the latter effect allows for transport of an electron (hole) in the form of a stable soliton-like wave packet which motion is controlled by the voltage applied to the metal gates as well as the gate geometry which determines the particle path. Spin rotations induced by the particle motion are employed in order to realize single spin qubit quantum gates, while the effect of the spin dependent trajectory is used to realize spin filtering devices which aim is to initialize and read out the spin state of a single charge carrier.

In order to prolong the electron spin qubit coherence time which is limited by the contact hyperfine interaction with nuclear spins, Si nuclear free material can be applied in the proposed nanodevices. Alternatively, the qubit can be encoded in the more immune to the decoherence spin state of a hole.

Furthermore, the proposed devices also make possible a fully controllable transport of electrons or holes, which spins carry the quantum information, and thus may be also useful for transferring the quantum information within the semiconductor nanostructures. Consequently, they may find applications for quantum communication in semiconductor nanostructures.

We have performed numerical (time dependent) simulations of all of the proposed nanodevices by solving iteratively the time dependent Schrödinger equation (within the effective mass theory) together with solving the Poisson equation in each time step of the numerical procedure in the three dimensional computational box containing the entire nanodevice. Similar methods were previously employed by my promotor in order to model (reproduce) theoretically with very high accuracy reach set of experimental results about properties of electrostatic quantum dots. Thus our work can be considered as a link between the theoretical proposal and an experimental realization.

Thanks to the fact that the proposed nanodevices realize operations within sub-nanoseconds on a spin qubit which is characterized by a coherence time of the order of hundreds of nanoseconds, their experimental realization would be an important step towards the physical implementation of quantum computers.

Podsumowanie

Niniejsza praca dotyczy projektowania, modelowania i komputerowej symulacji działania półprzewodnikowych nanourządzeń, które mogą być wykorzystane jako podstawowe elementy przyszłego komputera kwantowego. W projektowanych nanourządzeniach nośnik informacji kwantowej - kubit jest realizowany przez spin (wewnętrzny moment pędu) pojedynczego elektronu lub dziury uwięzionych w nanostrukturze półprzewodnikowej. Urządzenia zaprojektowane są w taki sposób aby spełniały podstawowe kryteria fizycznej implementacji komputerów kwantowych. Wymagają one między innymi możliwości precyzyjnego ustawiania stanu kubitów na początku realizowanego algorytmu kwantowego i odczytu (najlepiej w sposób nieniszczący lub rzutowy) na jego końcu oraz wykonywania w pełni kontrolowanych operacji na kubicie - realizacji jedno i dwukubitowych kwantowych bramek logicznych. Cała architektura komputera kwantowego musi ponadto spełniać kryterium skalowalności tzn. układ powinien się dać rozszerzyć na większą liczbę kubitów (rejestr kwantowy), które można w indywidualny sposób kontrolować nie zaburzając stanu pozostałych kubitów w rejestrze.

W pracy zaprojektowano nanourządzenia służące do ustawiania i odczytu spinu pojedynczego elektronu, oraz do wykonywania operacji jednokubitowych bramek kwantowych na spinie pojedynczej dziury. Zaproponowano również nanourządzenie "combo", w którym może być wykonana dowolna sekwencja jednokubitowych bramek kwantowych oraz zaprojektowano fragment skalowalnej architektury składającej się z takich nanourządzeń.

Niezwykle istotną cechą, odróżniającą nasze rozwiązania od innych dotychczasowych propozycji realizacji obliczeń kwantowych w nanostrukturach półprzewodnikowych jest możliwość ustawienia i odczytu spinu pojedynczego nośnika ładunku oraz wykonania na nim innych operacji bez użycia zewnętrznego pola magnetycznego (z wyjątkiem jednego nanourządzenia z rozdziału (3)). Operacje wykonywane przez zaprojektowane nanourządzenia kontrolowane są wyłącznie przy użyciu słabych statycznych pól elektrycznych, które są generowane lokalnie przez napięcia przyłożone do metalowych elektrod ułożonych na powierzchni nanostruktury. Dzięki temu możliwa jest kontrola pojedynczych kubitów w rejestrze kwantowym bez zaburzania stanu pozostałych kubitów, co jest warunkiem realizacji skalowalnej struktury.

Kontrola spinu elektronu (dziury) bez użycia pola magnetycznego jest możliwa dzięki wykorzystaniu oddziaływania spin-orbita oraz efektu samoogniskowania funkcji falowej elektronu (dziury) wywołanego oddziaływaniem nośnika ładunku z ładunkiem indukowa-

nym na metalowych elektrodach ułożonych na powierzchni nanostruktury. Pierwszy efekt wiąże ruch elektronu (dziury) z ich stanem spinowym co umożliwia realizację obrotu spinu powodowanego przez ruch nośnika ładunku lub odwrotnie uzyskanie trajektorii cząstki zależnej od jej stanu spinowego. Natomiast drugi efekt pozwala na kontrolowany napięciami przyłożonymi do metalowych elektrod transport elektronu (dziury) w postaci stabilnego pakietu falowego mającego charakter solitonu. Obroty spinu indukowane ruchem wykorzystane są do realizacji jednobitowych bramek kwantowych, natomiast efekt zależnej od spinu trajektorii do realizacji filtrów spinowych mających za zadanie ustawiać i odczytywać stan spinowy pojedynczego nośnika ładunku. Ze względu na fakt, że zaprojektowane nanourządzenia umożliwiają kontrolowany transport elektronów lub dziur, których spin jest nośnikiem informacji, mogą być przydatne do przesyłania informacji kwantowej wewnątrz półprzewodnikowych nanostruktur i tym samym znaleźć zastosowanie w komunikacji kwantowej w nanoukładach półprzewodnikowych.

Ponieważ algorytmy wykonywane przez komputer kwantowy będą obejmowały co najmniej kilka tysięcy operacji, które łącznie muszą być zrealizowane w czasie mniejszym od tzw. czasu koherencji, kubit powinien być realizowany przez stan kwantowy który zachowuje koherencję odpowiednio długo. Zakodowanie informacji kwantowej w stanie spinowym dziury pozwala wydłużyć czas koherencji w porównaniu z kubitem zrealizowanym na stanie spinowym elektronu. Ponieważ proponowane nanourządzenia wykonują operacje w czasie rzędu ułamków pikosekund na kubicie, którego czas koherencji jest rzędu setek nanosekund, ich eksperymentalna implementacja może być ważnym krokiem w kierunku fizycznej realizacji komputerów kwantowych.

W pracy wykonano numeryczne symulacje działania wszystkich zaproponowanych nanourządzeń poprzez iteracyjne rozwiązywanie zależnego od czasu równania Schroedingera z jednoczesnym obliczaniem aktualnego potencjału uwięzienia i pola elektrycznego poprzez rozwiązywanie w każdej chwili czasowej równania Poissona w trójwymiarowym obszarze przestrzennym obejmującym nanourządzenie. Identyczne metody obliczeniowe pozwoliły w przeszłości odtworzyć bogate spektrum wyników eksperymentalnych dotyczące własności elektrostatycznych kropek kwantowych. Dzięki temu niniejszą pracę można traktować jako ogniwo łączące teoretyczny opis nanourządzenia z jego eksperymentalną realizacją.

Samenvatting

In deze thesis ontwerpen, modelleren en simuleren we halfgeleider nanodevices die gebruikt kunnen worden als bouwstenen van een toekomstige kwantumcomputer. In deze nieuw ontworpen nanodevices wordt de basiseenheid van kwantuminformatie - de qubit - gecodeerd in de spin van een elektron of holte, opgesloten in de halfgeleider nanostructuur waarin kwantumstippen en draden gemaakt zijn.

De voorgestelde nanodevices zijn zodanig ontworpen dat ze voldoen aan de basis criteria voor de fysische implementatie van kwantumcomputatie. Deze basis criteria zijn de mogelijkheid om de toestand van een qubit te initialiseren en uit te lezen na de uitvoering van een zeker algoritme (en mogelijk in een niet-destructieve manier), en de volledig controleerbare manipulatie van deze qubit, i.e. de realisatie van een of twee-qubit logische operaties. Daarnaast moet de qubit gekarakteriseerd worden door een lange coherentietijd. De gehele computerarchitectuur moet ook volledig schaalbaar zijn, wat betekent dat het moet mogelijk zijn om kwantumregisters op te bouwen uit vele qubits, die individueel gecontroleerd moeten kunnen worden zonder de toestand van andere qubits in het register te verstoren.

In het bijzonder hebben we nanodevices ontworpen en gesimuleerd die het toelaten om de spin van een elektron te initialiseren en uit te lezen, en devices waarin de spin van een holte kan gemanipuleerd worden door kwantum gates. We hebben ook een "combo" nanodevice ontworpen waarin een arbitraire opeenvolging van kwantum logische gates kan gerealiseerd worden. En eveneens hebben we een onderdeel van een schaalbare architectuur opgebouwd uit dergelijke "combo" devices, met vier holte spin qubits.

Het feit dat spin manipulatie, initialisatie en uitlezing in de voorgestelde nanodevices geen gebruik maken van een uitwendig aangelegd magneetveld (behalve één nanodevice in hoofdstuk 3) maakt onze voorstellen uniek onder de voorstellen gebaseerd op elektron en holte qubits in halfgeleider nanostructuren. De voorgestelde devices manipuleren de spin qubits enkel met statische elektrische velden die lokaal gegenereerd worden door spanningen aan te leggen op metaal elektrodes bovenop de nanostructuren. Het laat toe om individuele qubits te manipuleren in het kwantumregister zonder de toestand van andere qubits te verstoren, essentieel voor de realisatie van een schaalbare architectuur.

Controle over de elektron (holte) spin qubits zonder een magneetveld is mogelijk door de combinatie van de spin-baan interactie en het zelf-focusing effect van een elektron (holte) golf functie die aanwezig is in geïnduceerde kwantumstippen en draden. Het

eerste effect koppelt de bewegings vrijheidsgraad met de spin vrijheidsgraad van een elektron(holte) wat leidt tot spin rotatie geïnduceerd door de beweging van het deeltje en vice versa. Dit resulteert in een baan die afhankelijk is van de spin. Het tweede effect leidt tot het transport van een elektron (holte) in de vorm van een soliton-achtig golfpakket waarvan de beweging bepaald wordt door de spanning aangelegd op de metaal elektroden en door de geometrie van deze elektroden. Spin rotaties die door de beweging geïnduceerd worden worden gebruikt om één spin kwantum gates te realiseren, terwijl het spin afhankelijke traject gebruikt wordt om een spin filter te realiseren. Een spin filter wordt dan weer gebruikt voor de initialisatie en uitlezing van de spin toestand van een enkele spin ladingsdrager.

Om de elektron spin coherentietijd, die gelimiteerd wordt door de hyperfijn interactie met de nucleaire spins, te verlengen kunnen we de voorgestelde nanodevices realiseren in Si. Een alternatief is om de qubit te coderen in de spin toestand van een holte die meer immuun is voor decoherentie.

Daarnaast maken de voorgestelde devices ook het controleerbaar transport mogelijk van elektronen of holten waarvan de spin de kwantum informatie dragen, en kunnen dus ook nuttig zijn voor de transfer van kwantum informatie in halfgeleider nanostructuren.

We hebben in deze thesis numerieke (tijdsafhankelijke) simulaties uitgevoerd van alle voorgestelde nanodevices door iteratief de tijdsafhankelijke Schrödingervergelijking op te lossen (binnen de effectieve massa benadering) samen met de Poisson vergelijking, in elke tijdsstap van de numerieke procedure in een drie-dimensionale doos die het hele nanodevice bevat. Analoge methoden werden reeds gebruikt door mijn promotor om theoretisch een aantal resultaten i.v.m. de eigenschappen van elektrostatische kwantumstippen erg accuraat te modelleren. Daarom kan deze thesis beschouwd worden als de link tussen een theoretisch voorstel en de experimentele realisatie.

Dankzij het feit dat de operaties in de voorgestelde nanodevices gerealiseerd worden in subnanoseconden op een spin qubit die gekarakteriseerd wordt door een coherentietijd van de orde van honderden nanoseconden, kan hun experimentele realisatie een belangrijke stap zijn in de fysische implementatie van een kwantumcomputer.

References

- [1] R. P. Poplavskii, “*Thermodynamical models of information processing*”, Uspekhi Fizicheskikh Nauk **115** (3) 465 (1975).
- [2] R. S. Ingarden, “*Quantum Information Theory*”, Reports on Mathematical Physics, **10**, 43, (1976).
- [3] R.P. Feynman, “*Simulating Physics with Computers*”, Int. J. Theor. Phys. **21** 467 (1982).
- [4] P. Benioff, “*Quantum mechanical hamiltonian models of turing machines*”, J. Stat. Phys. **29**, 515 (1982).
- [5] R.P. Feynman, “*Quantum mechanical computers*”, Opt. News **11**, 11 (1985).
- [6] D. Deutsch, “*Quantum computational networks*”, Proc. R. Soc. Lond. A **400** 97-117 (1985)
- [7] D. Deutsch, “*Quantum theory, the church-turing principle and the universal quantum computer*”, Proc. R. Soc. Lond. A 400:97-117 (1985).
- [8] D. Deutsch, R. Jozsa, “*Rapid Solution of Problems by Quantum Computation*” Proc. R. Soc. Lond. A 439:553-58 (1992).
- [9] P. W. Shor, “*Algorithms for Quantum Computation: Discrete Logarithms and Factoring*”, Proceedings of the 35th Annual Symposium on the Foundations of Computer Science (IEEE Press, Los Alamitos, 1994), p. 124
- [10] P. W. Shor, “*Polynomial-Time Algorithms for Prime Factorization and Discrete Logarithms on a Quantum Computer*” . SIAM J. Comput. 26:1484-509 (1997).
- [11] L. K. Grover, “*Quantum Mechanics Helps in Searching for a Needle in a Haystack*”, Phys. Rev. Lett. **79** 325 (1997).
- [12] L. K. Grover, “*Quantum Computers Can Search Arbitrarily Large Databases by a Single Query*” Phys. Rev. Lett. **79** 4709 (1997).
- [13] K. H. Han, Jong-Hwan Kin, “*Genetic Quantum Algorithm and its Application to Combinatorial Optimization Problem*” Congress of Evolutionary Computation, Piscataway, NJ, (2000).

-
- [14] K. L. Brown, W. J. Munro, V. M. Kendon, “*Using Quantum Computers for Quantum Simulation*”, Entropy **12** 2268 (2010).
- [15] P. W. Shor, “*Scheme for reducing decoherence in quantum computer memory*”, Phys. Rev. A, **52**, 4 (1995).
- [16] A. R. Calderbank and Peter W. Shor, “*Good quantum error-correcting codes exist*”, Phys. Rev. A **54**, 1098 (1996).
- [17] A. M. Steane, “*Error Correcting Codes in Quantum Theory*”, Phys. Rev. Lett. **77**, 793 (1996).
- [18] J. Preskill, “*Reliable quantum computers*”, Proc. R. Soc. Lond. A. **454**, 385 (1998).
- [19] P. Aliferis and J. Preskill, “*Fault-tolerant quantum computation against biased noise*”, Phys. Rev. A **78**, 052331 (2008).
- [20] A. Aspect, P. Grangier, and G. Roger, “*Experimental Realization of Einstein-Podolsky-Rosen-Bohm Gedankenexperiment: A New Violation of Bell’s Inequalities*”, Phys. Rev. Lett. **49**, 91 (1982).
- [21] M. A. Nielsen and I. L. Chuang, “*Quantum Computation and Quantum Information*”, Cambridge University Press, Cambridge, 2000.
- [22] T. D. Ladd, F. Jelezko, R. Laflamme, Y. Nakamura, C. Monroe, and J. L. O’Brien, “*Quantum computers*”, Nature(London) **464**, 45 (2010).
- [23] D. Loss, DP DiVincenzo, “*Quantum computation with quantum dots*” Phys. Rev. A **57**, 120 (1998).
- [24] A. Imamoglu, D. Awschalom, G. Burkard, D.P. DiVincenzo, D. Loss, M. Sherwin, and A. Small, “*Quantum Information Processing Using Quantum Dot Spins and Cavity QED*” 1999. Phys. Rev. Lett. **83**, 4204 (1999).
- [25] V. Cerletti, W. A. Coish, O. Gywat, and D. Loss, “*Recipes for spin-based quantum computing*”, Nanotechnology **16**, R27 (2005).
- [26] R. A. Zak, B. Rothlisberger, S. Chesi, D. Loss, “*Quantum Computing with Electron Spins in Quantum*”, Riv. Nuovo Cimento **33**, 345 (2010).

-
- [27] C. Kloeffel and D. Loss, “*Prospects for Spin-Based Quantum Computing*”, *Annu. Rev. Condens. Matter Phys.* **4**, 51 (2013).
- [28] J. I. Cirac and P. Zoller, “*Quantum Computations with Cold Trapped Ions*” *Phys. Rev. Lett.* **74** 4091 (1995).
- [29] Q. A. Turchette, C.J. Hood, W. Lange, H. Mabuchi, H.J. Kimble, “*Measurement of Conditional Phase Shifts for Quantum Logic*”, *Phys. Rev. Lett.* **75** 4710 (1995).
- [30] T. Pellizzari, S. A. Gardiner, J. I. Cirac, and P. Zoller, “*Decoherence, continuous observation, and quantum computing: A cavity QED model*”, *Phys. Rev. Lett.* **75** 3788 (1995).
- [31] A. Imamoglu, D. D. Awschalom, G. Burkard, D. P. DiVincenzo, D. Loss, M. Sherwin, and A. Small, “*Quantum Information Processing Using Quantum Dot Spins and Cavity QED*”, *Phys. Rev. Lett.* **83**, 4204 (1999).
- [32] A. Rauschenbeutel, G. Nogues, S. Osnaghi, P. Bertet, M. Brune, J. M. Raimond, and S. Haroche, “*Coherent Operation of a Tunable Quantum Phase Gate in Cavity QED*”, *Phys. Rev. Lett.* **83**, 5166 (1999).
- [33] N. A. Gershenfeld, and I. L. Chuang, “*Bulk spin resonance quantum computation*”, *Science* **275**, 350 (1997).
- [34] D. G. Cory, A. F. Fahmy, and T. F. Havel, “*Ensemble quantum computing by NMR spectroscopy*” *Proc. Natl Acad. Sci. USA* **94**, 1634 (1997).
- [35] A. Shnirman, G. Schön, Z. Hermon, “*Quantum Manipulations of Small Josephson Junctions*”, *Phys. Rev. Lett.* **79** 2371 (1997).
- [36] A. J. Leggett, “*Superconducting Qubits—a Major Roadblock Dissolved?*”, *Science* **296**, 861 (2002).
- [37] G. Blatter, “*The qubit duet*”, *Nature* **421**, 196 (2003).
- [38] J. Clarke, “*Flux Qubit Completes the Hat Trick*”, *Science* **299**, 1850 (2003).
- [39] H. Mooij, “*The Road to Quantum Computing*”, *Science* **307**, 1210 (2005).
- [40] J. Q. You and F. Nori, “*Superconducting circuits and quantum information*”, *Physics Today* **58**, 42 (2005)

-
- [41] E. Knill, R. Laflamme, G.J. Milburn, “*A scheme for efficient quantum computation with linear optics*”, Nature (London) **409**, 46 (2001)
- [42] M.N. Leuenberger, D. Loss, “*Quantum Computing in Molecular Magnets*”, Nature (London) **410**, 789 (2001).
- [43] L. Bogani and W. Wernsdorfer, “*Molecular spintronics using single-molecule magnets*”, Nature Materials **7**, 179 (2008).
- [44] F. Meier, J. Levy, D. Loss, “*Quantum computing with spin cluster qubits*”, Phys. Rev. Lett. **90** 047901 (2003).
- [45] B.E. Kane, “*A silicon-based nuclear spin quantum computer*”, Nature (London) **393** 133 (1998).
- [46] Vrijen R, Yablonovitch E, Wang KL, Jiang HW, Balandin AA, V. Roychowdhury, T. Mor, and D. DiVincenzo, “*Electron-spin-resonance transistors for quantum computing in silicon-germanium heterostructures*”, Phys. Rev. A **62**, 012306 (2000).
- [47] F. Jelezko , J. Wrachtrup, “*Single defect centres in diamond: A review*”, Phys. Status Solidi A **203**, 3207 (2006).
- [48] R. Hanson, D. D. Awschalom, “*Coherent manipulation of single spins in semiconductors*”, Nature (London) **453**, 1043 (2008).
- [49] P. Maletinsky, S. Hong, M. S. Grinolds, B. Hausmann, M. D. Lukin, R. L. Walsworth, M. Loncar, and A. Yacoby, “*A robust scanning diamond sensor for nanoscale imaging with single nitrogen-vacancy centres*” Nature Nanotech. **7** 320 (2012).
- [50] A. Mizel, M. Mitchell, and M. L. Cohen, “*Energy barrier to decoherence*”, Phys. Rev. A **63**, 040302(R) (2001).
- [51] E. Farhi, J. Goldstone, S. Gutmann, J. Laplan, A. Lundgren, and D. Preda, “*A Quantum Adiabatic Evolution Algorithm Applied to Random Instances of an NP-Complete Problem*” Science **292**, 472 (2001).
- [52] A. M. Childs, E. Deotto, E. Farhi, J. Goldstone, S. Gutmann, and A. J. Landahl “*Quantum search by measurement*”, Phys. Rev. A **66**, 032314 (2002).

-
- [53] M. Steffen, W. van Dam, T. Hogg, G. Breyta, and I. Chuang, “*Experimental Implementation of an Adiabatic Quantum Optimization Algorithm*”, Phys. Rev. Lett. **90**, 067903 (2003).
- [54] A. Y. Kitaev, “*Fault-tolerant quantum computation by anyons*”, Ann. Phys. **303**, 2 (2003).
- [55] M. H. Freedman, A. Kitaev, and Z. Wang, “*Simulation of topological field theories by quantum computers*”, Commun. Math. Phys. **227**, 587 (2002).
- [56] C. Nayak, S. H. Simon, A. Stern, M. Freedman, and S. Das Sarma, “*Non-Abelian anyons and topological quantum computation*”, Rev. Mod. Phys. **80**, 1083 (2008).
- [57] A. Stern, N. H. Lindner, “*Topological Quantum Computation From Basic Concepts to First Experiments*”, Science **339**, 1179 (2013).
- [58] J. Alicea, Y. Oreg, G. Refael, F. von Oppen, and M. P. A. Fisher, “*Non-Abelian statistics and topological quantum information processing in 1D wire networks*”, Nature Physics **7**, 412 (2011).
- [59] J. Leinaas and J. Myrheim, “*On the theory of identical particles*”, Nuovo Cimento **B37**, 1 (1977).
- [60] F. Wilczek, “*Quantum Mechanics of Fractional-Spin Particles*”, Phys. Rev. Lett. **49**, 957 (1982).
- [61] E. Majorana, “*Teoria simmetrica dell’elettrone e del positrone*”, Nuovo Cimento **5**, 171 (1937).
- [62] F. Wilczek, “*Majorana returns*”, Nature Phys. **5**, 614 (2009).
- [63] C. Monroe, D. M. Meekhof, B. E. King, W. M. Itano, and D. J. Wineland, “*Demonstration of a Fundamental Quantum Logic Gate*”, Phys. Rev. Lett. **75**, 4714 (1995).
- [64] D. Leibfried, R. Blatt, C. Monroe, and D. Wineland, “*Quantum dynamics of single trapped ions*”, Rev. Mod. Phys. **75**, 281 (2003).
- [65] C. R. Monroe, and D. J. Wineland, “*Quantum Computing with Ions*”, Scientific American (2008)

-
- [66] P.Goy, J.M.Raimond, M.Gross and S.Haroche, “*Observation of cavity-enhanced single atom spontaneous emission*”, Phys. Rev. Lett. **50**, 1903 (1983).
- [67] M. Brune, S. Haroche, J. M. Raimond, L. Davidovich, and N. Zagury, “*Manipulation of photons in a cavity by dispersive atom-field coupling: Quantum-nondemolition measurements and generation of Schrödinger cat states*”, Phys. Rev. A **45**, 5193 (1992).
- [68] M. Brune, E. Hagley, J. Dreyer, X. Maitre, A. Maali, C. Wunderlich, J. M. Raimond, and S. Haroche, “*Observing the Progressive Decoherence of the Meter in a Quantum Measurement*”, Phys. Rev. Lett. **77**, 4887 (1996).
- [69] S. Osnaghi, P. Bertet, A. Auffeves, P. Maioli, M. Brune, J. M. Raimond, and S. Haroche, “*Coherent Control of an Atomic Collision in a Cavity*”, Phys. Rev. Lett. **87**, 037902 (2001).
- [70] J. M. Raimond, M. Brune, and S. Haroche, “*Manipulating quantum entanglement with atoms and photons in a cavity*”, Rev. Mod. Phys. **73**, 565 (2001).
- [71] W. H. Zurek, “*Decoherence and the Transition From Quantum to Classical*”, Phys. Today **44** (10), 36 (1991).
- [72] W. H. Zurek, “*Decoherence, einselection, and the quantum origins of the classical*”, Rev. Mod. Phys. **75**, 715 (2003).
- [73] D. Aharonov, “*Quantum to classical phase transition in noisy quantum computers*”, Phys. Rev. A **62**, 062311 (2000).
- [74] D. P. DiVincenzo and D. Loss, “*Quantum Information is Physical*”, Superlattices and Microstructures **23**, 419 (1998).
- [75] D. P. DiVincenzo, “*The physical implementation of quantum computation*”, Fortschr. Phys. **48**, 771 (2000).
- [76] A. Barenco, C. H. Bennett, R. Cleve, D.P. DiVincenzo, N. Margolus, P. Shor, T. Sleator, J. A. Smolin, and H. Weinfurter, “*Elementary gates for quantum computation*”, Phys. Rev. A **52**, 3457 (1995).
- [77] S. Lloyd “*Almost Any Quantum Logic Gate is Universal*”, Phys. Rev. Lett. **75**, 346 (1995).

-
- [78] Q. A. Turchette, C. J. Hood, W. Lange, H. Mabuchi, and H. J. Kimble, “*Measurement of conditional phase shifts for quantum logic*”, Phys. Rev. Lett. **75**, 4710 (1995).
- [79] R. Hanson, L. P. Kouwenhoven, J. R. Petta, S. Tarucha, and L. M. K. Vandersypen, “*Spins in few-electron quantum dots*”, Rev. Mod. Phys. **79**, 1217 (2007).
- [80] S. Amasha, K. MacLean, I. P. Radu, D. M. Zumbüh, M. A. Kastner, M. P. Hanson, and A. C. Gossard, “*Electrical Control of Spin Relaxation in a Quantum Dot*”, Phys. Rev. Lett. **100**, 046803 (2008).
- [81] J. R. Petta, A. C. Johnson, J. M. Taylor, E. A. Laird, A. Yacoby, M. D. Lukin, C. M. Marcus, M. P. Hanson, and A. C. Gossard, “*Coherent Manipulation of Coupled Electron Spins in Semiconductor Quantum Dots*”, Science **309**, 2180 (2005).
- [82] J. M. Elzerman, R. Hanson, L. H. Willems van Beveren, B. Witkamp, L. M. K. Vandersypen, and L. P. Kouwenhoven, “*Single-shot read-out of an individual electron spin in a quantum dot*”, Nature (London) **430**, 431 (2004).
- [83] R. Hanson, L. H. Willems van Beveren, I. T. Vink, J. M. Elzerman, W. J. M. Naber, F. H. L. Koppens, L. P. Kouwenhoven, and L. M. K. Vandersypen, “*Single-Shot Readout of Electron Spin States in a Quantum Dot Using Spin-Dependent Tunnel Rates*”, Phys. Rev. Lett. **94**, 196802 (2005).
- [84] T. Meunier, I. T. Vink, L. H. Willems van Beveren, F. H. L. Koppens, H. P. Tranitz, W. Wegscheider, L. P. Kouwenhoven, and L. M. K. Vandersypen, “*Nondestructive measurement of electron spins in a quantum dot*”, Phys. Rev. B **74**, 195303 (2006).
- [85] F. H. L. Koppens, C. Buizert, K. J. Tielrooij, I. T. Vink, K. C. Nowack, T. Meunier, L. P. Kouwenhoven, and L. M. K. Vandersypen, “*Driven coherent oscillations of a single electron spin in a quantum dot*”, Nature (London) **442**, 766 (2006).
- [86] A. Morello, J. J. Pla, F. A. Zwanenburg, K. W. Chan, K. Y. Tan, H. Huebl, M. Möttönen, C. D. Nugroho, C. Yang, J. A. van Donkelaar, A. D. C. Alves, D. N. Jamieson, C. C. Escott, L. C. L. Hollenberg, R. G. Clark, and A. S. Dzurak, “*Single-shot readout of an electron spin in silicon*”, Nature (London) **467**, 687 (2010).
- [87] A. J. Ramsay, S. J. Boyle, R. S. Kolodka, J. B. B. Oliveira, J. Skiba-Szymanska, H. Y. Liu, M. Hopkinson, A. M. Fox, and M. S. Skolnick “*Fast Optical Preparation,*

- Control, and Readout of a Single Quantum Dot Spin*”, Phys. Rev. Lett. **100**, 197401 (2008).
- [88] D. Press, T. D. Ladd, B. Zhang, and Y. Yamamoto, “*Complete quantum control of a single quantum dot spin using ultrafast optical pulses*”, Nature (LONDON) **456**, 218 (2008).
- [89] K. C. Nowack, F. H. L. Koppens, Yu. V. Nazarov, and L. M. K. Vandersypen, “*Coherent Control of a Single Electron Spin with Electric Fields*”, Science **318**, 1430 (2007).
- [90] S. Nadj-Perge, S. M. Frolov, E. P. A. M. Bakkers and L. P. Kouwenhoven, “*Spin-orbit qubit in a semiconductor nanowire*”, Nature (London) **468**, 1084 (2010).
- [91] S. Nadj-Perge, V. S. Pribiag, J. W. G. van den Berg, K. Zuo1, S. R. Plissard, E. P. A. M. Bakkers, S. M. Frolov, and L. P. Kouwenhoven, “*Spectroscopy of Spin-Orbit Quantum Bits in Indium Antimonide Nanowires*”, Phys. Rev. Lett. **108**, 166801 (2012).
- [92] R. Hanson and D. D. Awschalom, “*Coherent manipulation of single spins in semiconductors*”, Nature (London) **453**, 1043 (2008).
- [93] R. Brunner, Y.-S. Shin, T. Obata, M. Pioro-Ladriere, T. Kubo, K. Yoshida, T. Taniyama, Y. Tokura, and S. Tarucha, “*Two-Qubit Gate of Combined Single-Spin Rotation and Interdot Spin Exchange in a Double Quantum Dot*”, Phys. Rev. Lett. **107**, 146801 (2011).
- [94] K. C. Nowack, M. Shafiei, M. Laforest, G. E. D. K. Prawiroatmodjo, L. R. Schreiber, C. Reichl, W. Wegscheider, L. M. K. Vandersypen, “*Single-Shot Correlations and Two-Qubit Gate of Solid-State Spins*”, Science **333**, 1269 (2011).
- [95] D. D. Awschalom , L. C. Bassett, A. S. Dzurak, E. L. Hu, and J. R. Petta, “*Quantum Spintronics: Engineering and Manipulating Atom-Like Spins in Semiconductors*” Science **339**, 1174 (2013).
- [96] L. M. K. Vandersypen, M. Steffen, G. Breyta, C. S. Yannoni, M. H. Sherwood, and I. L. Chuang, “*Experimental realization of Shor’s quantum factoring algorithm using nuclear magnetic resonance*”, Nature (London) **414**, 883 (2001).

-
- [97] C.-Y. Lu, D. E. Browne, T. Yang, and J.-W. Pan, “*Demonstration of a Compiled Version of Shor’s Quantum Factoring Algorithm Using Photonic Qubits*”, Phys. Rev. Lett. **99**, 250504 (2007).
- [98] B. P. Lanyon, T. J. Weinhold, N. K. Langford, M. Barbieri, D. F. V. James, A. Gilchrist, and A. G. White, “*Experimental Demonstration of a Compiled Version of Shor’s Algorithm with Quantum Entanglement*”, Phys. Rev. Lett. **99**, 250505 (2007).
- [99] E. Lucero, R. Barends, Y. Chen, J. Kelly, M. Mariantoni, A. Megrant, P. O’Malley, D. Sank, A. Vainsencher, J. Wenner, T. White, Y. Yin, A. N. Cleland, and John M. Martinis, “*Computing prime factors with a Josephson phase qubit quantum processor*”, Nature Physics **8**, 719 (2012).
- [100] E. Martin-López, A. Laing, T. Lawson, R. Alvarez, X.-Q. Zhou, and J. L. O’Brien, “*Experimental realization of Shor’s quantum factoring algorithm using qubit recycling*”, Nature Photonics **6**, 773 (2012).
- [101] D. P. DiVincenzo, D. Bacon, J. Kempe, G. Burkard, and K. B. Whaley, “*Universal quantum computation with the exchange interaction*”, Nature (London) **408**, 339 (2000).
- [102] V. N. Golovach, M. Borhani, and D. Loss, “*Electric-dipole-induced spin resonance in quantum dots*”, Phys. Rev. B **74**, 165319 (2006).
- [103] S. Dehdal and C. Emary, “*Spin-Orbit-Driven Coherent Oscillations in a Few-Electron Quantum Dot*”, Phys. Rev. Lett. **94**, 226803 (2005).
- [104] C. Flindt, A. S. Sorensen, and K. Flensberg, “*Spin-Orbit Mediated Control of Spin Qubits*”, Phys. Rev. Lett. **97**, 240501 (2006).
- [105] I. A. Merkulov, Al. L. Efros, and M. Rosen, “*Electron spin relaxation by nuclei in semiconductor quantum dots*”, Phys. Rev. B **65**, 205309 (2002).
- [106] A. V. Khaetskii, D. Loss, and L. Glazman, “*Electron Spin Decoherence in Quantum Dots due to Interaction with Nuclei*”, Phys. Rev. Lett. **88**, 186802 (2002).
- [107] Ł. Cywiński, W. M. Witzel, and S. Das Sarma, “*Electron Spin Dephasing due to Hyperfine Interactions with a Nuclear Spin Bath*”, Phys. Rev. Lett. **102**, 057601 (2009).

-
- [108] W. A. Coish and J. Baugh, “*Nuclear spins in nanostructures*”, Phys. Status Solidi B **246**, 2203 (2009).
- [109] J. Fischer and D. Loss, “*Dealing with Decoherence*”, Science **324**, 1277 (2009).
- [110] H. Bluhm, S. Foletti, I. Neder, M. Rudner, D. Mahalu, V. Umansky, A. Yacoby, “*Dephasing time of GaAs electron-spin qubits coupled to a nuclear bath exceeding 200 us*”, Nature Phys. **7**, 109 (2010).
- [111] G. Burkard, “*Positively spin coherent*”, Nature Materials **7**, 100 (2008).
- [112] M. H. Kolodrubetz, J. R. Petta, “*Coherent holes in a semiconductor quantum dot*”, Science **325**, 42 (2009).
- [113] A. Tartakovskii, “*Holes avoid decoherence*”, Nature Photonics **5**, 647 (2011).
- [114] J. Fischer, W. A. Coish, D. V. Bulaev, and D. Loss, “*Spin decoherence of a heavy hole coupled to nuclear spins in a quantum dot*”, Phys. Rev. B **78**, 155329 (2008).
- [115] C. Testelin, F. Bernardot, B. Eble, and M. Chamarro, “*Hole-spin dephasing time associated with hyperfine interaction in quantum dots*”, Phys. Rev. B **79**, 195440 (2009).
- [116] B. Eble, C. Testelin, P. Desfonds, F. Bernardot, A. Balocchi, T. Amand, A. Miard, A. Lemaitre, X. Marie, and M. Chamarro, “*Hole-Nuclear Spin Interaction in Quantum Dots*”, Phys. Rev. Lett. **102**, 146601 (2009).
- [117] P. Fallahi, S. T. Yilmaz, and A. Imamoglu, “*Measurement of a Heavy-Hole Hyperfine Interaction in InGaAs Quantum Dots Using Resonance Fluorescence*”, Phys. Rev. Lett. **105**, 257402 (2010).
- [118] P. Desfonds, B. Eble, F. Frasn, C. Testelin, F. Bernardot, M. Chamarro, B. Urbaszek, T. Amand, X. Marie, J.-M. Gérard, V. Thierry-Mieg, A. Miard, and A. Lemaitre, “*Electron and hole spin cooling efficiency in InAs quantum dots: The role of nuclear field*”, Appl. Phys. Lett. **96**, 172108 (2010).
- [119] E. A. Chekhovich, A. B. Krysa, M. S. Skolnick, and A. I. Tartakovskii, “*Direct Measurement of the Hole-Nuclear Spin Interaction in Single InP/GaInP Quantum Dots Using Photoluminescence Spectroscopy*”, Phys. Rev. Lett. **106**, 027402 (2011).

-
- [120] Z. K. Keane, M. C. Godfrey, J. C. H. Chen, S. Fricke, O. Klochan, A. M. Burke, A. P. Micolich, H. E. Beere, D. A. Ritchie, K. V. Trunov, D. Reuter, A. D. Wieck, and A. R. Hamilton, “*Resistively Detected Nuclear Magnetic Resonance in n- and p-Type GaAs Quantum Point Contacts*”, Nano Lett. **11**, 3147 (2011).
- [121] K. Yano and D. K. Ferry, “*Single-electron solitons*” Superlattices Microstruct. **11**, 61 (1991).
- [122] S. Bednarek, B. Szafran, and K. Lis, “*Electron soliton in semiconductor nanostructures*” Phys. Rev. B **72**, 075319 (2005).
- [123] S. Bednarek, B. Szafran, K. Lis, “*Self-focusing of a quantum-well confined electron wave packet interacting with a metal plate*”, Phys. Stat. Sol. (b) **243** 2811 (2006).
- [124] S. Bednarek, B. Szafran, “*Energy dissipation of electron solitons in a quantum well*” Phys. Rev. B **73**, 155318 (2006).
- [125] S. Bednarek, B. Szafran, R. J. Dudek, K. Lis, “*Induced quantum dots and wires: Electron storage and delivery*” Phys. Rev. Lett. **100**, 126805 (2008).
- [126] S. Bednarek, B. Szafran, “*Spin rotations induced by an electron running in closed trajectories in gated semiconductor nanodevices*” Phys. Rev. Lett. **101**, 216805 (2008).
- [127] S. Bednarek, B. Szafran, “*Gated combo nanodevice for sequential operations on single electron spin*”, Nanotechnology **20**, 065402 (2009).
- [128] G. Dresselhaus, “*Spin-Orbit Coupling Effects in Zinc Blende Structures*”, Phys. Rev. **100**, 580 (1955).
- [129] E. I. Rashba, Fiz. Tverd. Tela (Leningrad) **2**, 1224 (1960) [Sov. Phys. Solid State **2**, 1109 (1960)].
- [130] Y.A. Bychkov and E.I. Rashba, “*Oscillatory effects and the magnetic susceptibility of carriers in inversion layers*”, J. Phys. C **17**, 6039 (1984).
- [131] S. Bednarek, K. Lis, B. Szafran, “*Quantum dot defined in a two-dimensional electron gas at n-AlGaAs/GaAs heterojunction: Simulation of electrostatic potential and charging properties*” Phys. Rev. B **77**, 115320 (2008).

-
- [132] J. M. Elzerman, R. Hanson, L. H. Willems van Beveren, L. M. K. Vandersypen, and L. P. Kouwenhoven, “*Excited-state spectroscopy on a nearly closed quantum dot via charge detection*”, Appl. Phys. Lett. **84**, 4617 (2004).
- [133] S. Cortez, O. Krebs, S. Laurent, M. Senes, X. Marie, P. Voisin, R. Ferreira, G. Bastard, J. M. Gerard, and T. Amand, “*Optically Driven Spin Memory in n-Doped InAs-GaAs Quantum Dots*”, Phys. Rev. Lett. **89**, 207401 (2002).
- [134] A. Shabaev, Al. L. Efros, D. Gammon, and I. A. Merkulov, “*Optical readout and initialization of an electron spin in a single quantum dot*”, Phys. Rev. B **68**, 201305(R) (2003).
- [135] O. Gywat, H.-A. Engel, D. Loss, R. J. Epstein, F. M. Mendoza, and D. D. Awschalom, “*Optical detection of single-electron spin decoherence in a quantum dot*”, Phys. Rev. B **69**, 205303 (2004).
- [136] A. S. Bracker, E. A. Stinaff, D. Gammon, M. E. Ware, J. G. Tischler, A. Shabaev, Al. L. Efros, D. Park, D. Gershoni, V. L. Korenev, and I. A. Merkulov, “*Optical Pumping of the Electronic and Nuclear Spin of Single Charge-Tunable Quantum Dots*”, Phys. Rev. Lett. **94**, 047402 (2005).
- [137] M. Atature, J. Dreiser, A. Badolato, A. Hogege, K. Karrai, and A. Imamoglu, “*Quantum-Dot Spin-State Preparation with Near-Unity Fidelity*”, Science, **312**, 551 (2006).
- [138] K. Ono, D. G. Austing, Y. Tokura, and S. Tarucha, “*Current Rectification by Pauli Exclusion in a Weakly Coupled Double Quantum Dot System*”, Science, **297**, 1313 (2002).
- [139] A. C. Johnson, J. R. Petta, C. M. Marcus, M. P. Hanson and A. C. Gossard, “*Singlet-triplet spin blockade and charge sensing in a few-electron double quantum dot*”, Phys. Rev. B, **72**, 165308 (2005).
- [140] S. Datta and B. Das, “*Electronic analog of the electrooptic modulator*”, Appl. Phys. Lett. **56**, 665 (1990).
- [141] J. Schliemann, C. Egues, J, and D. Loss, “*Nonballistic Spin-Field-Effect Transistor*”, Phys. Rev. Lett. **90**, 146801 (2003).

-
- [142] J.E. Hirsch, “*Spin Hall Effect*”, Phys. Rev. Lett. **83**, 1834 (1999).
- [143] M. I. Dyakonov and V. I. Perel’ “*Possibility of orientating electron spins with current*”. Sov. Phys. JETP Lett. **13**, 467 (1971).
- [144] M.I. Dyakonov and V.I. Perel’. “*Current-induced spin orientation of electrons in semiconductors*”. Phys. Lett. A **35** (6) 459 (1971).
- [145] Y. Kato, R. C. Myers, A. C. Gossard, D. D. Awschalom “*Observation of the Spin Hall Effect in Semiconductors*”, Science **306** 1910 (2004).
- [146] J. Wunderlich, B. Kaestner, J. Sinova and T. Jungwirth, “*Experimental Observation of the Spin-Hall Effect in a Two-Dimensional Spin-Orbit Coupled Semiconductor System*”, Phys. Rev. Lett. **94** 047204 (2005).
- [147] J. C. Egues “*Spin-Dependent Perpendicular Magnetotransport through a Tunable ZnSe/Zn_{1-x}Mn_xSe Heterostructure: A Possible Spin Filter?*” Phys. Rev. Lett. **80**, 4578 (1998).
- [148] M. Field, C. G. Smith, M. Pepper, D. A. Ritchie, J. E. F. Frost, G. A. C. Jones, and D. G. Hasko, “*Measurements of Coulomb blockade with a noninvasive voltage probe*”, Phys. Rev. Lett. **70**, 1311 (1993).
- [149] D. Heiss, S. Schaeck, H. Huebl, M. Bichler, G. Abstreiter, J. J. Finley, D. V. Bulaev, and D. Loss, “*Observation of extremely slow hole spin relaxation in self-assembled quantum dots*”, Phys. Rev. B **76**, 241306 (2007).
- [150] B. D. Gerardot, D. Brunner, P. A. Dalgarno, P. Öhberg, S. Seidl, M. Kroner., K. Karrai, N. G. Stoltz, P. M. Petroff, and R. J. Warburton, “*Optical pumping of a single hole spin in a quantum dot*”, Nature (London) **451**, 441 (2008).
- [151] F. Fras, B. Eble, P. Desfonds, F. Bernardot, C. Testelin, M. Chamarro, A. Miard, and A. Lemaitre, “*Hole-spin initialization and relaxation times in InAs/GaAs quantum dots*”, Phys. Rev. B **84**, 125431 (2011).
- [152] D. V. Bulaev and D. Loss, “*Electric Dipole Spin Resonance for Heavy Holes in Quantum Dots*”, Phys. Rev. Lett. **98**, 097202 (2007).

-
- [153] J. C. Budich, D. G. Rothe, E. M. Hankiewicz, and B. Trauzettel, “*All-electric qubit control in heavy hole quantum dots via non-Abelian geometric phases*”, Phys. Rev. B **85**, 205425 (2012).
- [154] C. Hsieh, R. Cheriton, M. Korkusinski, and P. Hawrylak, “*Valence holes as Luttinger spinor based qubits in quantum dots*”, Phys. Rev. B **80**, 235320 (2009).
- [155] T. Andlauer and P. Vogl, “*Electrically controllable g tensors in quantum dot molecules*”, Phys. Rev. B **79**, 045307 (2009).
- [156] R. Roloff, T. Eissfeller, P. Vogl, and W. Pötz, “*Electric g tensor control and spin echo of a hole-spin qubit in a quantum dot molecule*”, New J. Phys. **12**, 093012 (2010).
- [157] K. De Greve, P. L. McMahon, D. Press, T. D. Ladd, D. Bisping, C. Schneider, M. Kamp, L. Worschech, S. Höfling, A. Forchel, and Y. Yamamoto, “*Coherent control and suppressed nuclear feedback of a single quantum dot hole qubit*”, Nature Physics **7**, 872 (2011).
- [158] A. Greilich, S. G. Carter, D. Kim, A. S. Bracker, and D. Gammon, “*Optical control of one and two hole spins in interacting quantum dots*”, Nature Photonics **5**, 702 (2011).
- [159] T. M. Godden, J. H. Quilter, A. J. Ramsay, Yanwen Wu, P. Brereton, S. J. Boyle, I. J. Luxmoore, J. Puebla-Nunez, A. M. Fox, and M. S. Skolnick, “*Coherent Optical Control of the Spin of a Single Hole in an InAs/GaAs Quantum Dot*”, Phys. Rev. Lett. **108**, 017402 (2012).
- [160] K. Müller, A. Bechtold, C. Ruppert, C. Hautmann, J. S. Wildmann, T. Kaldewey, M. Bichler, H. J. Krenner, G. Abstreiter, M. Betz, and J. J. Finley, “*High-fidelity optical preparation and coherent Larmor precession of a single hole in an (In,Ga)As quantum dot molecule*”, Phys. Rev. B **85**, 241306 (2012).
- [161] B. Eble, P. Desfonds, F. Fras, F. Bernardot, C. Testelin, M. Chamarro, A. Miard, and A. Lemaitre, “*Hole and trion spin dynamics in quantum dots under excitation by a train of circularly polarized pulses*”, Phys. Rev. B **81**, 045322 (2010).

- [162] F. Fras, B. Eble, F. Bernardot, C. Testelin, M. Chamarro, A. Miard, and A. Lemaitre, “*Optical pumping and reversal of hole spin in InAs/GaAs quantum dots*”, Appl. Phys. Lett. **100**, 012104 (2012).
- [163] A. J. Ramsay, S. J. Boyle, R. S. Kolodka, J. B. B. Oliveira, J. Skiba-Szymanska, H. Y. Liu, M. Hopkinson, A. M. Fox, and M. S. Skolnick, “*Fast Optical Preparation, Control, and Readout of a Single Quantum Dot Spin*”, Phys. Rev. Lett. **100**, 197401 (2008).
- [164] T. M. Godden, J. H. Quilter, A. J. Ramsay, Y. W. Wu, P. Brereton, I. J. Luxmoore, J. Puebla, A. M. Fox, and M. S. Skolnick, “*Fast preparation of a single-hole spin in an InAs/GaAs quantum dot in a Voigt-geometry magnetic field*”, Phys. Rev. B **85**, 155310 (2012).
- [165] V. S. Pribiag, S. Nadj-Perge, S. M. Frolov, J. W. G. van den Berg, I. van Weperen, S. R. Plissard, E. P. A. M. Bakkers, and L. P. Kouwenhoven, “*Electrical control of single hole spins in nanowire quantum dots*”, Nature Nanotechnology **8**, 170 (2013).